SC-RR-65-551

EG

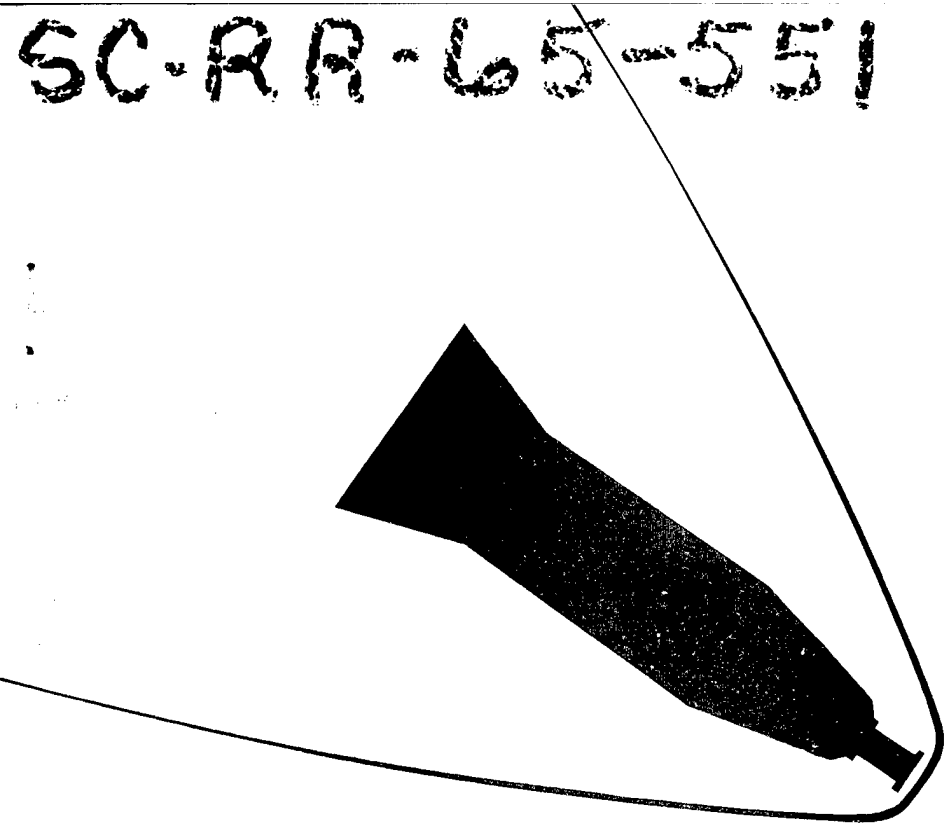

SC-RR-65-551

DISTRIBUTION STATEMENT A
Approved for Public Release
Distribution Unlimited

AEROSPACE NUCLEAR SAFETY

ROVER POSTOPERATIONAL DESTRUCT INSTRUMENTATION DEVELOPMENT

SANDIA CORPORATION

PRIME CONTRACTOR TO THE
UNITED STATES ATOMIC
ENERGY COMMISSION
ALBUQUERQUE, NEW MEXICO
LIVERMORE, CALIFORNIA

Issued by Sandia Corporation,
a prime contractor to the
United States Atomic Energy Commission

Printed in USA. Price $4.00. Available from the Clearinghouse for Federal Scientific and Technical Information, National Bureau of Standards, U. S. Department of Commerce, Springfield, Virginia

SC-RR-65-551

ROVER POSTOPERATIONAL DESTRUCT INSTRUMENTATION DEVELOPMENT

R. E. Berry, 9312
J. P. Martin, 9232

December 1965

Approved by V. E. Blake
V. E. Blake, 9310

A. Y. Pope
A. Y. Pope, 9300

ABSTRACT

This report presents the results of the instrumentation development tests conducted to determine the techniques, instrumentation, and physical layout needed for performing a full-scale destruct test of a mockup ROVER/NERVA space propulsion engine.

SUMMARY

In partial fulfillment of its responsibility to the AEC for the safety analyses of nuclear power supplies to be used in space, Sandia Corporation performed a series of development tests in preparation for a full-scale destruct test of the ROVER/NERVA space propulsion engine. The data from the full-scale test are necessary before the safety analysis of the nuclear space engine can be completed.

The development tests furnished the following information:

1. The debris pattern from a four-explosive charge, scale model is a four-jet pattern with the jets originating at 45 degrees between the explosive charges.
2. The debris size and distribution is repeatable and the size ranges from 0.5 micron to 4760 microns.
3. The velocity of the debris particles was from about 350 to 450 feet per second.
4. Scale models simulating the real item must be used to be assured of proper debris distribution pattern.
5. Rotating polystyrene foam particle catchers and velocity measuring devices are satisfactory and will produce the desired data.
6. Air sampling is necessary to obtain information on the particle sizes below 20 microns.
7. The 2-pound per cubic foot foam was superior for particle collection.
8. The pressure to be expected is about 50 percent of that pressure created by an uncased charge of the same weight.

The development tests were very successful in providing the techniques, instrumentation, and physical layout information needed for performing a full-scale destruct test on a mockup ROVER/NERVA space propulsion engine.

TABLE OF CONTENTS

LIST OF ILLUSTRATIONS

LIST OF ILLUSTRATIONS (cont)

LIST OF ILLUSTRATIONS (cont)

ACKNOWLEDGMENT

The design assistance and field support provided by personnel from other organizations within Sandia Corporation has played a significant part in the successful completion, within limited time scales, of this program.

ROVER POSTOPERATIONAL DESTRUCT INSTRUMENTATION DEVELOPMENT

Introduction

Sandia Corporation is responsible to the AEC for the safety analyses of nuclear power supplies used and being proposed for use in space and has the authority to perform any tests needed to substantiate the analyses or to provide data to be used in the safety assessment.

At the request of the joint AEC/NASA Space Nuclear Propulsion Office, Sandia Corporation is assisting Aberdeen Proving Grounds to obtain source data for computer analyses of radioactive material fallout resulting from the chemical explosive destruction in space of a ROVER/NERVA nuclear propulsion engine. The analysis of the data obtained from these tests will provide the information needed for the design of the instrumentation for a full-scale destruct test of a mockup ROVER/NERVA space propulsion engine. The source data required for the analyses includes the debris space distribution, debris size and mass, and debris velocity as a function of size.

A total of 24 tests were conducted to obtain these source data which were used for computer analyses and for the development of instrumentation for collecting the data. These tests were divided into groups, each group having a specific purpose.

Group 1. Tests 1 through 6.
Evaluation of polystyrene foam as a particle collector.

Group 2. Tests 7 through 12. Sled Tests 1 through 6.
Evaluation of velocity measuring techniques.

Group 3. Tests 13 through 23.
Evaluation of mass balance techniques and instrumentation layout to be used on the full-scale destruct test.

This report describes the tests conducted to obtain samples of the nuclear materials and presents the results obtained from an analysis of the data.

Objectives

The primary objective of the development model tests was to establish an adequate method for collecting debris. Secondary objectives were to determine the debris spatial distribution and to measure the debris velocity as a function of particle size and mass.

Description of Tests

The primary objective was approached by developing an adequate collection media -- Group 1 tests. Group 2 tests were conducted to evaluate velocity measurement techniques, and Group 3 tests were conducted to evaluate the instrumentation and techniques to be used in a full-scale test. These last tests were performed to establish a high confidence factor for satisfactory completion of a full-scale test.

Group 1 Tests

In these tests, a solid graphite test device (Figure 1) was employed to acquire information about the debris distribution pattern and to evaluate the polystyrene foam plastic (various densities) as a particle collection medium. Reactor grade graphite 3-3/4-inch square was used to fabricate the 4-inch diameter by 7-inch long test device. The centrally located hole was loaded with Comp C4 explosive. The test was also to provide an estimate of velocity as established by particle penetration into the foam plastic.

Minimum instrumentation was used in these tests to promote better photographic coverage.

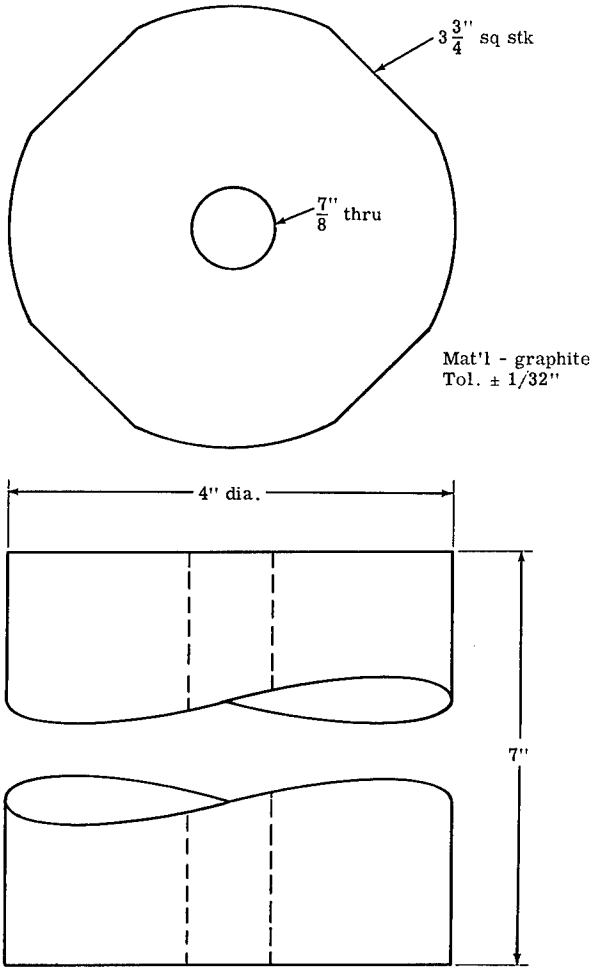

Figure 1. PODS Test Device

Tests 1 and 2 -- These two tests were performed to establish an approximate overpressure level, an indication of particle penetration, and to photograph the debris cloud.

The physical layout of these tests is shown in Figure 2.

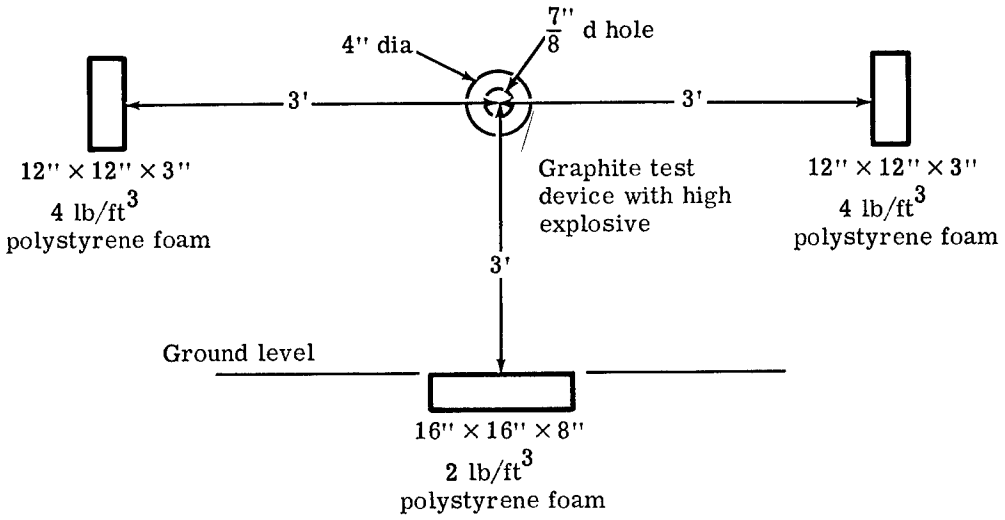

Figure 2. Physical Layout for PODSIT Tests 1 and 2

The results from the pressure transducers and the effectiveness of the foam plastic particle collector are tabulated in Appendix A.

Polystyrene foam was effective in collecting graphite particles (Figure 3). Pressure of 2.6 psi at 3 feet was satisfactorily measured. The velocity indication was unsatisfactory because no definite depth versus particle size was evident. This part of the test did indicate that penetration tests under controlled conditions, i.e., known velocity and known particle size, would be necessary before any useful velocity versus penetration depth data could be acquired.

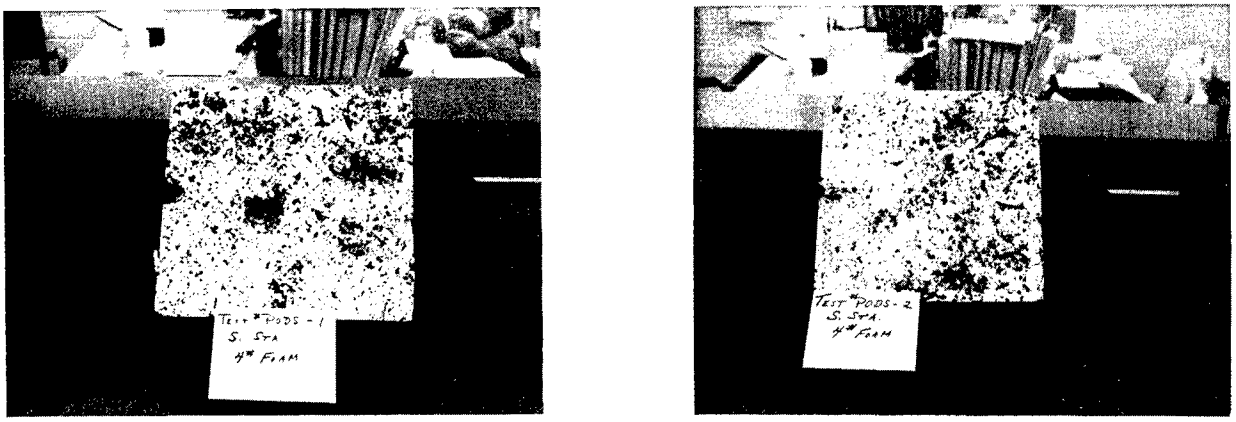

Figure 3. Polystyrene Foam Plastic After Impact of Graphite Particles

Tests 3 and 4 -- The overpressure measured during the previous tests indicated that greater distance was needed to reduce damage to the foam plastic support structures. This was also indicated by the foam plastic being torn from their mounts. Because insufficient distribution information was acquired in Tests 1 and 2, the physical layout for Tests 3 and 4 (Figure 4) was devised.

This physical layout was intended to establish particle distribution around a horizontally suspended test device and to provide some average velocity data on the graphite particles.

To reduce the overpressure and to improve particle collection, three changes were made:

1. The weight of explosive was reduced by placing the explosive in an aluminum thimble. Figure 5 shows the configuration of the aluminum thimble. This action also tended to give a more even debris cloud.
2. The foam plastic particle collectors were installed at 4 feet instead of 3 feet.
3. The test device was ringed with foam plastic particle collectors. Seven collectors were used instead of three.

The velocity data acquisition was attempted with a Time-of-Arrival (TOA) gage. The gage incorporated two principles:

1. Particles which had passed through a 1/2-inch wide by 1-inch long slot in a rotating aluminum plate were collected in fixed polystyrene foam. This concept was intended to sample along the depth of the particle cloud by excluding those particles which did not align with the slot.
2. An accelerometer was used to sense the impact of the particles.

Figure 6 is a photograph of the Time-of-Arrival gage.

One final addition to the physical layout was an 8 x 8-foot backboard painted white with 12 x 12-inch black cross hatching. This backboard provided a better background for photographing the black graphite particles and a measuring reference for velocity determination.

The data from these tests are tabulated in Appendix A.

The overpressure was reduced to 1.1 psi at 3.5 feet. The foam plastic particle collectors indicated that the debris pattern was not spherical, because the foam collectors at 45 degrees to the longitudinal axis of the test device received a greatly reduced number of graphite particles. The table in Appendix A illustrates this phenomena. Further, Tests 1 and 2 were recalculated to determine whether better agreement would be shown in a model other than spherical.

The literature explains that, when firing a cylindrical charge, the debris pattern is cylindrical. This debris pattern is defined by establishing a plane at 10 degrees from the plane of the end surface of the cylinder being destroyed. Figure 7 is a representation of the debris cloud expected from a cylindrical explosive charge in a cylindrical object to be destroyed.

Using this cylindrical debris cloud concept instead of the spherical model used in Tests 1 and 2 gives superior agreement between the theoretical quantity of material to be collected in the polystyrene foam and the actual amount collected. The table in Appendix A shows the comparison between the spherical model and the cylindrical model. From this point forward only the cylindrical model was used.

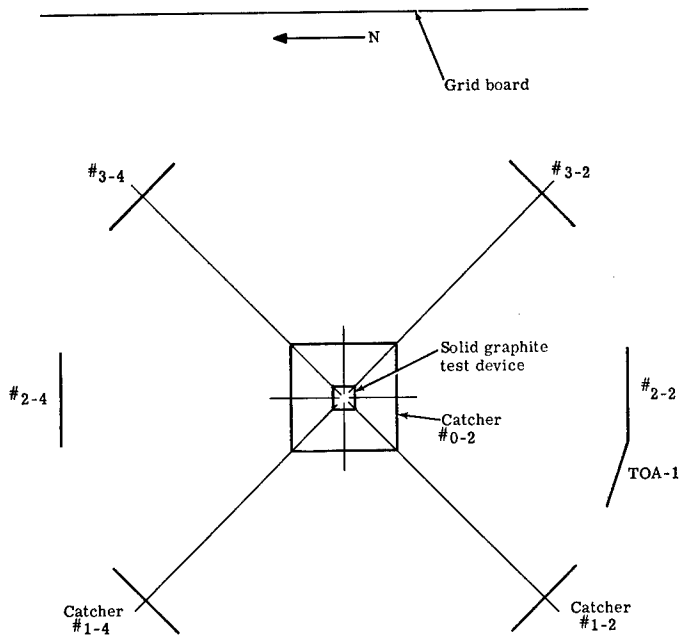

Plan View

Notes:
All catchers numbered -2 are 16" x 16" x 8", those numbered -4 are 12" x 12" x 3".

All catchers, except #0-2, are to be mounted perpendicular with the centerline of the catcher 3 feet above ground surface and the face of the catcher 3 feet from the test device.

Catcher #0-2 mounted at ground plane with horizontal centerline of test item 3 feet above face of catcher.

TOA-1 is to be a box 8" x 8" x 8" mounted with its centerline 3 feet above ground surface, open face toward test specimen, 3 feet away.

Grid board 8' x 8' central to test specimen 4 feet distance, white background, 2-inch black gridlines on 12-inch centers.

Figure 4. Physical Layout PODSIT - Tests 3 and 4

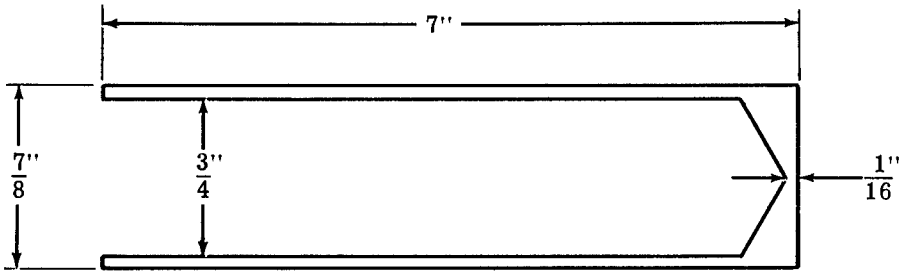

Figure 5. Aluminum Thimble

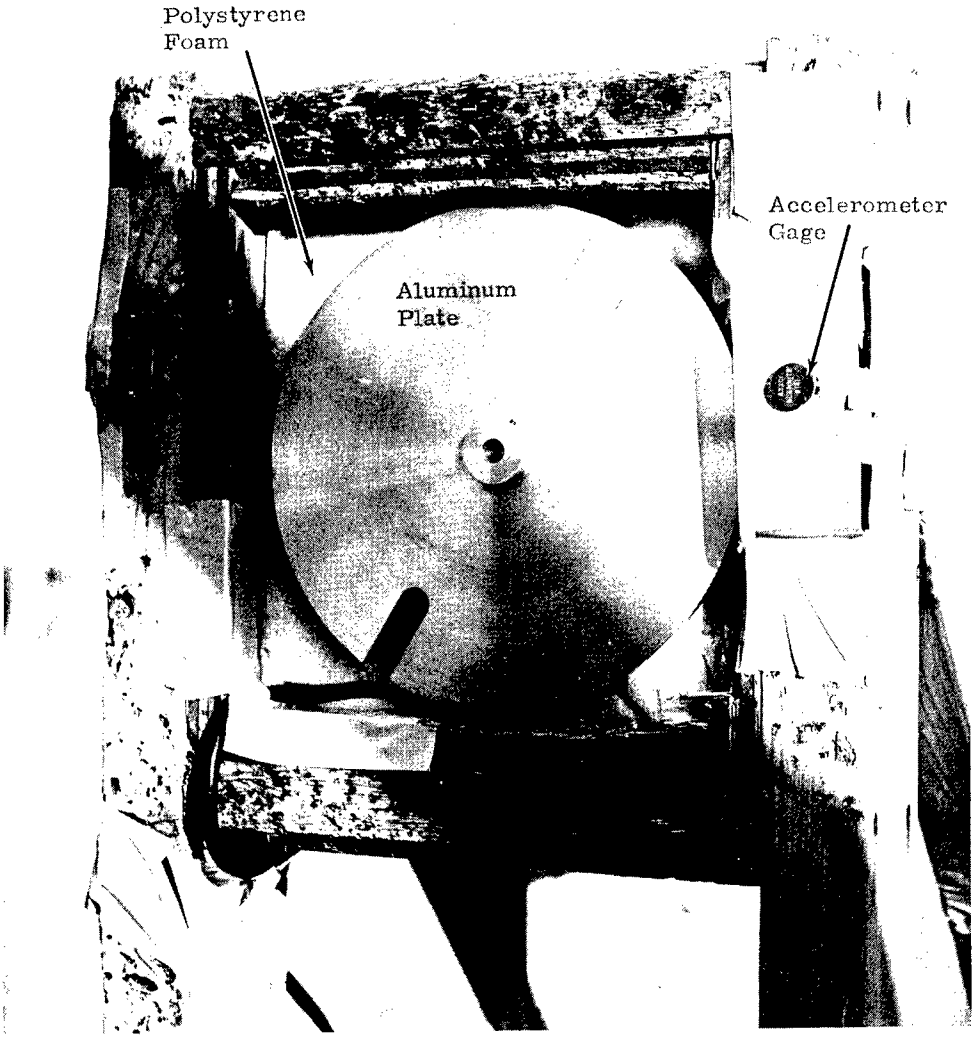

Figure 6. Time-of-Arrival (TOA) Gage

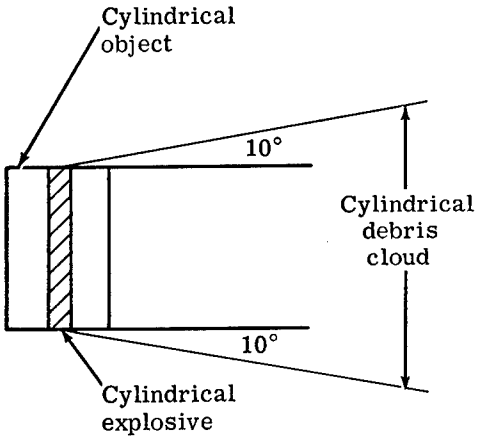

Figure 7. Debris Cloud Shape from a Cylindrical Test Device and Explosive Charge

The TOA gage did not function as intended, and therefore no velocity data were acquired. Either the overpressure or the impact of particles damaged the TOA and caused the rotating disc to stop. The accelerometer was damaged by impact.

Test 5 -- The previous tests indicated that velocity might very well be calculated from the passage of the debris cloud across the grid on the backboard. The location of other instrumentation devices interfered with a clear view of the debris cloud; therefore, the physical layout was modified for this test. Figure 8 shows the physical layout for Test 5.

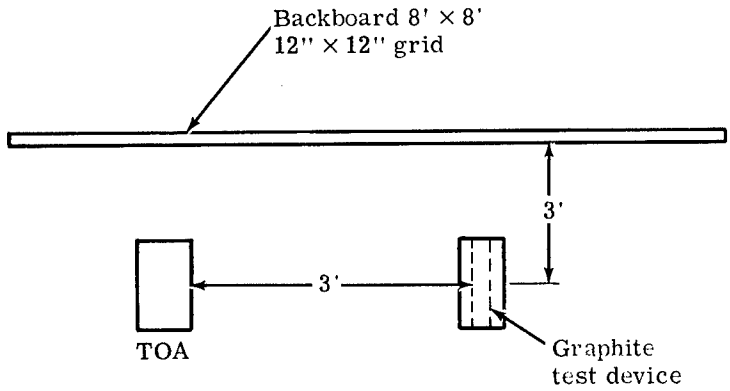

Figure 8. Physical Layout for Test 5

This test was performed strictly for the purpose of determining the velocity of the leading edge of the particle cloud. The TOA gage malfunctioned and did not provide any data, but the photographic film was read and velocity data were obtained. These data indicate an average velocity of about 900 feet per second. A tabulated list of velocities appears in Appendix A.

Test 6 -- The previous tests indicated that the backboard was effective and that the collection devices were effective only when positioned within the cylindrical area encompassed by the debris cloud.

Analyzing the information from all previous tests provided data which were used to design the next test.

The test was designed to determine the most effective distance for particle collection and whether a reduced density foam at greater distance was as effective as the heavier material close to ground zero.

No new concepts or instrumentation were placed in this test. Figure 9 illustrates the physical layout used to acquire more particle collection data and to acquire more velocity data.

Data from this test are tabulated in Appendix A.

This test served to illustrate that all particle foam plastic collection surfaces must be perpendicular to a line from the geometric center of the test device and the geometric center of the collection surface. The "look" angle is important to the efficient collection of graphite particles.

The TOA gage again did not provide any velocity information.

The use of a lower density foam plastic (2 lbs/ft^3) is more effective for collecting the graphite particles but must be installed at a greater distance from ground zero to prevent excessive particle damage.

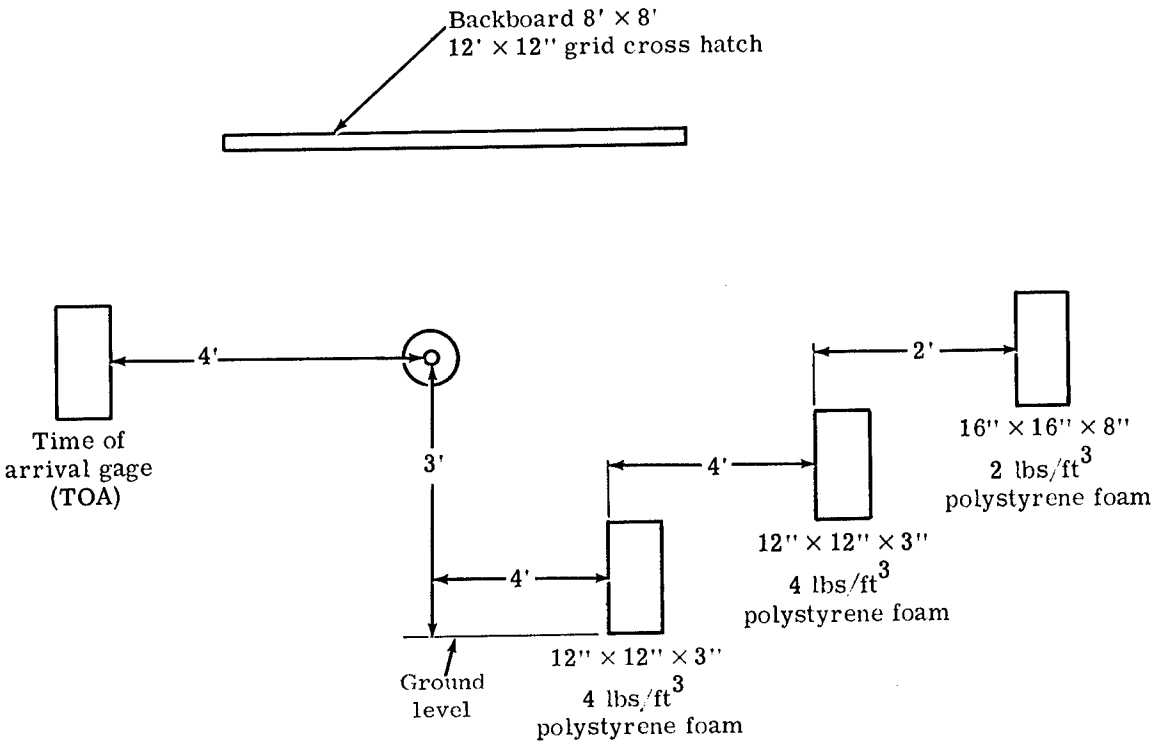

Figure 9. Physical Layout for Test 6

This test was the conclusion of the Group 1 tests used to evaluate the polystyrene foam plastic as a particle collection material.

General Discussion -- The Group 1 tests served to establish the following general information:

1. The debris pattern is symmetricl and radial when observed along the longitudinal axis of the test device (see Figure 10).
2. The use of polystyrene foam for particle collection is satisfactory.
3. The use of 2 lb/ft^3 polystyrene foam is superior to 4 lb/ft^3 foam when the distance is adjusted so that excessive damage to the foam is prevented.

The Group 1 tests also served to point up the following areas where further investigation would be necessary and where new techniques were needed to procure the needed data:

1. Photographic coverage indicated that the debris pattern perpendicular to the longitudinal axis was other than circular.
2. The determination of velocity as a function of penetration depth into the polystyrene foam would require additional testing under more controlled conditions.

Considering all information acquired and all information known to be lacking, the Group 2 tests, including the sled tests, were outlined as shown in Appendix B (Test Plan for ROVER Postoperational Destruct Systems Instrumentation Tests).

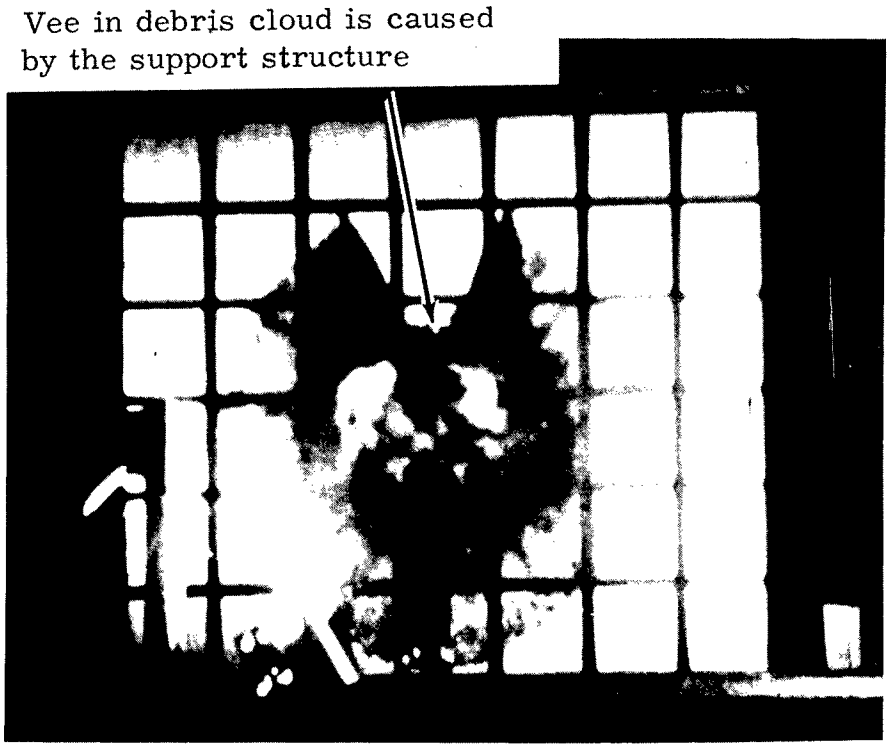

Figure 10. Debris Pattern for Group 1 Tests

Group 2 Tests

This group of tests (Tests 7 through 12 and the sled tests) was designed from the data and information acquired during the Group 1 test series. There was one major difference in the Group 2 tests. These tests were to be completed in 1 month (six tests) and multiple instrumentation was to be evaluated. The time limitation was imposed for the purpose of deciding whether a full-scale destruct test could be instrumented and conducted in approximately 3 months. Further, there must be a high level of confidence that data could be obtained or the full-scale test would not be instrumented.

To give the best possible instrumentation system available in the limited time, each test was designed to provide a maximum amount of data. All suggested concepts and techniques which appeared feasible were tested. Only those techniques which produced data or appeared to have promise of producing data were carried from one test to the next test.

The TOA, the fixed foam particle collector, and the pressure transducers used in the Group 1 tests were also used in this test series.

The following new items were evaluated in these tests:

1. Crystal Shock Wave Gages -- These gages operate on the piezoelectric principal; when the thin wafer is flexed or broken by the shock wave, a small current is generated. Figure 11 shows the gages mounted for test. Recording of the current generated will allow the calculation of shock wave velocity.

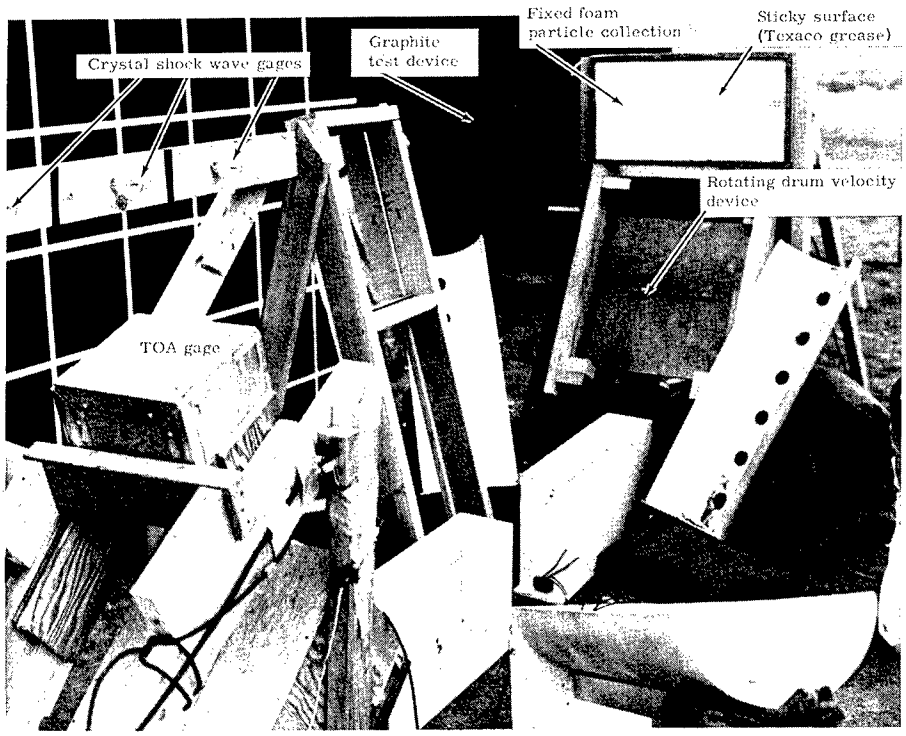

Figure 11. Gages Mounted for Group 1 Tests

2. Rotating Foam Disc Particle Collector and Velocity Device -- This device is an adaptation of the fixed foam particle collector with the added feature of attempting to separate the particles making up the debris cloud. Further, by measuring the rotational velocity of the device prior to test, the difference in velocity from leading particles to trailing particles could be determined. Another feature was the marking of the foam surface at zero time in order to calculate average velocity from firing to impact.

3. Rotating Foam Drum Particle Collector and Velocity Device -- The principle for the rotating drum is the same as for the rotating disc. The one large advantage of the drum over the disc is the possible variation in rotational speed due to belt and pulley drive and also the size of the drum collection area is larger. Figure 12 shows the front view of the rotating disc particle collector. Figure 13 shows the foam after test with particles embedded in both the disc and the drum.

4. Wire Mesh Velocity Gage -- The wire mesh velocity gage, a frame covered with a very fine wire, was used to obtain particle velocity. Figure 14 shows the wire mesh velocity gage.

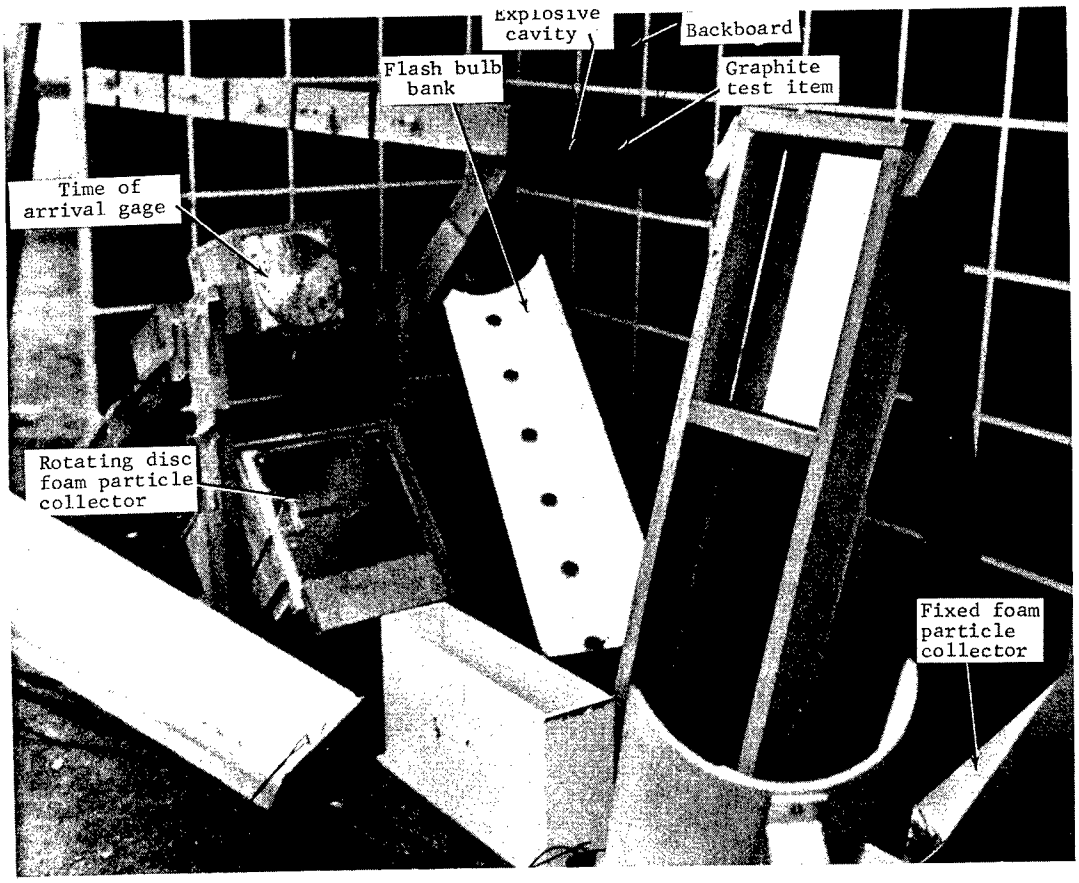

Figure 12. Physical Layout for a Development Test

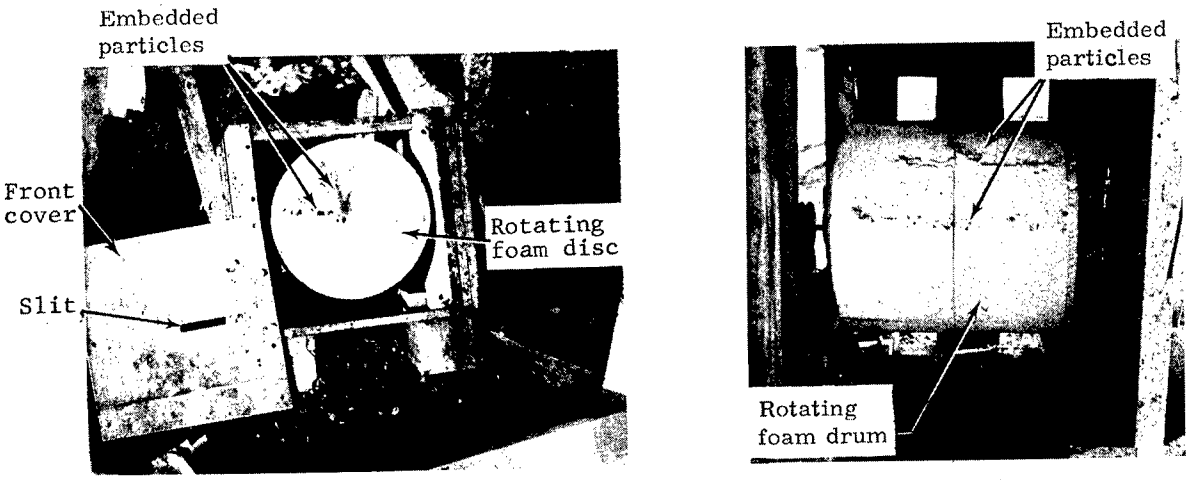

Figure 13. Rotating Foam Velocity Devices with Embedded Graphite Particles

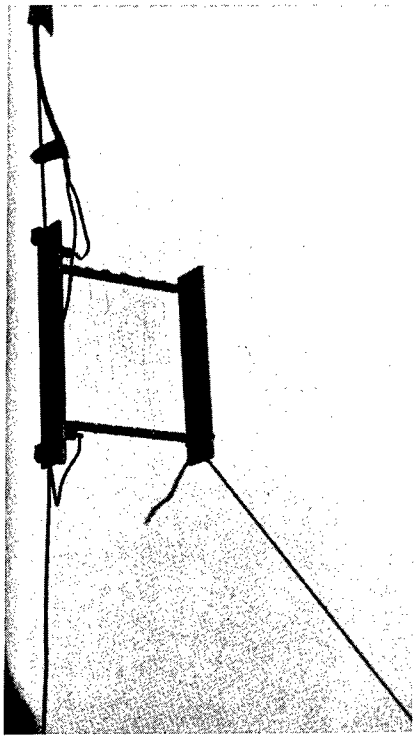

Figure 14. Wire Mesh Velocity Gage

5. Sticky Face Foam Collector -- The loss of the very small or slow speed particles caused the use of a sticky face on the fixed foam particle collector. The material was a Texaco grease which could be dissolved in trichloroethylene solvent (see Figure 11).

6. Photoelectric Cell Velocity Device -- This device operated on the principle that the graphite particles would block the light source from the collector and give an indication of time as the successive photocell light sources are blocked.

Test 7 -- The test device (described for the Group I tests) was fired with the longitudinal axis horizontal; however, many new instrumentation concepts were tested.

Figure 15 shows the physical layout used for Tests 7 and 8.

Although the crystal shock wave gages functioned satisfactorily in other tests, they did not function in this test. The shock wave was so weak that little or no flexing was produced and therefore no signal was obtained.

The rotating foam disc and foam drum devices were found to be functional and, with refinements, were used throughout the entire test program.

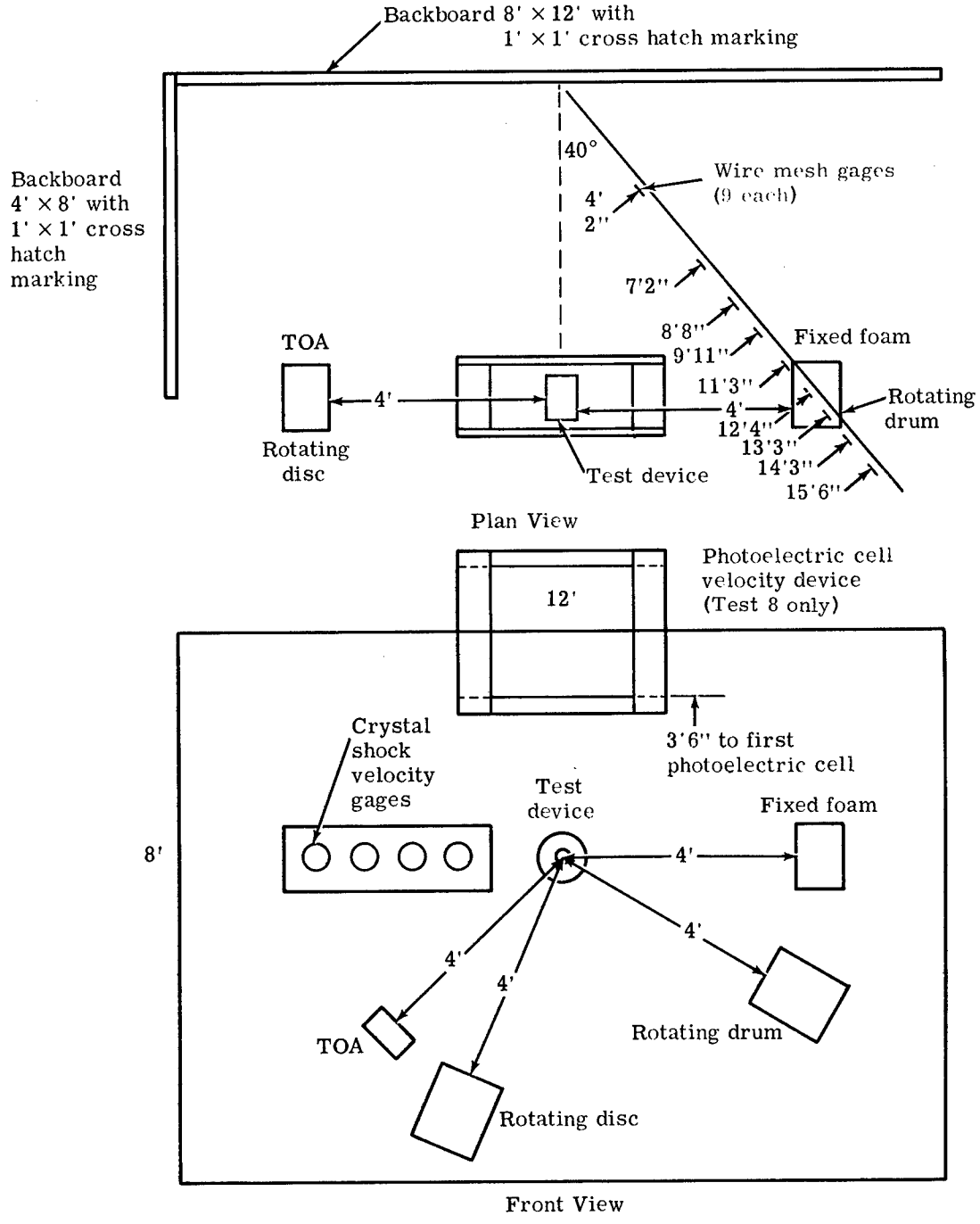

Figure 15. Physical Layout for Tests 7 and 8

The wire mesh velocity gage was satisfactory, but the particle that breaks the circuit is not collected, and, therefore the particle size cannot be determined. Further, it is not known whether the particle which broke the wire mesh came from the leading or trailing portion of the particle cloud.

These gages did produce data and appear to have potential with further development.

The sticky face foam collector functioned well except that it tended to dry out when put on too early and collected extraneous material before and after the test; this resulted in cleaning problems. Figure 16 compares the sticky face versus nonsticky face particle collection.

The test results are tabulated in Appendix A.

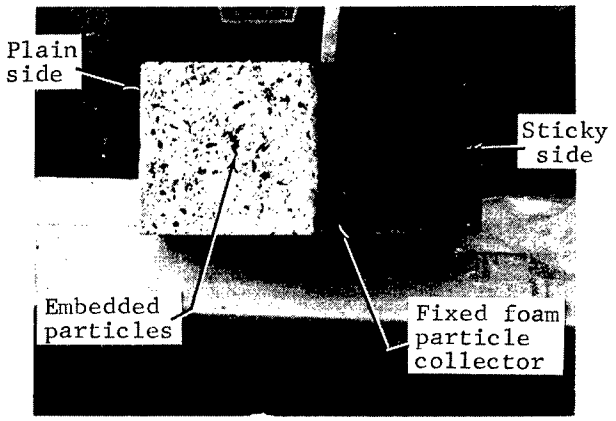

Figure 16. Comparison of Sticky Face versus Nonsticky Face Particle Collection

In general, the results were encouraging; both rotating foam velocity devices functioned, but velocity could be determined only from the rotating disc. The wire mesh velocity gage gave limited data but indicated that more data could be obtained by better placement of the gages. The fixed foam plastic particle collector functioned satisfactorily, and the grease appeared to collect the small particles and the slow moving particles. The pressure transducer functioned, giving a pressure of 0.9 psi at 4 feet.

Other items which were tested but failed to produce results are the crystal shock wave gages and the TOA gage.

Test 8 -- This test was performed with the same physical layout used in Test 7 except for the addition of a photoelectric cell velocity device. Figure 15 presents the physical layout for this test and shows the photoelectric device. Even though some of the devices failed on the previous test, they were used in this test to minimize the setup time.

The rotating foam plastic particle collectors functioned but the zero time was not present and velocity determination was impossible. The fixed foam particle collector functioned with a collection efficiency of about 82 percent. More data than previously obtained were recorded by the wire mesh gages which indicated an average velocity of 1065 fps at 3 feet tapering to 710 fps at 5.75 feet.

The photoelectric cell velocity device did not function because the flash bulbs used to illuminate the area for camera coverage completely saturated the collector cells prior to actual particle arrival. The TOA and the crystal shock wave gages did not function.

All data from this test are tabulated in Appendix A.

Test 9 -- The devices dropped from further use were the crystal shock wave gages and the photoelectric cell velocity device.

The one major change was the rotation of the graphite test device, so that the longitudinal axis was vertical.

The physical layout for this test is shown in Figure 17.

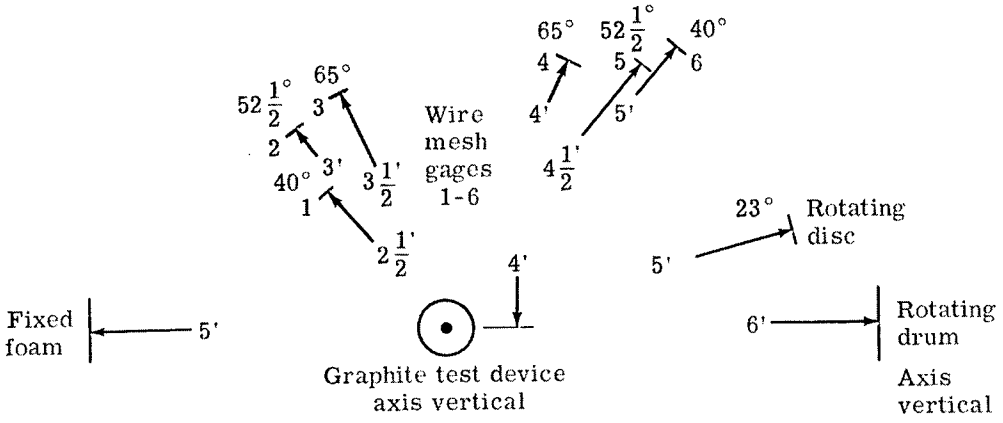

Figure 17. Physical Layout for Test 9

Figure 18 shows the graphite test device hanging vertically and the wire mesh gages around the test device.

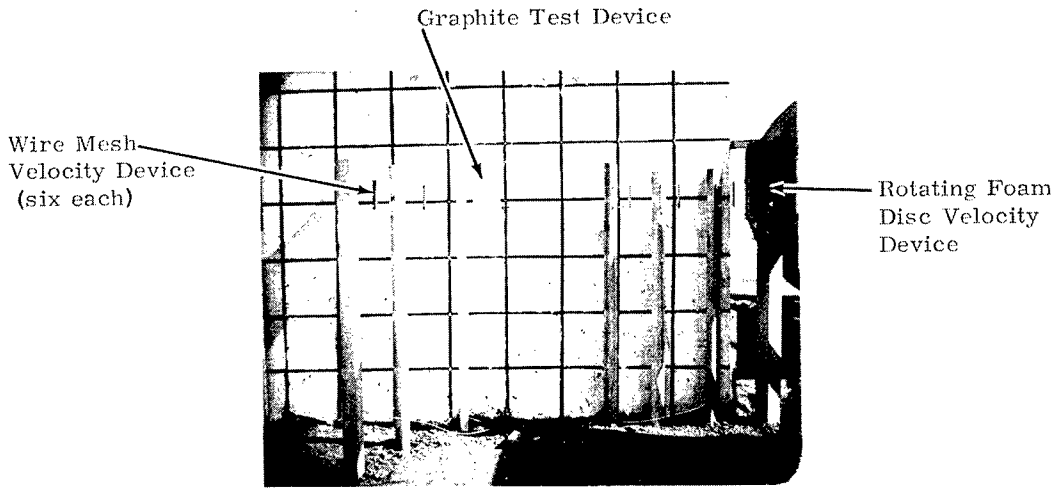

Figure 18. Test Setup with Graphite Test Device Axis Vertical

This test served to verify the shape of the debris cloud as described in Figure 7. Figure 19 shows the imprint of the graphite impact on the backboard. Calculating the spread indicates that the debris is well within the 10 degrees specified. Figure 20 verifies the donut shape of the debris cloud.

Figure 19. Debris Pattern on Backboard Test 9

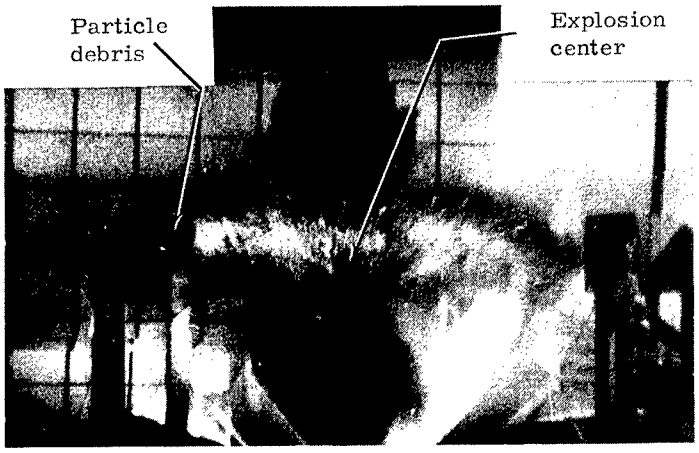

Figure 20. Shape of Debris Cloud

Data were obtained from the wire mesh velocity gages, the rotating foam disc velocity gage, and the photographic film coverage. The rotating foam drum velocity gage functioned, but no zero time was distinguishable and the data were useless.

The data, tabulated in Appendix A, are compared to that of the other tests.

Test 10 -- This test setup was similar to Test 9 except for the addition of two new concepts. A microphone and a strain gage sensor for velocity measurement or time of arrival were used. The physical layout is shown in Figure 21.

The microphone failed to give any data but the strain gage sensor recorded an average velocity of 882 fps at 66 inches.

The other devices used were pressure gages, time of arrival gage, rotating foam disc, rotating foam drum, wire mesh velocity gages, and cameras. All devices and cameras functioned, but the data were lost on the rotating foam drum because no zero time was recorded; the photographic coverage was lost because the flash bulbs triggered early. The other devices produced data which are shown in detail in Appendix A.

The pressure was 0.7 psi at 2 feet, and average velocities ranged between 684 and 966 fps (depending on the distance from ground zero).

Tests 11 and 12 -- The same physical layout was employed for Tests 11 and 12. Figure 22 shows the the location of instrumentation for these two tests.

The pressure apparently increased slightly, 1.3 psi at 4.0 feet and 1.0 psi at 46 inches, because of the addition of a 0.032-inch aluminum sleeve over the graphite cylinder.

The velocities observed were 608 to 1150 fps at 5 feet from ground zero. The vibration sensor and the microphone velocity devices gave limited information, but these velocities were so high that some phenomena other than particle impact must have caused the output. No further development is planned for these devices.

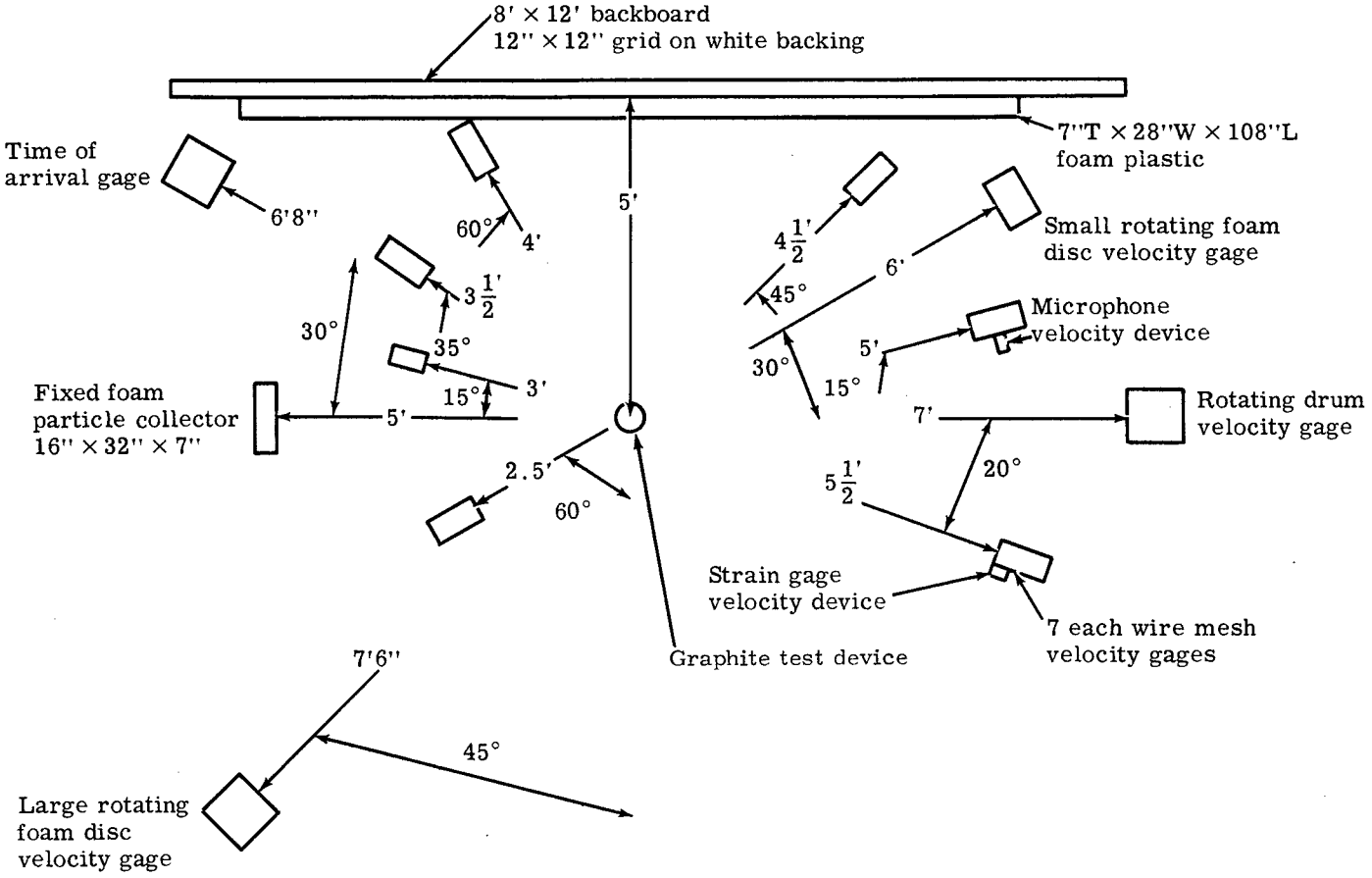

Figure 21. Physical Layout for Test 10

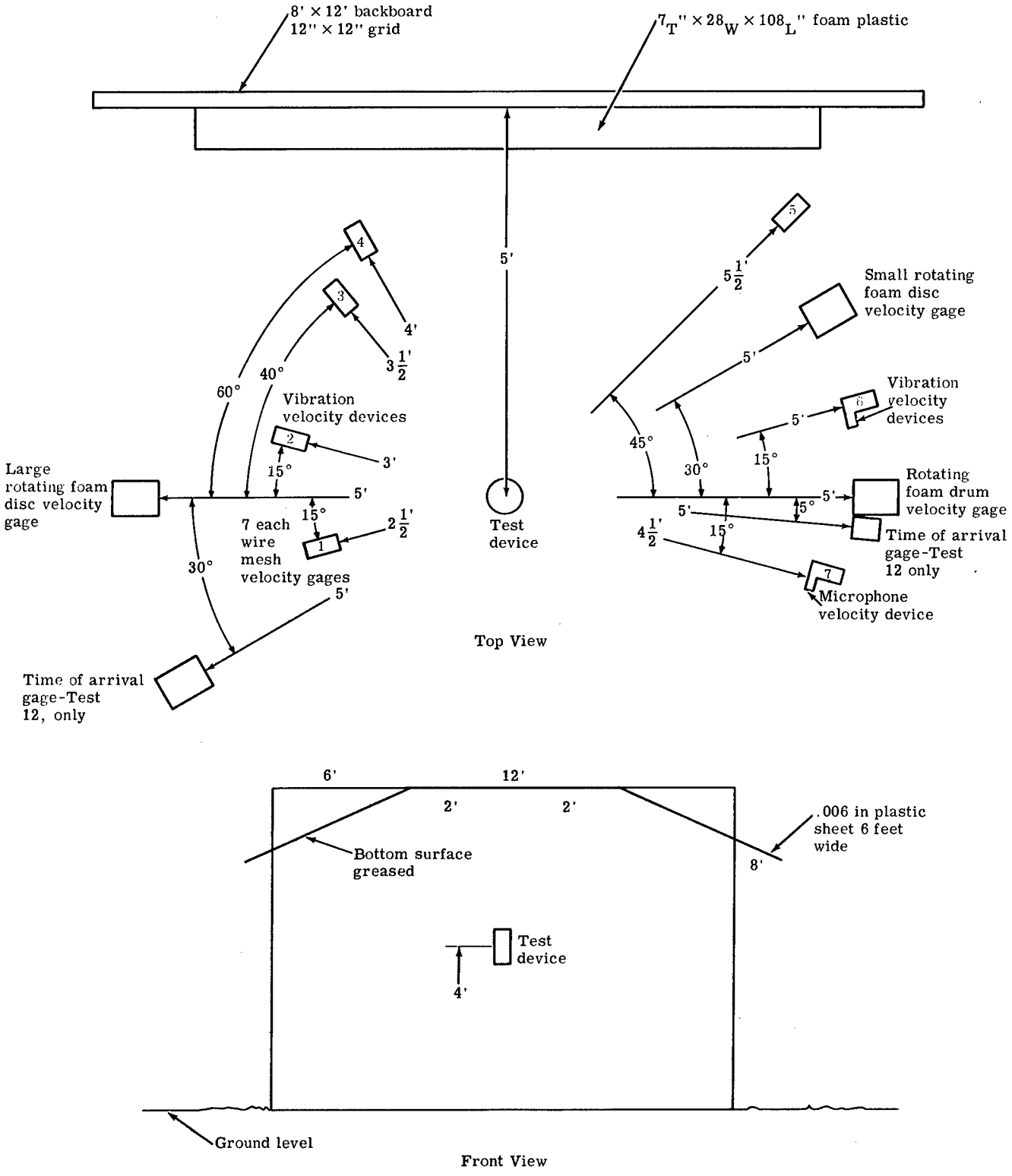

Figure 22. Physical Layout for Tests 11 and 12

Sled Tests -- These tests were designed to provide data, under controlled conditions, about the relationship of particle size and velocity as a function of penetration depth.

Graphite bars were crushed and the size graded through standard Tyler screens. Three sizes were selected for testing; 13.5 mm (0.530 inch); 4.76 mm (0.185 inch); and 2.38 mm (0.093 inch). Actually, the particles used were those particles which passed through the next larger screen and did not pass through the designated screen.

Two of the above graphite particle sizes were dropped from an overhead hopper which straddled the sled track and were collected in polystyrene foam carried on the front of the rocket powered sled. The polystyrene foam was analyzed for particle penetration and then dissolved to recover the impacted graphite particles. These recovered particles were resized through standard screens to determine if secondary breakup were caused by impact.

Figure 23 shows the hopper which was designed for the exit of single particles in a two-dimensional particle stream. Two sizes of particles were dropped simultaneously.

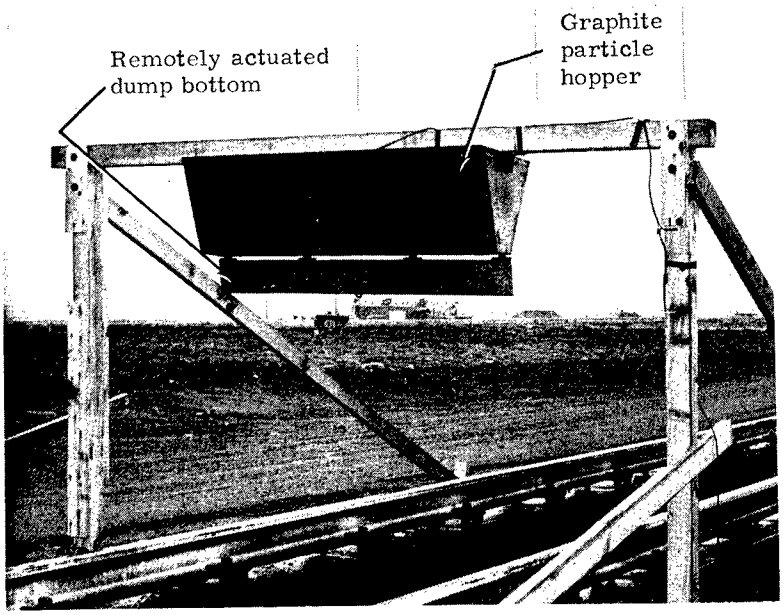

Figure 23. View of Graphite Particle Hopper Used in Sled Tests of Fixed Foam Particle Collectors

Figure 24 presents a side view of the rocket sled which carries the polystyrene foam at high velocity through the stream of graphite particles. Figure 25 is a photograph of the polystyrene foam after being impacted by the graphite particles.

Although six sled tests were originally scheduled, only the following four test runs were completed:

Sled 1 - 750 fps, 0.185 and 0.530-inch particles

Sled 2 - 750 fps, 0.093 and 0.185-inch particles

Sled 3 - 1125 fps, 0.093 and 0.185-inch particles

Sled 4 - 1125 fps, 0.093 and 0.185-inch particles

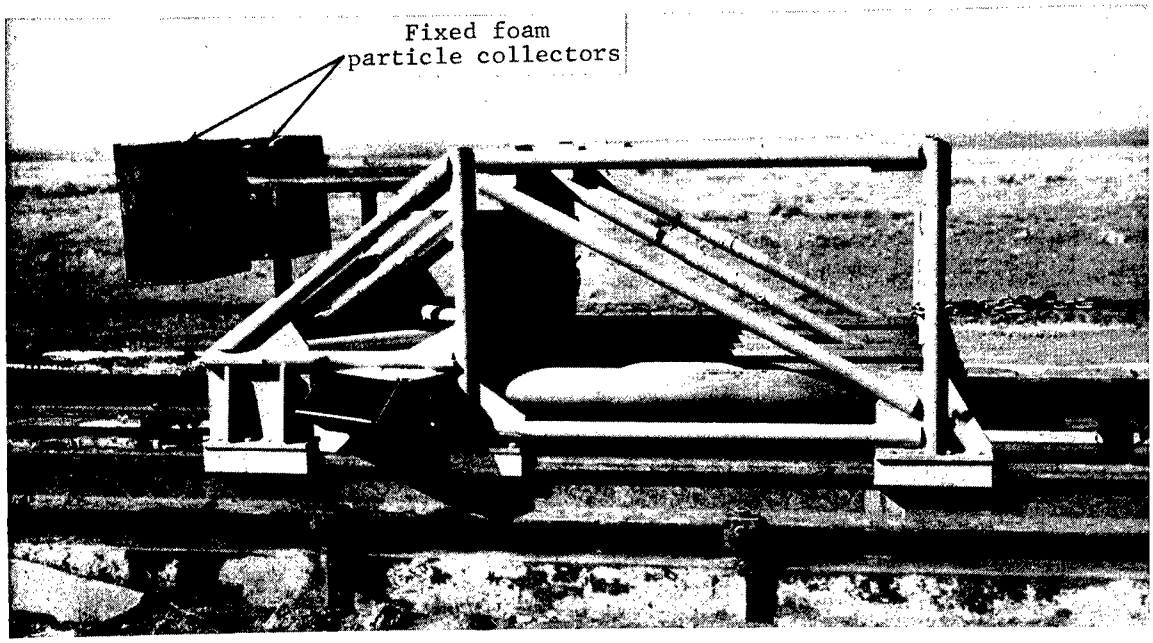

Figure 24. Rocket Sled Used in Graphite Particle Fragmentation Test

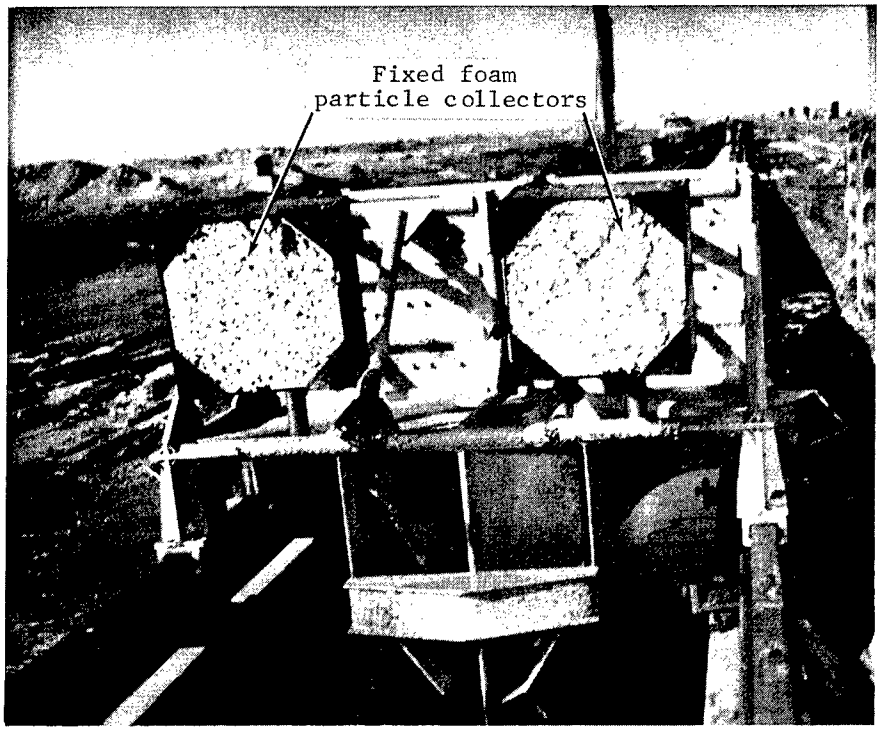

Figure 25. Fixed Foam Particle Collectors After Sled Test

Figures 26 and 27 are prints of an X-ray film showing the polystyrene foam used on Sled 4. The X-rays were to establish a finite or average penetration depth for the specific size particle at a specific velocity. Although the tests served to illuminate the problem areas, no distinct penetration depth was established.

This technique has marginal value because during an actual explosive destruct test, the particle velocities are variable, the particle sizes are variable, and the debris cloud is three dimensional. The ideal condition of one velocity, one particle size, and one particle thick cloud cannot be realized. The development of this technique will require a large number of tests to establish any statistically reliable velocity, size, penetration data.

Also, superimposed impacts tend to skew any data that might be obtained from a single impact. The graphite particles, which were collected from the polystyrene foam and rescreened, show a very small percentage of fracture. The tabulated results are found in Appendix B.

General Discussion of Group 2 Tests -- This group of tests was performed to provide data which would indicate whether a full-scale test could be instrumented with a high level of confidence. This objective was accomplished and the data revealed that instrumentation of a full-scale test was feasible. The use of pressure transducers, rotating foam velocity devices, fixed foam particle collectors and cameras would assure the collection of the required debris distribution, size, and velocity data from the destruct test of a full-scale ROVER/NERVA engine mockup.

Evaluation of all previous tests indicated the following:

1. A one-sixth scale model device duplicating the propulsion engine as closely as possible should be employed in the Group 3 tests.
2. The scale model device should be fired with the longitudinal axis vertical to take advantage of the 360-degree debris pattern and the donut shape.
3. Cameras should be located at about the same level as the device and perpendicular to the device axis.
4. All particle collection and velocity devices must be at the same height as the test device, and the collection face must be perpendicular to the test device longitudinal axis.
5. Rotating foam plastic particle collectors and velocity devices should be used in the Group 3 tests.
6. Pressure transducers should be used in the Group 3 tests.
7. Fixed foam plastic particle collectors should be used in the Group 3 tests.
8. Air sampling of the airborne cloud should be attempted.

Group 3 Tests

This indicates only 11 tests, but jetting caused by the four explosive charges produced a different debris pattern than experienced on previous tests. A repeat test (Test 13A) was performed with the longitudinal axis horizontal to observe the new debris cloud pattern.

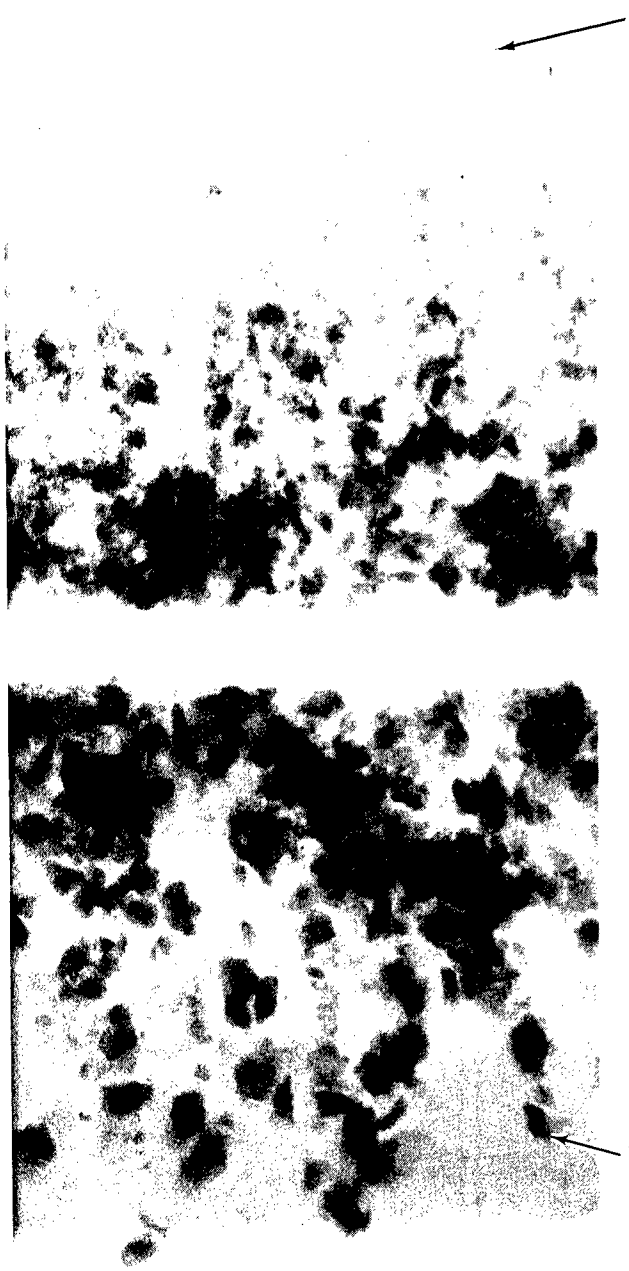

Figure 26. X-Ray Film Print of Polystyrene Foam Used on Sled 4

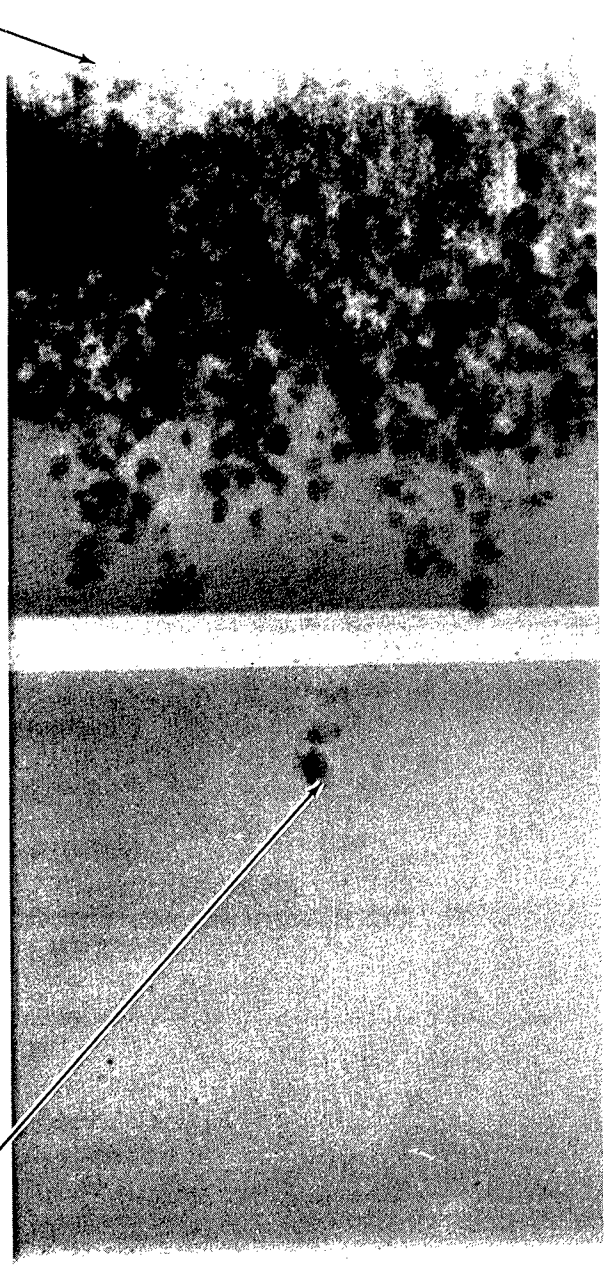

Figure 27. X-Ray Film Print of Polystyrene Foam Used on Sled 4

This group of tests was subdivided into three categories:

1. One test (13) was performed to establish the debris pattern and to verify the information on debris distribution observed in the previous test series. However, the appearance of two distinct holes in the backboard (see Figure 28) showed the need for another test, 13A, in this category.

2. Five tests (14, 15, 18, 19, and 21) were scheduled to establish the debris pattern and particle size distribution resulting from a totally contained test firing.

   These tests being totally contained were also expected to give a mass balance evaluation versus the particle size distribution.

   The short time period prior to the preparation for the full-scale test reduced the number of tests actually performed to four. Test 21 was not conducted.

3. Five tests (16, 17, 20, 22, and 23) were performed for the evaluation of instrumentation techniques and repeatability of collected data prior to preparing for the full-scale test.

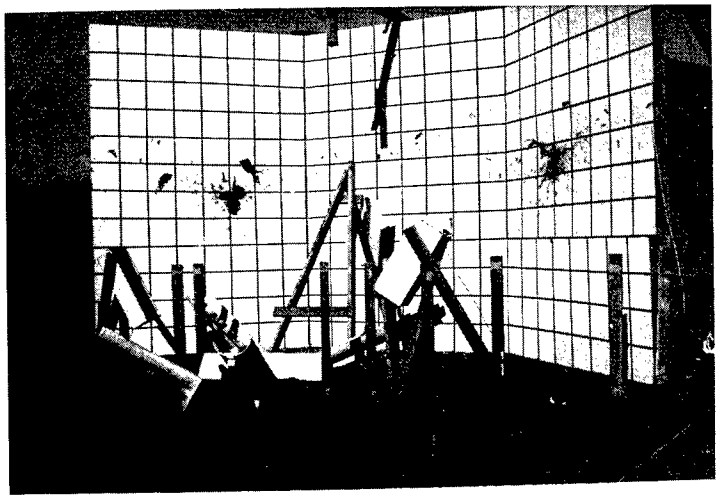

Figure 28. Debris Pattern

A scale model ROVER/NERVA propulsion engine was employed in the performance of these Group 3 tests. The scale model is defined on Sandia Drawing, N95405. Those components and features which were considered important to the overall explosive reaction were duplicated in the scale model. Figures 29, 30, 31, and 32 show the components and subassemblies of the 1/6 scale model ROVER /NERVA space propulsion engine. Figure 33 shows the assembled scale model.

At the initiation of the Group 3 tests, the full-scale test instrumentation was selected; the tests served to proof test the instrumentation principle and to provide a high level of confidence that the data required would be collected during the full-scale destruct test.

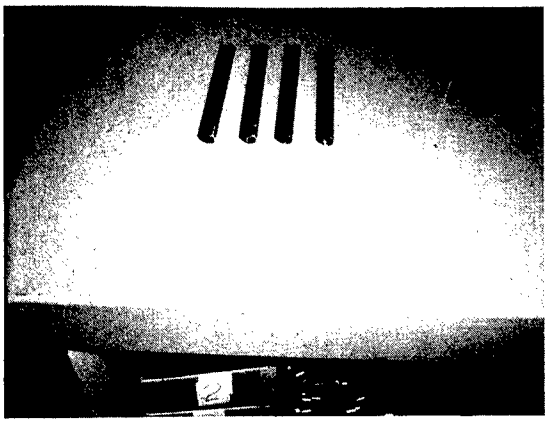

Figure 29. Steel Cylinders for Packaging the High Explosive

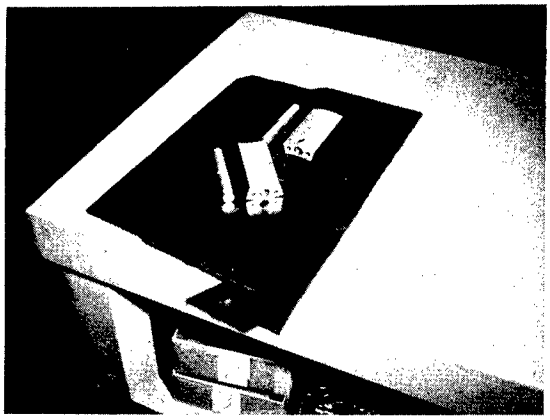

Figure 30. Simulated Reflector Segments and Control Drums

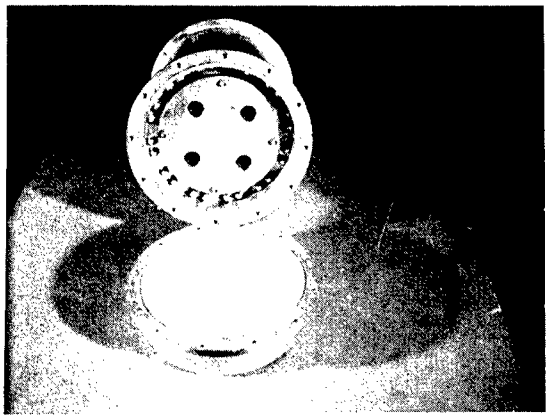

Figure 31. Assembled Scale Model Space Engine with Top Removed

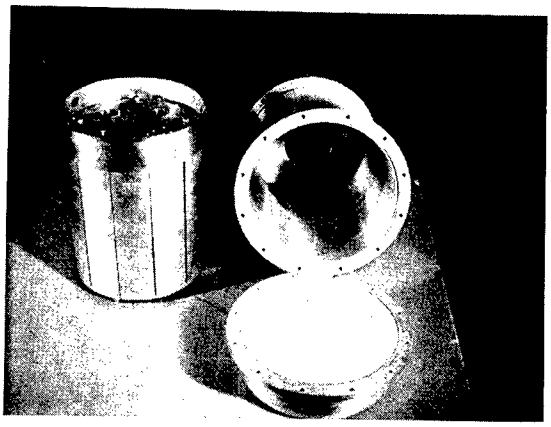

Figure 32. Simulated Core Removed from Pressure Vessel

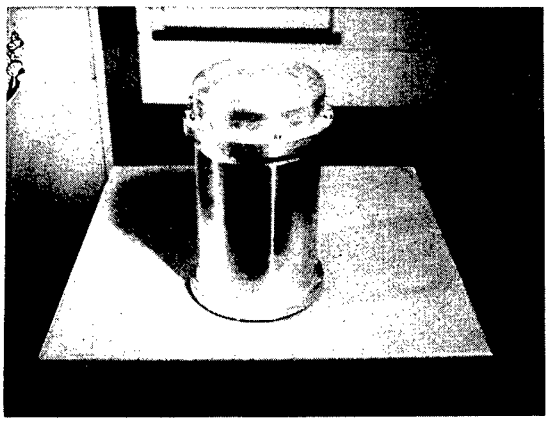

Figure 33. Assembled ROVER/NERVA Propulsion Engine, Scaled Model

Tests 13 and 13A (Debris Pattern Class A Tests) -- The debris pattern observed in the previous tests indicated that firing the device with its longitudinal axis vertical provided the best cloud shape for particle collection; therefore, in the first test of this series, the device was oriented in this way. However, the debris pattern (Figure 28) indicated that the 1/6 scale model was not reacting or disassembling in the same debris pattern observed during the previous explosive destruct tests (see Figure 19).

Figure 34 shows the physical layout used for Test 13. The expected debris pattern was a uniform debris impact across the backboard. Figure 35 presents photographs of the backboard before and after the destruct test. This odd debris pattern led to the physical layout used in Test 13A. Figure 36 shows the physical layout used in Test 13A.

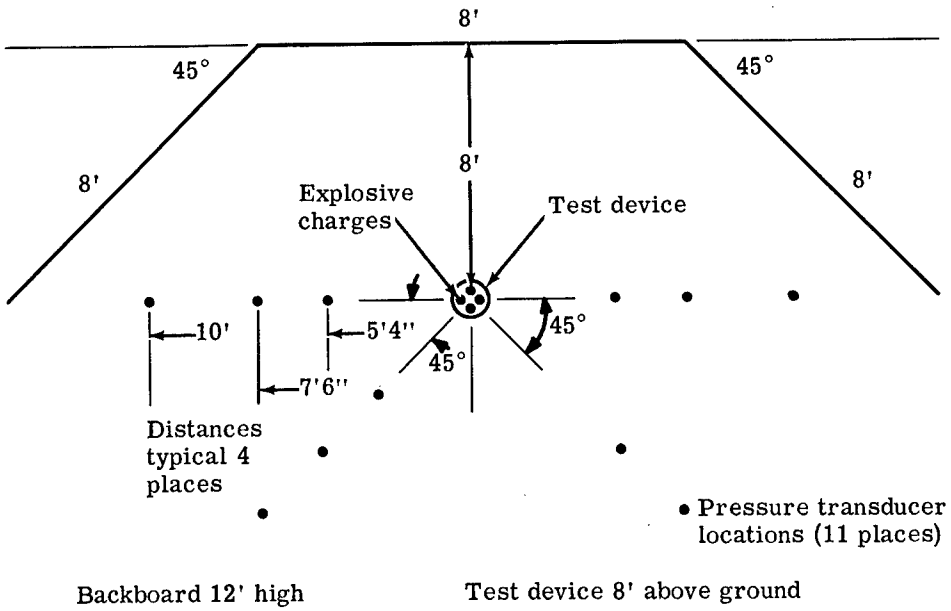

Figure 34. Physical Layout for Test 13

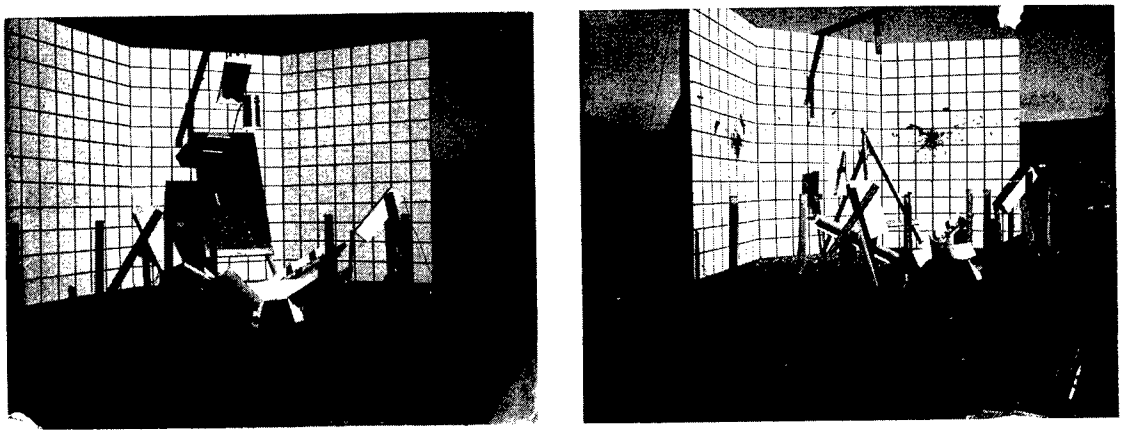

Before Test After Test

Figure 35. Test 13 Physical Layout Before and After Test

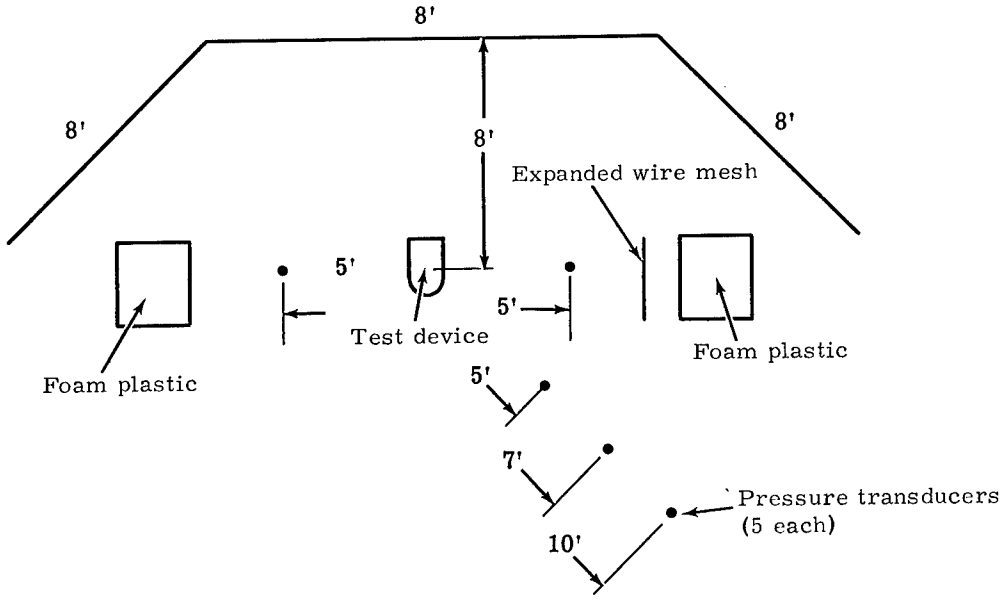

Top View

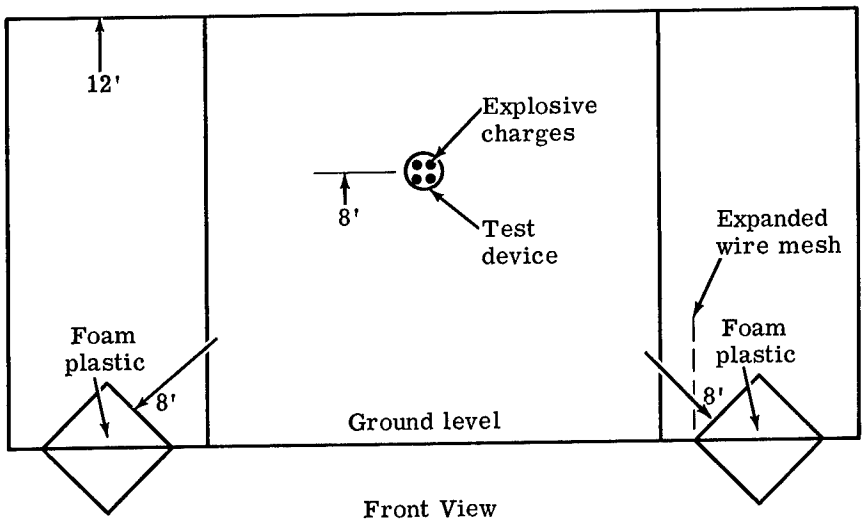

Front View

Figure 36. Physical Layout for Test 13A

The foam plastic particle catchers were used in Test 13A in an attempt to determine how much material was contained in the concentration observed in Figure 28. Figure 37 shows photographs of the backboard before and after Test 13A. This indicated that no debris, except for the simulated nozzle, traveled in a direction parallel to the longitudinal axis of the test device. Figure 38, which shows the foam plastic particle catchers after the destruct test, indicates a further change in the debris pattern. The centerline of the test device was aligned with the geometric center of the foam plastic particle collector. Figure 38 also shows that the expanded wire mesh was not effective for stopping the metal pieces and also that the debris did not follow a radial line but came out at a slight angle.

Figure 39 illustrates the debris pattern resulting from Test 13A when four explosive charges were used for the destruct system.

These two tests served to establish the need for a new approach to the instrumentation philosophy to be used in the full-scale destruct test.

Pressure from these tests ranged from 7 psi at 64 inches to 2.5 psi at 120 inches. The velocity of the jets, obtained from the photographic film, was about 380 feet per second.

Tests 14, 15, 18, 19, and 21 (Totally Contained, Class B Test) -- These tests were performed in a totally enclosed facility. Tests 14, 15, and 18 were performed in a 10-foot diameter steel pipe whose ends were covered with plywood. Figure 40 is a photograph of the steel pipe, showing the plywood end covering.

Test 19 was performed in a 30-foot diameter steel pipe and Test 21 was not fired.

Figure 41 is a photograph of the 30-foot diameter steel pipe facility. Again, the open end was closed with plywood providing a totally enclosed structure.

These four tests very successfully established the debris pattern and also enabled recovery of a mass balance of 88 percent graphite. This percentage is increased to about 90 when the data from air sampling are included.

Pressures observed during these tests were about 62 psi at 2 feet, 25 psi at 4 feet, and 8 psi at 6 feet.

Figure 42 is a photograph of the inside surfaces of the 10-foot diameter pipe showing the instrumentation used for air sampling and pressure.

Figure 43 is a photograph of the vacuum pumps and associated equipment used for air sampling.

Figure 44, a photograph of the 10-foot pipe after Test 15, shows the concentration of debris, both with respect to longitudinal distribution and to radial distribution.

Figure 45, a photograph of the debris impact resulting from the explosive destruct of a scale model device, illustrates the deviation from radial distribution caused by explosive burning. The black strip was aligned with the geometric centerline of the scale model device. From this picture, the angle can be calculated; the impact is about 6 inches offset and the distance from ground zero was 46 inches.

$$\alpha = \arctan \frac{6}{46} = 7.4^{\circ}$$

The above angle was used in the outside test setups and in preparation for the full-scale test.

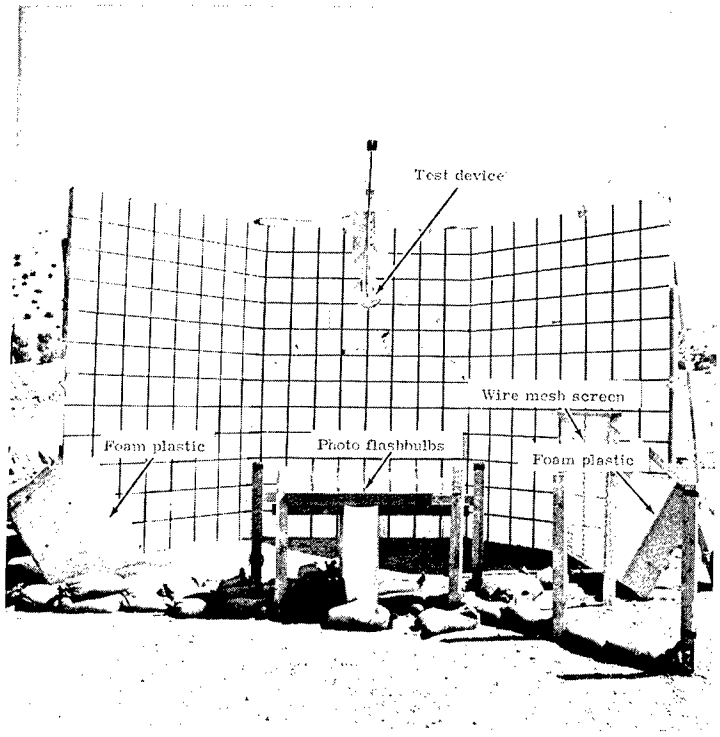

Before Test

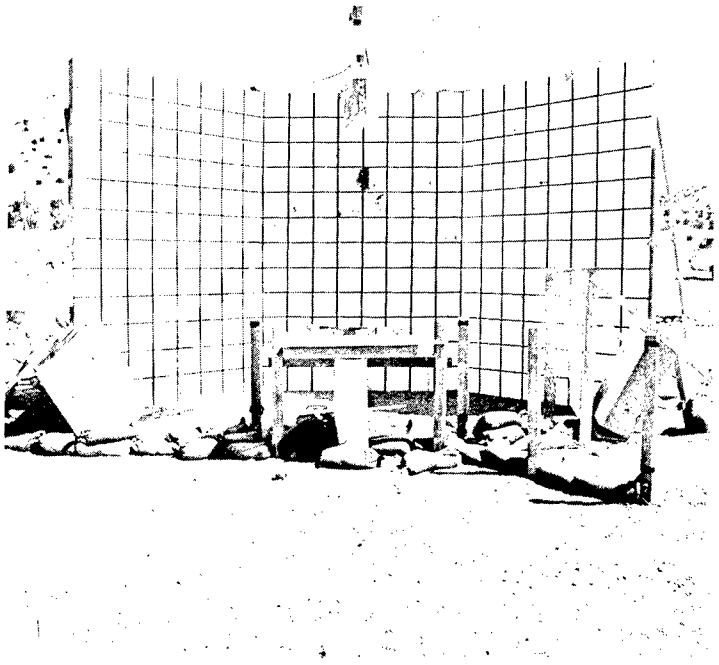

After Test

Figure 37. Test Backboard Before and After Test 13A

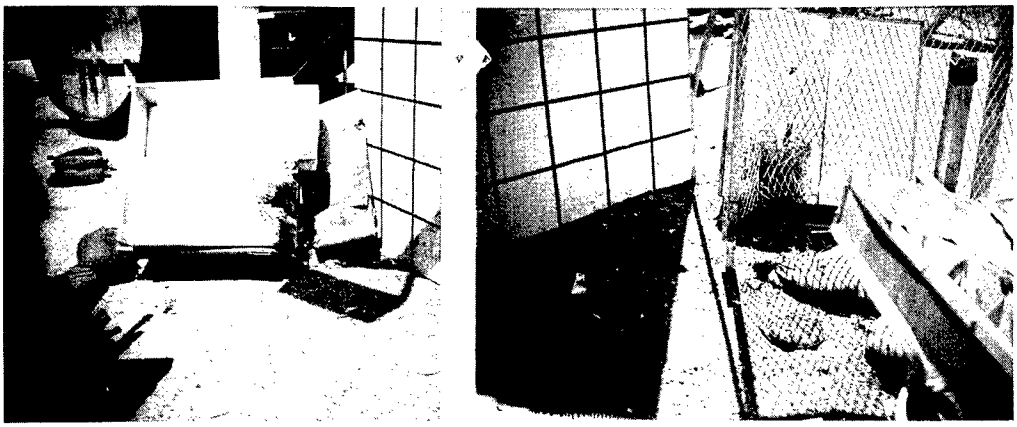

Figure 38. Debris Impact in Foam Plastic

Figure 39. Debris Pattern Resulting from the Destruct of a Scale Model Device

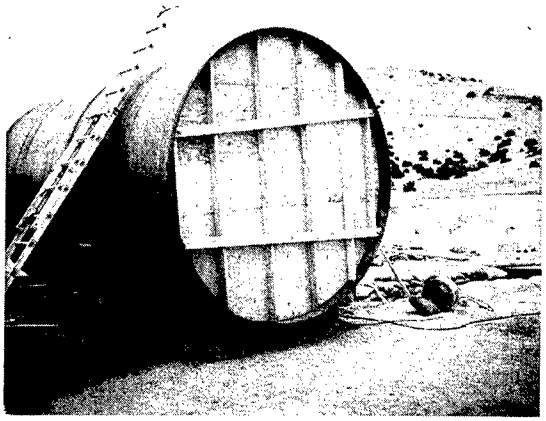

Figure 40. Ten-Foot Diameter Steel Pipe with Plywood End Covering

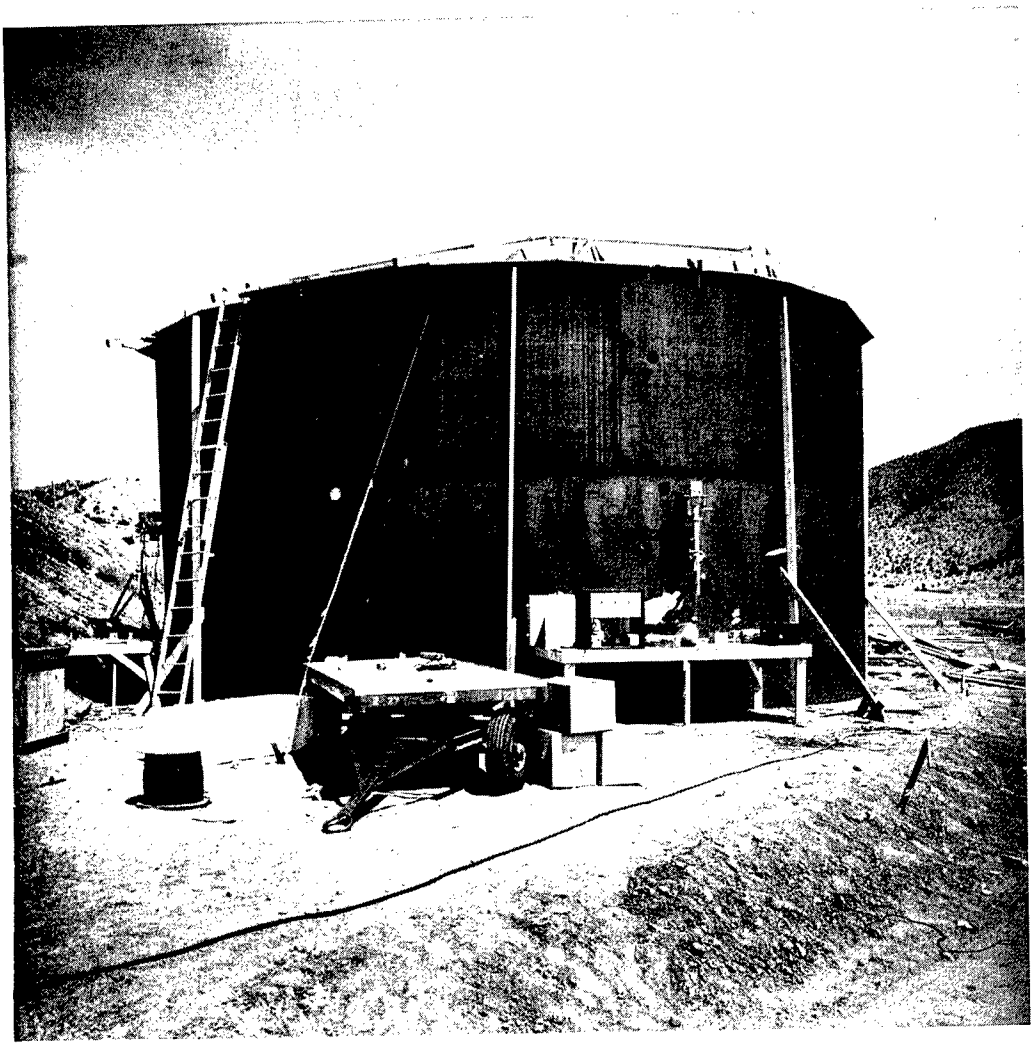

Figure 41. Thirty-Foot Diameter Steel Tank

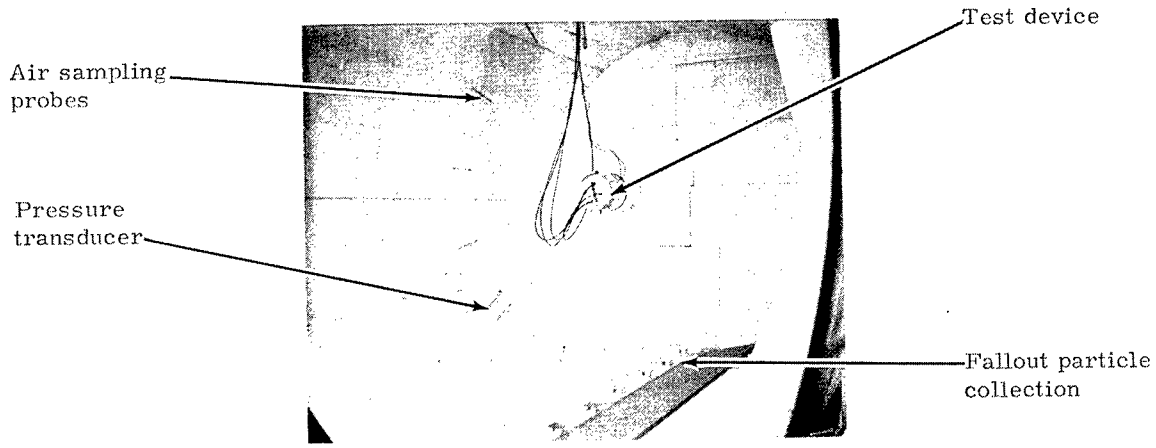

Figure 42. Instrumentation Inside the 10-Foot Diameter Pipe

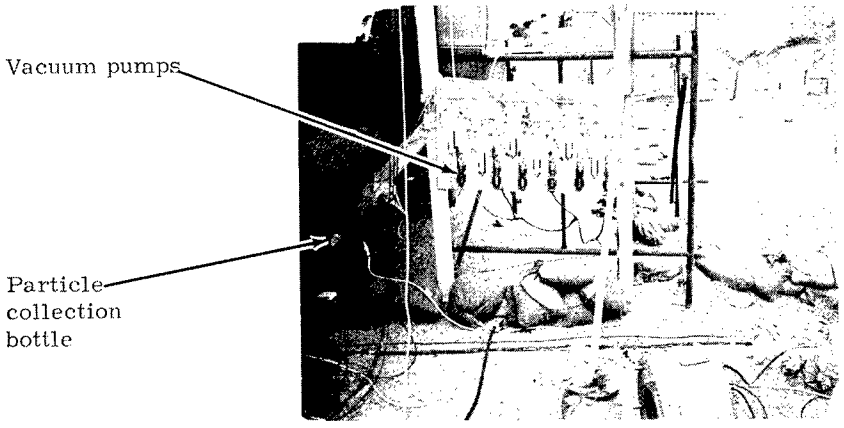

Figure 43. Air Sampling Pump Array Used With 10-Foot Diameter Steel Pipe

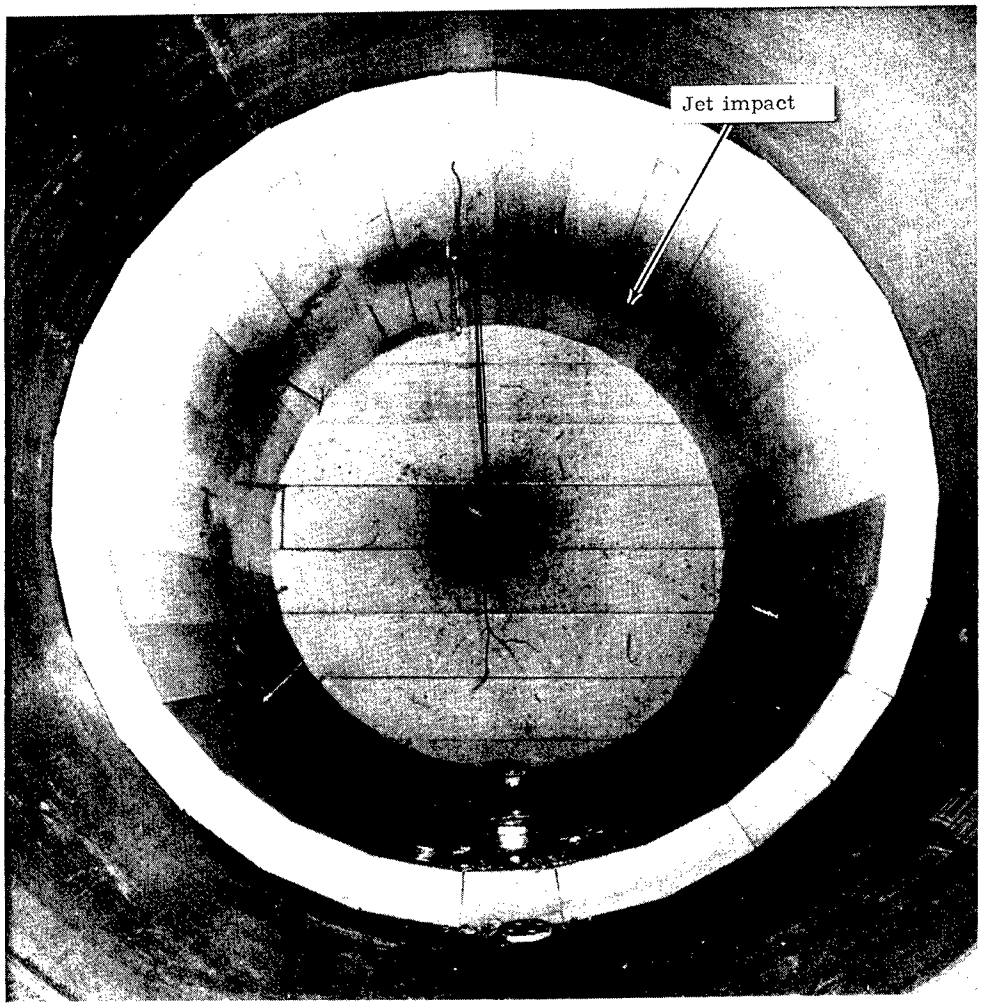

Figure 44. Debris Impact After Explosive Destruct of a Scale Model

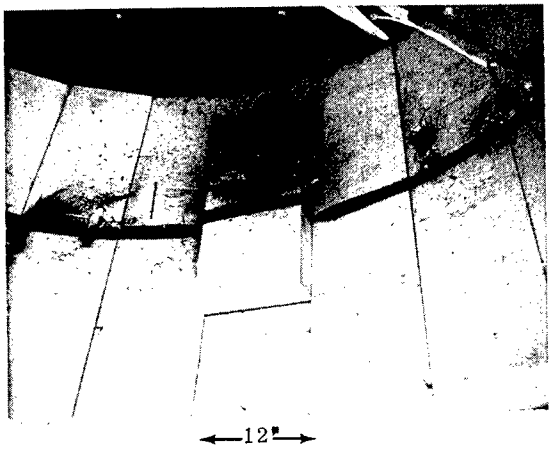

Figure 45. Jet Impact Showing Deviation Due to Explosive Propagation

Figure 46 shows the same type of debris pattern shown in Figure 45, but this test was performed in a 30-foot diameter steel pipe. Again the offset due to explosive propagation is shown, and the relative lack of debris between the jets is demonstrated.

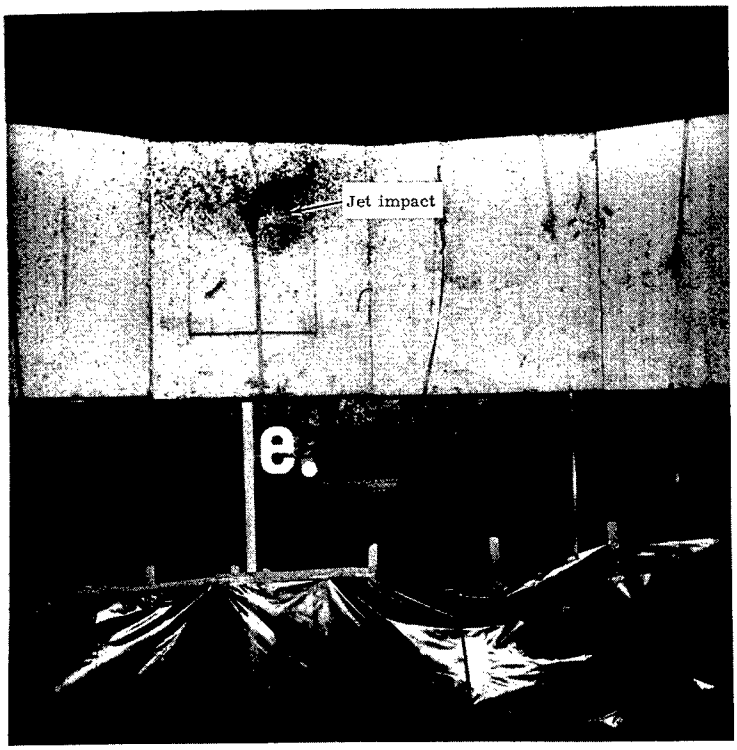

Figure 46. Debris Pattern After Explosive Destruct of a Scale Model in the 30-Foot Diameter Steel Pipe

Tests 16, 17, 20, 22, and 23 (Outside or "Swimming Pool", Class C Tests) -- These tests were fired in the outside facility referred to as the "swimming pool." Figure 47 shows the physical layout for this group of tests.

The primary purpose for these tests was the proof of principle for the coming full-scale destruct test. These tests also served to establish an optimum distance for rotating foam particle catchers and velocity devices. Further, it demonstrated that protection of the data collection devices was not feasible and that duplicate instrumentation should be used to assure the data collection.

From the standpoint of mass balance, these tests were not as valuable as the totally contained tests but did serve to demonstrate that a small sample will give a representative description of the particle sizes to be expected. The graphite collection techniques used were successful in obtaining debris samples which were 32 to 54 percent of the total graphite in the simulated core.

In addition to graphite particle collection using the fixed foam technique and the rotating foam velocity devices, air sampling devices, polyethylene sheet fallout particle collectors, pressure transducers, metal particle deflectors, and photographic data collectors were evaluated during the Class C tests.

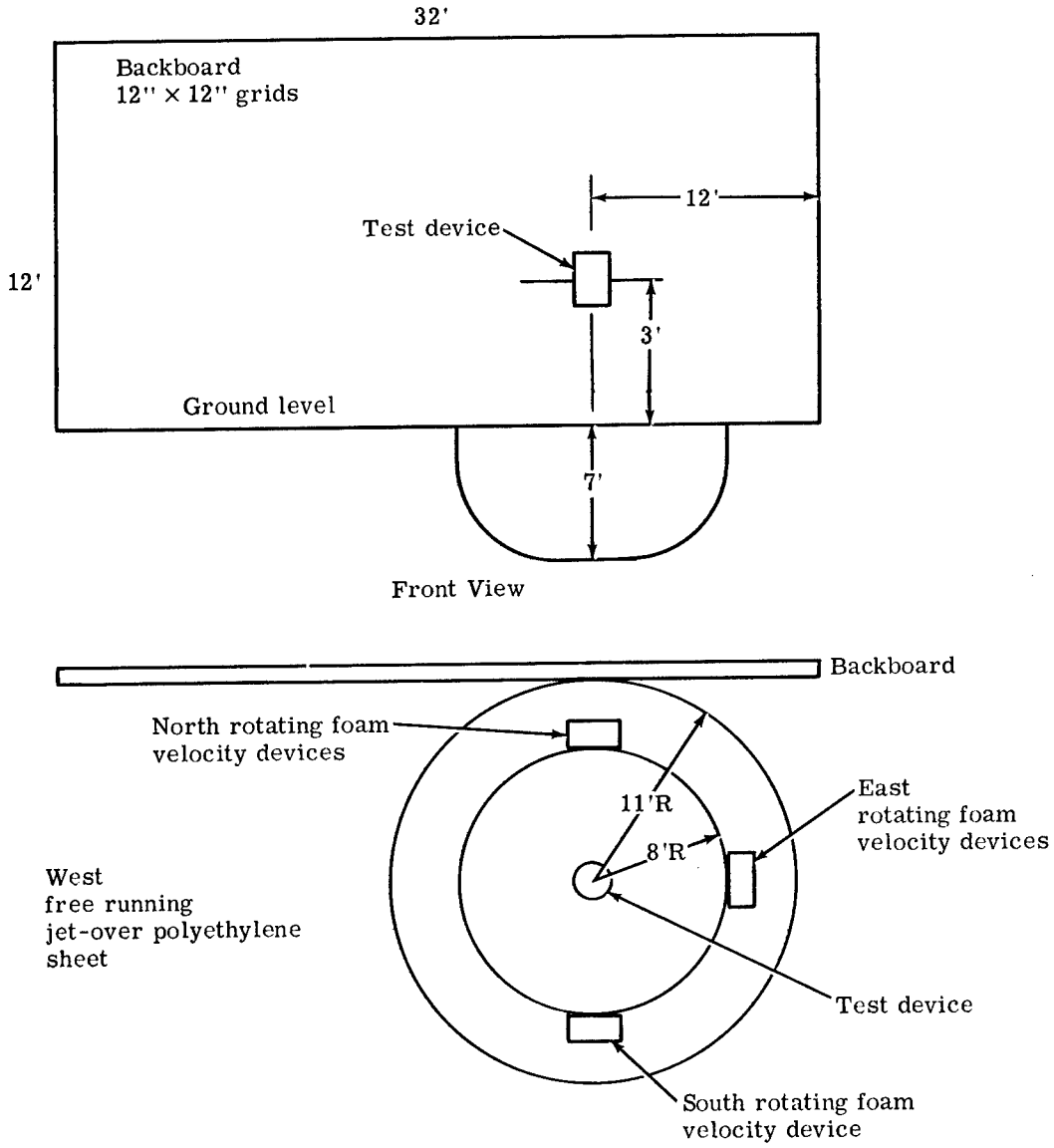

Figure 47. Physical Layout for Group 3 Class C Tests

Figure 48 shows the physical layout for Test 16 and illustrates the use of deflector structures. The use of a heavier expanded screen and the use of a 1 x 0.125-inch steel strap mounted on edge are shown. Figures 49 and 50 show the damage incurred and that this type of deflector is ineffective.

In Test 17, the physical layout used was the same as for Test 16, but, because one of the four explosive charges did not fire, the debris pattern was changed sufficiently to prevent any usable data collection. This test did demonstrate that to be assured of efficient core destruction (reduced to small particles) the four charges must be fired with reasonable simultaneity.

Figures 51 and 52 show the shifting of the debris pattern caused by the misfire.

The shaped charge effect observed in this test caused ejection of the fuel elements (which were about 2/3 of the full length used in the scale model).

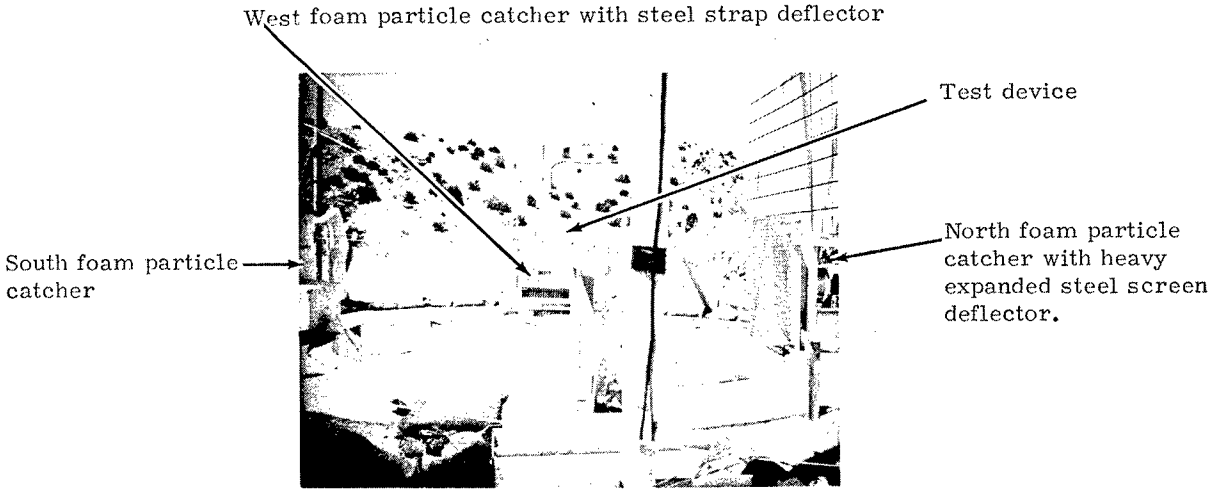

Figure 48. Physical Layout for Test 16

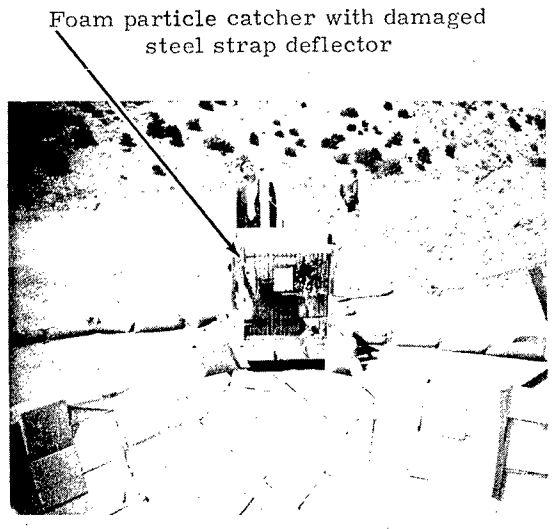

Figure 49. Damage to 1 x 0.125-inch Steel Strap Deflector

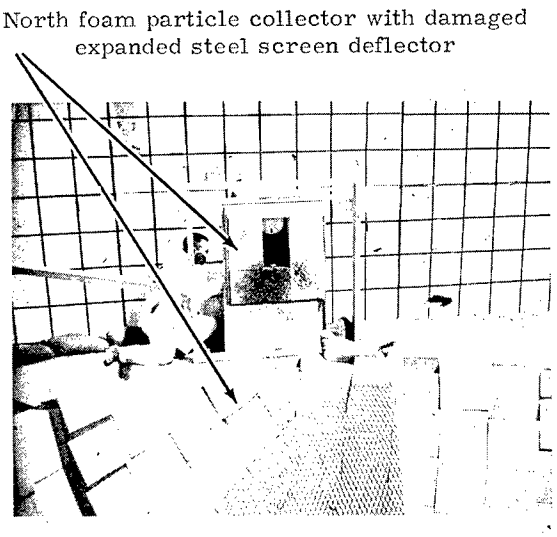

Figure 50. Foam Particle Catcher with Damaged Expanded Screen Deflector

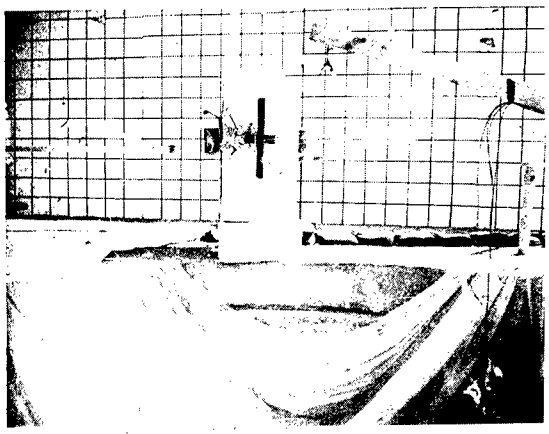

Figure 51. Test 17 Deflection on North Foam Catcher

Figure 52. Test 17 Debris Missed South Catcher

The final three tests were performed with a minimum of mishap and produced a high level of confidence in the data collection technique.

Test 22, which was prematurely fired, gave no camera coverage; however, all other systems functioned properly. Particle collection was good.

General Discussion of Group 3 Tests -- These tests served to define the full-scale physical layout, and they gave confidence in the instrumentation techniques to be used.

The tests established the debris size, shape, and pattern to be expected during the full-scale destruct test and provided the information necessary to the proper placement of instruments for data collection.

Finally, these tests provided data concerning the way graphite fuel elements break up during explosive destruct.

Test Results

The test program was successful in establishing techniques for collecting the debris resulting from the explosive destruct of a scale model ROVER/NERVA reactor. Furthermore, techniques were devised for the determination of debris spatial distribution and for measuring debris velocity as a function of particle size and mass. This information established the feasibility of conducting a full-scale explosive destruct test of a ROVER/NERVA space propulsion engine.

The following instrumentation and techniques would be required for the successful completion of a full-scale test:

1. Two-pound per cubic foot polystyrene foam is required for graphite particle collection and subsequent particle sizing and size distribution.

2. Rotating polystyrene foam particle collectors and velocity devices would be required for establishing the velocity, as a function of size, of graphite core material.

3. Pressure transducers would be required for establishing the overpressure as a function of distance from ground zero.

4. Air sampling would be required to establish the particle sizes which remain airborne and the quantity of material contained in the airborne cloud.

5. Photographic coverage would be required to establish the debris cloud shape and to document the destruct test.

These instrumentation devices and techniques for employment are verified by data contained in Appendixes C, D, and E.

The curves in Appendix C are plots of the weight percent of the total collected material by specific size ranges. Not all tests were fired for particle collection, and some tests are not plotted. The first curve shows the envelope which encompasses the extremes of the percentages and gives an idea of the spread among the tests.

The curves in Appendix D are plots of the accumulative weight percent that is collected in each size range. A curve is plotted for each test which was performed to collect graphite particles, and the first curve is an envelope which encompasses all test data.

The curves in Appendix E are plots of representative velocities of the graphite particles. These velocities were obtained from the photographic film taken during the development destruct tests.

Timing marks were not placed on some of the film, and therefore velocity data could not be determined from those tests.

A complete tabulation of the data used to complete the curves in Appendices C and D are contained in "Development Report on the Rover Destruct Tests" (SC-DC-65-1758). Also contained in this report are more refined data and linear plots of the data that appears on semi-log paper in this report.

APPENDIX A

COMPOSITE OF DEVELOPMENT TEST DATA

Test No.	Graphite weight (grams)	Explosive weight (grams)	Pressure (psi)	Polystyrene foam area (in^2)	Percent of total material available collected	Theoretical weight collected (grams) Cylindrical model	Theoretical weight collected (grams) Spherical model	Actual weight collected (grams)	Percent efficiency of collection Spherical model	Percent efficiency of collection Cylindrical model
1	2258.79 Hung Horizontal	102 - Comp C4	2.6 @ 3 ft					No recovery		
2	2268.96 Hung Horizontal	102 - Comp C4	1.4 @ 3 ft							
South 3'				144		72.2	20.33	———		
North 3'				144		72.2	20.33	49.9	245.8	70
Ground 3'				256		128.3	36.14	89.4	248.3	70
3	2250.18	76.5 Comp C4	No data							Cylindrical Model
0-2 Ground				256		129.8		106.33		81.9
1-2 SW	Hung Horizontal	al Sleeve		256		———		7.14		———
(all 3') 2-2 South		49.2 grams		256		129.8		109.54		84.4
3-2 SE				256		———		.70		———
1-4 NW				144		———		7.49		———
2-4 North				144		72.9		49.65		68.0
3-4 NE				144		———		.78		———
4	2240.31	75.9 Comp C4	1.1 @ 3.5'							
0-2 Ground	Hung Horizontal	al Sleeve		256		129.3		102.8		79.5
1-2 SW				256		———		4.0		———
(all 3') 2-2 South		48.8 grams		256		129.3		105.5		81.6
3-2 SE				256		———		4.2		———
1-4 NW				144		———		3.4		———
2-4 North				144		72.6		55.1		75.9
3-4 NE				144		———		6.0		———
5	2257.74 Hung Horizontal	69.22 Comp C4	0.9 @ 3.5'					No recovery		
6	2240.84	75.9 Comp C4	0.8 @ 3.9'							
4#/ft^3 4'	Hung Horizontal			144		40.50		16.92		41.8
4#/ft^3 8'				144		13.05		10.16		77.8
2#/ft^3 10'				256		15.38		12.89		83.8
7	2261.96 Hung Horizontal	68.4 Comp C4 al Sleeve 52.4	0.9 @ 4.0'	144		45.16		42.64		94.5
				144 greased face		45.16		38.17		84.6
8	2260.2	67.84 Comp C4 al Sleeve 52.16	1.1 @ 4.0'	288		90.26		74.14		82.2
9	2268.0	67.9 Comp C4 52.3 al Sleeve	0.8 @ 4.0'	432		92.35		87.89		95.2
10	2247.2	70.25 Comp C4 52.35 al Sleeve	0.7 @ 2.0'	1512*		*1-59.3	5-71.0	*1-42.7	5-82.0	*1-72.0 5-115
						2-64.5	6-70.1	2-43.8	6-46.1	2-68.0 6- 65
						3-67.6	7-67.6	3-41.9	7-34.7	3-62.0 7- 51
						4-70.1	8-64.5	4-50.0	8-36.0	4-71.3 8- 55
							9-59.3		9-27.9	9- 47
11	2255.7 External al Sleeve	69.4 Comp C4 52.5 al Sleeve	1.3 @ 4.0'	1512*		*1-59.5	5-71.3	*1-50.3	5-64.3	*1-84.5 5- 90
						2-64.7	6-70.4	2-43.1	6-58.0	2-66.6 6- 82
						3-67.9	7-67.9	3-41.7	7-39.2	3-61.3 7- 57
						4-70.4	8-64.7	4-39.5	8-25.3	4-56.1 8- 39
							9-59.5		9-24.6	9- 41
12	2253.2 External al Sleeve	68.65 Comp C4 52.35 al Sleeve	2.0 @ 22.0' 1.0 @ 46.0'			Same as 236-11		Collected material was not processed		None
13	Not recorded	TNT 230 grams	15 @ 4' 7 @ 5'4" 3 @ 7'6" 2.5 @ 10'	None		NA		NA		NA
13A	6397.5	TNT 230 grams	17 @ 4' 6.5 @ 6' 4.0 @ 8' 3.0 @ 10'	3200		NA		Debris missed collectors No data		NA
14 Pipe 10'	6512	DATB 220 grams	12 @ 4'	Totally contained	100.	6512		6537.57		NA
15 Pipe 10'	6602	DATB 220 grams	65 @ 2' 30 @ 4' 8 @ 6'	Totally contained	100.	6602		6636.30		NA
16	6751.5	DATB 220 grams	12 @ 4' 5 @ 8' 3 @ 12'	NA	53.9	NA		3641.6		NA
17	6810	DATB 220 grams	No data	NA		NA		No recovery		NA
18 Pipe 10'	6696.5	DATB 220 grams	60 @ 2' 22 @ 4' 7.5 @ 6'	Totally contained	87.4	6696.5		5847		NA
19 Pipe 30'	6537.6	DATB 220 grams	No data	Totally contained	88.1	6537.6		5757.4		NA
20	6810	DATB 220 grams	40 @ 3' 6 @ 6' 3.5 @ 3.5'	NA	42.5	NA		2891.6		NA
22	6537.6	DATB 220 grams	No data	NA	50.6	NA		3328.3		NA
23	6673.8	DATB 220 grams	No data	NA	31.7	NA		2113.2		NA

NA = Not Available

*This test area is divided into equal parts for particle evaluation.

mposite of Development Test Data

Time of arrival gage	Photographic	Rotating disc particle collector and velocity device (in/ms)	Rotating drum particle collector and velocity device (in/ms)	Wire mesh velocity device (in/ms)	Vibration sensor (in/ms)	Air Sampling: Number of particles	Air Sampling: Size and percentage	Fallout particle collectors	Remarks
	Good no timing								
	Good no timing								
Damaged from impact	Good no timing								
NA	Good no timing								
Malfunc-tioned	Very good								
Malfunc-tioned	Too much light no coverage								
No data	Good no timing	15.7 to 19.5 @ 4 ft	No zero time	6.4 @ 50 in. 10.5 @ 104 in.					
NA	Good no timing	No fiducial mark	No zero time	12.8 @ 36 in. 10.4 @ 51 in. 11.2 @ 42 in. 8.5 @ 69 in.					
NA	Very good	9.2—>11.9 @ 5 ft	No zero time	14.1 @ 30 in. 11.0 @ 48 in. 12.3 @ 36 in. 10.9 @ 54 in. 11.7 @ 42 in. 11.4 @ 60 in.					
9.4 i 11.6 in/ ms @ 70"	Flash bulbs early - no coverage	8.2—>11.5 in/ms @ 89 in.	8.7—>10.9 in/ms @ 84 in.	12.3 @ 30 in. 12.3 @ 36 in. 11.9 @ 48 in. 12 @ 54 in. 11.5 @ 60 in. 11.2 @ 66 in.					
NA	Good	86—>13.8 in/ms @ 60 in.	No zero time	Good response no zero time	No data				
NA	Good	7.3—>10.34 @ 60 in	No zero time		16.1 @ 32 in. 15.7 @ 41 in. 15.2 @ 52 in.				
NA	Very good	None used	None used		No further use in test				
NA	Very good no timing	None used	None used			No data			
NA	No coverage	10 foot diameter pipe	10 foot diameter pipe			No data		Poor data	
NA	No coverage	10 foot diameter pipe	10 foot diameter pipe			7.09×10^{12} to 1.12×10^{13} particles/ft^3	.5—>3μ 66.2% 3—>10μ 30% 10—>20μ 3.7% < 20μ .26%	.5—>3 57.5% 3—>10 33% 10—>20 8.5% < 20 1.0%	
No data	Good no timing	Timing paper lost on one disc	No data			7.54×10^{7} to 1.19×10^{9} particles/ft^3	.5—>3 67% 3—>10 29.2% 10—>20 3.8%	Windshift No data	
NA	Helicopter coverage good	No data	No data			No data		40' x 100' plastic along west jet - No data	Only 3 charges fired. Foam plastic particle collectors were not evaluated - No particle data from this test.
NA	No coverage	10 foot diameter pipe	10 foot diameter pipe			9.67×10^{9} to 21.8×10^{9} particles/ft^3	.5—>3 79.2% 3—>10 20.7% 10—>20 2.3% < 20	Not analyzed	
NA	Too much light washed out film	30 foot diameter pipe	30 foot diameter pipe			2.52% < 20μ 1.88% < 20μ	Sample collected in 5 min. after firing	None used	
No data	Good	No data	No data			No data		40' x 100' plastic along west jet	
No data	4 seconds premature no coverage	No zero time	No zero time			No data		None used	Firing occurred 4 seconds early
No data	Very good	No zero time	No zero time			No data		40' x 100' plastic under west jet	

APPENDIX B

TEST PLAN FOR ROVER POSTOPERATIONAL DESTRUCT SYSTEM INSTRUMENTATION TESTS

TEST PLAN FOR ROVER POSTOPERATIONAL DESTRUCT SYSTEM INSTRUMENTATION TESTS

Introduction

The design agency for the ROVER propulsion reactor has developed a destruct system which utilizes four explosive missiles injected into each quadrant of the reactor after mission completion. This system has been proved to effectively destroy the reactor but the size, distribution and velocity of the resulting particles are unknown. Further, Westinghouse Astronuclear Laboratory has developed a computer code called "Foot-print" which will give the distribution of particles on the earth's surface providing the size, distribution, and velocity are known at the time of beginning re-entry into the atmosphere.

The fact becomes readily apparent that in order to assess the safety of using the ROVER reactor in space one must be able to have quantitative data concerning the size, distribution, and velocity of particles resulting from a destroyed ROVER reactor.

Sandia Corporation has been requested to instrument all or part of a full-scale ROVER reactor test scheduled for the first week in May 1965. High quality data must be obtained from this test to support a request for reinstating the Reactor In Flight Test program (RIFT).

Data Requirements

The data requirements for the reactor destruct program are rather extensive and must be collected under adverse test conditions. The requirements as listed by the Space Nuclear Propulsion Office (SNPO) of the AEC are as follows:

1. Dynamics of the Destruct Event

   a. Velocity of fragments of core, reflector, and pressure vessel as functions of fragment size and time.

   b. Angular distribution of fragments of core, reflector, and pressure vessel as functions of fragment size and time.

   c. Reconstruction of geometry of debris pattern of test as a function of time on a triaxial coordinate system.

   d. Extrapolation of geometry of c above to vacuum destruct condition on triaxial coordinate system.

2. Particle Size Distribution

   a. Quantitative determination of particle size distribution of fuel fragments in sufficient detail to construct distribution curve with good level of confidence.

   b. Sampling fuel in metric system at points 30, 20, 10, 5, 1 mm and at 750, 500, 250, 100, 50, 1μ.

   c. Classifying fuel as to angularity, sphericity, 1/d, surface area, and density. (Fragment characterization).

   d. Qualitative determination of fragment size distribution of other engine components.

Starting at the end and progressing upward, the data required in item No. 2 is after-the-fact analysis of the particles collected during the destruct test.

Item 1d is a mathematical analysis of the data obtained in 1c.

Items 1a, 1b, and 1c are the areas where experimental data must be collected and that data reduced to produce usable criteria which can be inserted into the "Footprint" computer program.

Again starting at the end, the data required in item 1c probably can be obtained with a combination of high speed photography and data obtained from foam collectors (rotating and fixed foam collectors). Judicious placement of cameras and collectors and using at least 100 percent duplication will produce data from which the debris pattern can be reconstructed.

Item 1a and item 1b will be discussed together as the needed data and techniques being evaluated are interrelated. The particle size, velocity, and distribution will be obtained with the use of catcher devices covered with polystyrene foam and with electronic measuring equipment.

The techniques outlined above will theoretically produce data but these techniques must be tested and proved to be functional under the adverse conditions of an explosion environment.

Proof Tests

There are three series of tests

1. Instrumentation Evaluation Tests
2. Mass Balance Evaluation Tests
3. Proof of Principle Tests

which are expected to produce results that will be used in the design and location of instrumentation for the full scale destruct test.

1. Instrumentation Evaluation Tests -- These tests are numbered 7 through 12 and Sled 1 through 6. Each test is expected to yield data that will allow a better collection of data in the next test.

   Test 7

   Configuration - 4" diameter by 7" graphite cylinder suspended horizontally, all instrumentation at 4-foot radius, collection device faces normal to a line from ground zero to geometric center of device, rotating cylinder device axis parallel to graphite axis.

   Purpose - Evaluation of collection devices, velocity devices, and debris cloud shape and lighting for photography.

   Test 8

   Repeat 7 except graphite cylinder will be suspended vertically, the rotating cylinder axis will remain horizontal.

   Purpose - Same as 7 but with the addition of evaluation for repeatibility of the instrumentation to procure data.

   Test 9

   Repeat 8 except the rotating cylinder axis will be rotated to become parallel with the graphite axis.

   Purpose - Same as 8.

Test 10

Repeat the test above which appeared to give the most usable data, using refined techniques of particle collection, velocity measurement, and particle distribution.

Test 11 and Test 12

These two tests are the last of this series and are intended to give proof of principle before beginning the implementation of full-scale test hardware.

Sled 1 and Sled 2

Configuration - The foam will be attached to the leading surface of the sled; graphite particles will be dropped in front of the sled which is moving at 750 feet per second. These individual hoppers containing 0.093-inch diameter, 0.185-inch diameter, and 1/2-inch diameter graphite particles, respectively, will be used.

Purpose - To determine the depth of penetration as a function of particle size and velocity. Also, the foam will be analyzed to determine the percentage of secondary fracture of the graphite particles. Two sleds are being run to assure reproducible results.

Sled 3 and Sled 4

Configuration - Same as Sled 1 and Sled 2 except sled velocity will be 1125 feet per second.

Purpose - Same as Sled 1 and Sled 2.

Sled 5 and Sled 6

Configuration - Same as previous tests except sled velocity will be 1500 feet per second.

Purpose - Same as for previous tests.

At the conclusion of this series of evaluation tests, the results will be analyzed in detail, and design, fabrication, and test configuration will be selected for the full-scale test instrumentation.

2. Mass Balance Evaluation Tests

This series of tests is numbered 13 through 15 and is expected to establish the expected debris pattern and what percentage of complete containment of particles is necessary to give reliable data acquisition.

Test 13

Configuration - The ROVER reactor will be simulated with a 1/6 linear scaled model consisting of a solid graphite core, solid bar reflectors, a simulated pressure vessel, and using four volume scaled explosive charges (properly located). It will be suspended either horizontally or vertically as established by previous tests. Particle collectors, velocity measuring devices, and cameras will be placed at the appropriate distances to simulate full-scale test conditions.

Purpose - To observe debris cloud and to further evaluate instrumentation.

Test 14 and Test 15

Configuration - A 10-foot diameter by 15-foot long steel pipe will be completely lined with polystyrene foam, including the ends. A 1/6 scale model ROVER reactor will be suspended horizontally in the geometric center. Air outlets will be left at the top on both ends and over these outlets will be positioned air filters and air samplers.

Purpose - To obtain the particulate impact pattern in foam, to obtain sizes of particles which are airborne, and to allow a complete mass balance analysis. Further, to establish what percentage of collection area less than complete containment will be acceptable for full-scale testing.

3. Proof of Principle Tests

This series of tests numbered 16 through 20 are the final evaluation of the instrumentation, the instrumentation layout, and any special techniques established by previous tests. The full-scale test will be duplicated as nearly as possible using the 1/6 scale model ROVER reactor configuration.

Purpose - To establish that the instrumentation and location of instrumentation selected for the full-scale test will in fact produce the data required by the Space Nuclear Propulsion Office of the AEC. Five tests are being performed to give a reasonable confidence in success of data gathering.

Data Reduction

The data produced in this test series will come in the usual forms of magnetic tape and photographic film, but also will be collected by penetration into low density foam plastic. Each collecting media will be treated separately to produce the maximum quantity of useful information.

1. Fixed Foam Particle Collectors

The sequence of data reduction will be as follows:

a. X-ray the blocks perpendicular to the path of particle entry to get the average penetration depth of particles and size if possible.

b. Dissolve the blocks in trichloroethylene and recover all graphite particles. Centrifuge, evaporate, or filter the solution to assure collection of the extremely small particles.

c. Weigh the total graphite collected.

d. Separate the particles by screening into at least 10 sizes and no more than 20 sizes. Weigh each size category.

e. Classify each size category as to angularity, sphericity, 1/d, surface area, and density.

2. Rotating Foam Particle Collectors

The sequence of data reduction will be as follows:

a. Measure the arc distance from the fiducial mark to the first particles and to the last particles.

b. Using a random sampling technique, measure the angle of entry into the foam with respect to a radial line.

c. At the same time b above is performed, measure the depth of penetration of the particle.

d. Dissolve that portion of the cylinder plus sufficient excess at the trailing end to account for angle of entry of particles and recover all graphite particles. Centrifuge, evaporate, or filter the solution to assure collection of the extremely small particles.

e. Weigh the particles.

f. Separate the particles by screening into at least 10 sizes and no more than 20 sizes. Weigh each size category.

g. Classify each size category as to angularity, sphericity, 1/d, surface area, and density.

3. Sled Test Foam Particle Collectors

a. X-ray each block perpendicular to the path of particle entry to get the average depth of penetration of particles.

b. Slice each block in half from top to bottom as established by the position on the sled. Each block will be marked "top."

c. Dissolve one-half of each block and recover all graphite particles.

d. Weigh the total graphite collected.

e. Separate the particles by screening into five categories when starting with No. 8 particles, six categories when starting with No. 4 particles, and eight categories when starting with 1/2-inch particles. In all three cases use the same sizes for the smaller sizes.

f. Weigh each size category.

g. Using the other one-half block and starting from the rear surface, slice the block into 1/4-inch slices.

h. Examine each slice for penetration of particles and record the size and number until single particles are not distinguishable.

4. Magnetic Tape

Start all reduction from the time of the fiducial pulse.

a. Determine the rpm of rotating foam particle collectors.

b. Determine shock wave velocity.

c. Determine debris cloud velocity from the wire mesh gages.

d. Determine the debris cloud velocity from the photoelectric gages.

e. Determine the debris cloud time of arrival from the strain gage.

f. Determine time of arrival and overpressure associated with the shock wave and the debris cloud.

5. Photographic Film

Determine the velocity of the leading edge of the debris cloud and also the trailing edge if the trailing edge is distinguishable.

The urgency of this program and the need for immediate evaluation of data makes it necessary to request that magnetic tape and photographic film data reduction be completed 2 days after the test date.

APPENDIX C

ROVER/NERVA DEVELOPMENT DESTRUCT
(Particle Size versus Weight Percent)

The curves in this appendix show the percentage-by-weight of the total weight of material collected plotted against screen sizes. Also shown is the composite (maximum-minimum) curve for groups of tests which were performed on the same test configuration. These data are again plotted as weight percent against the screen size.

A solid graphite cylinder 4 inches in diameter by 7 inches in length was used for Tests 3 through 11. The 1/6 scale model test vessel was used for the remaining tests.

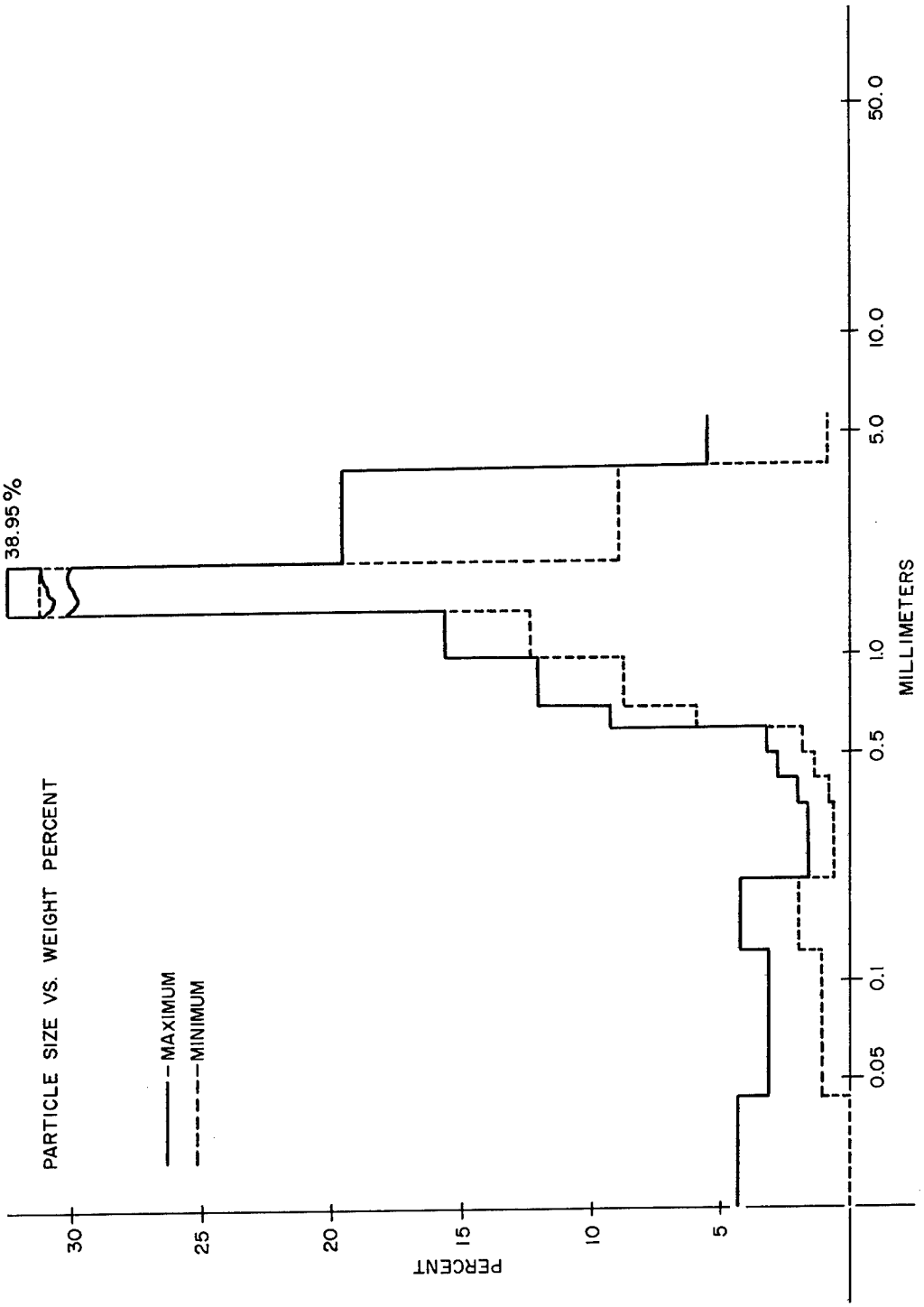

Figure C-1. Maximum-Minimum Curves for Tests 3, 6, 7, 8, 9, 10, and 11

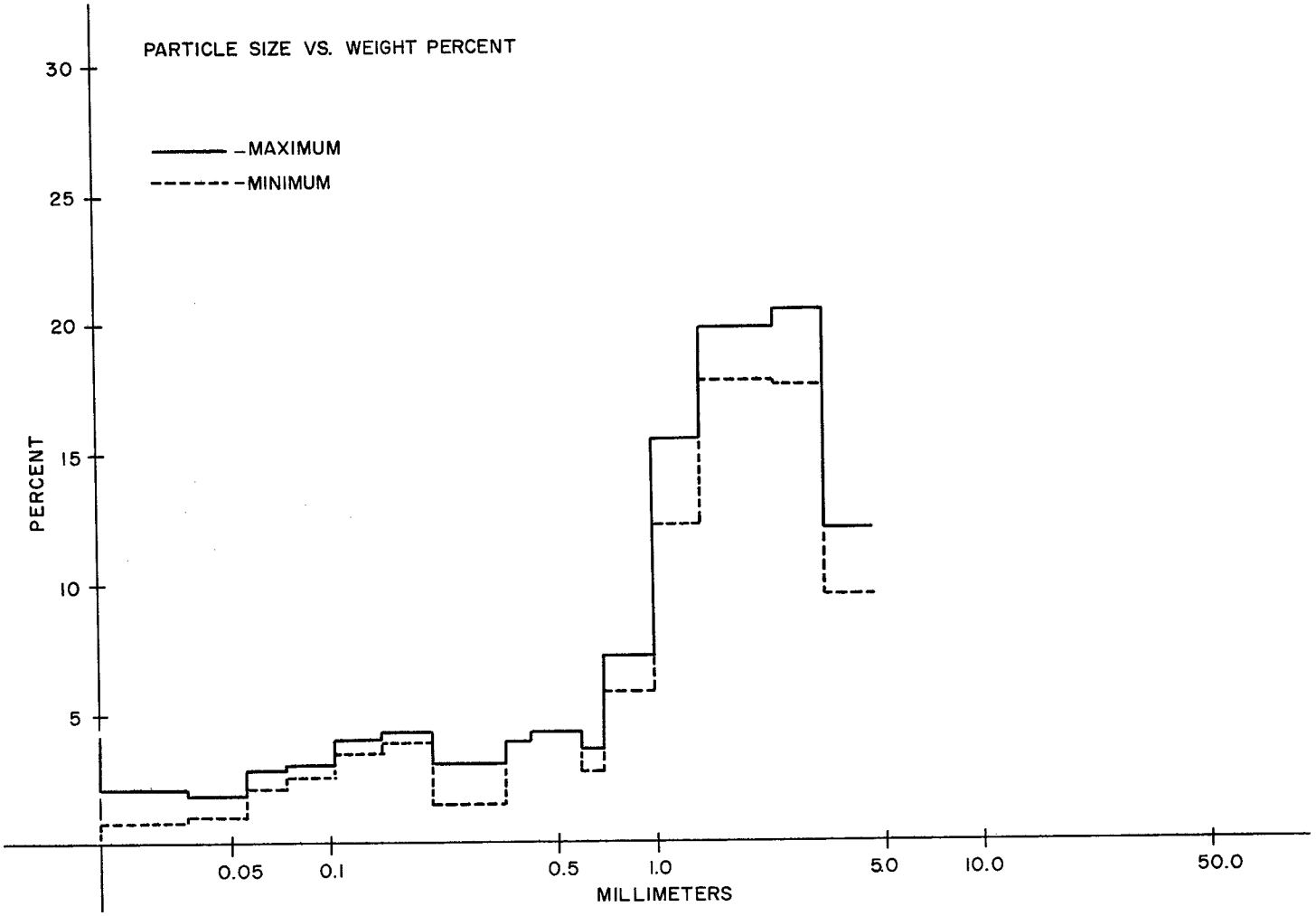

Figure C-2. Maximum-Minimum Curves for Tests 14, 15, 18, and 19

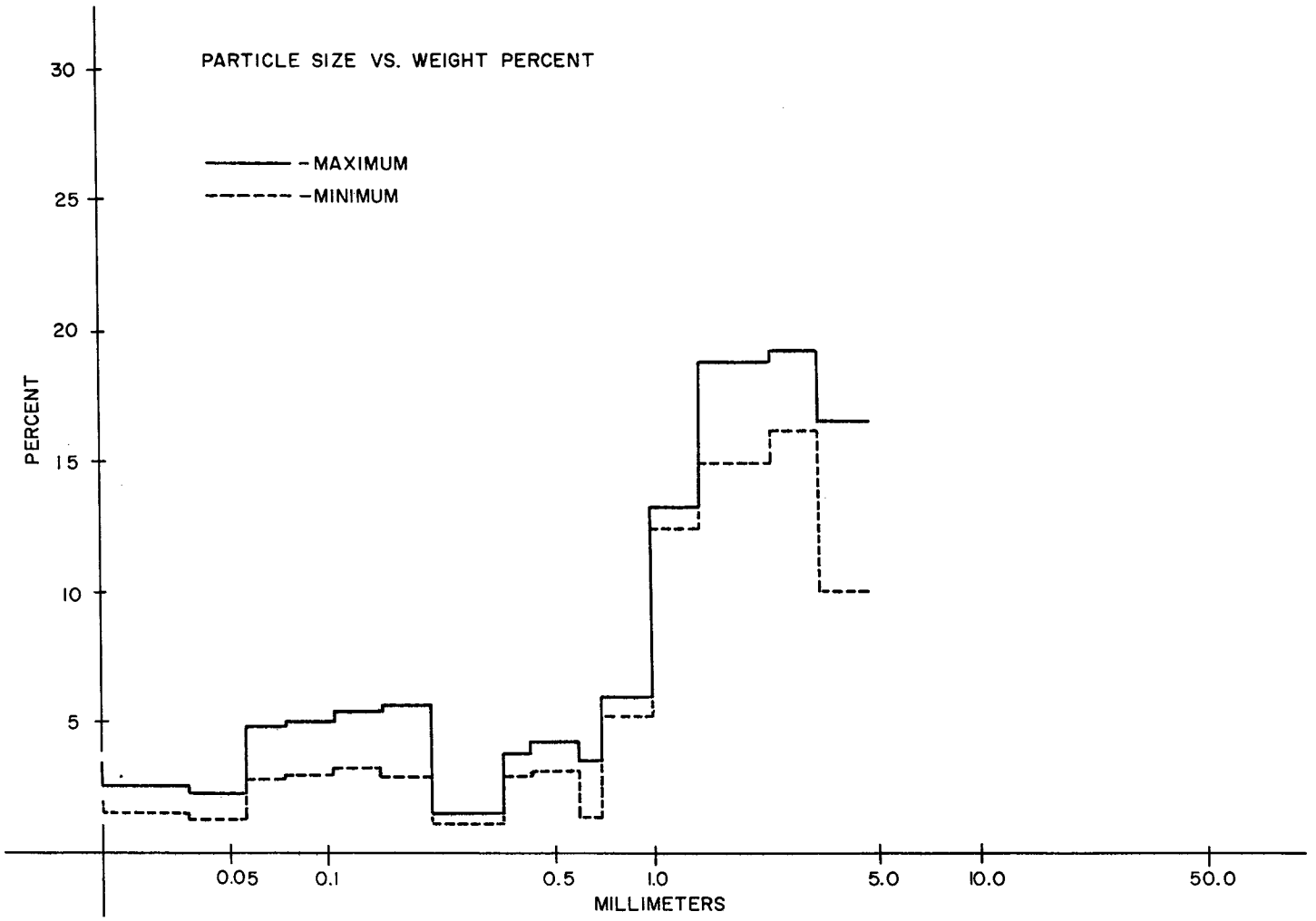

Figure C-3. Maximum-Minimum Curves for Tests 16, 20, 22, and 23

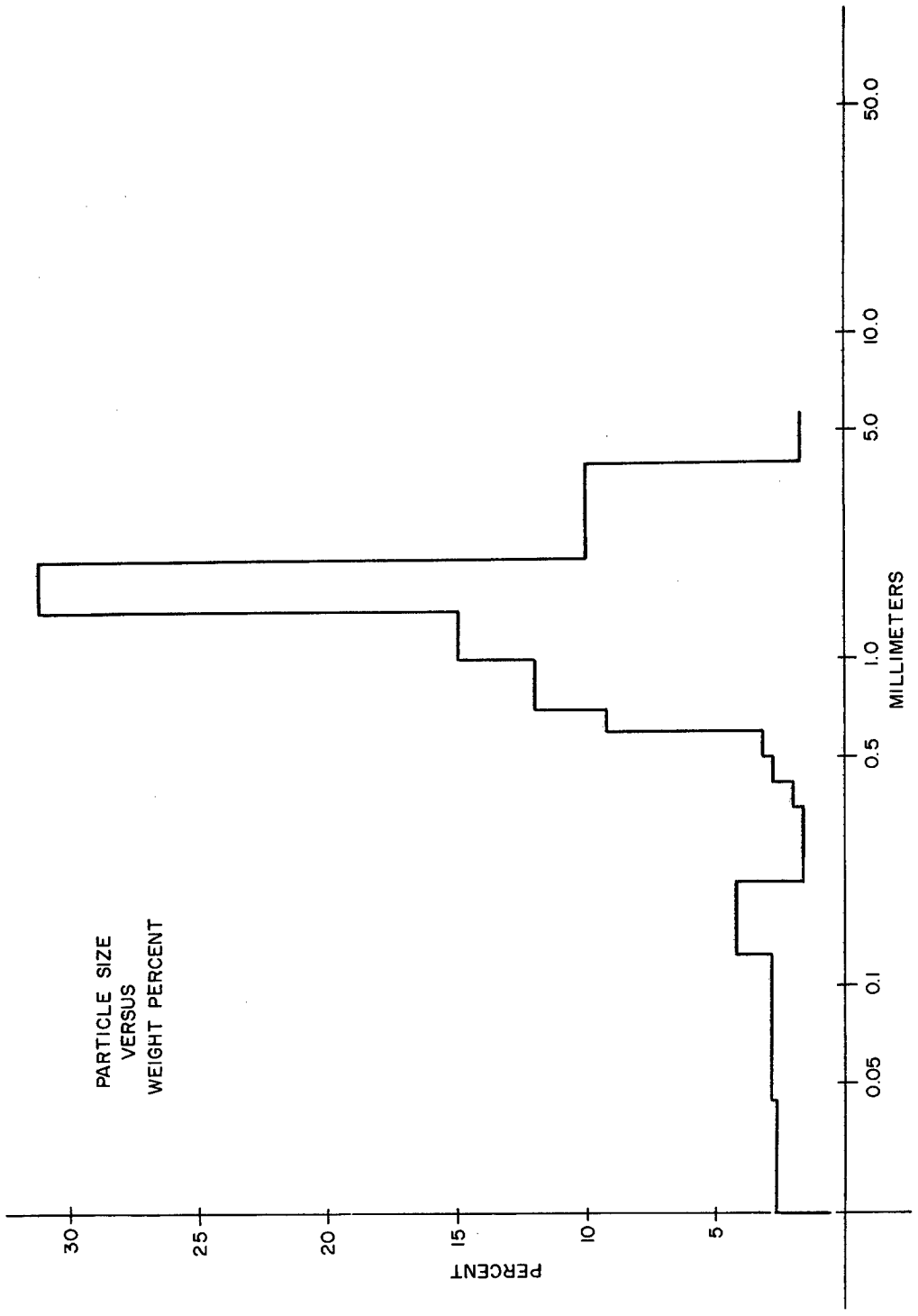

Figure C-4. Test 3

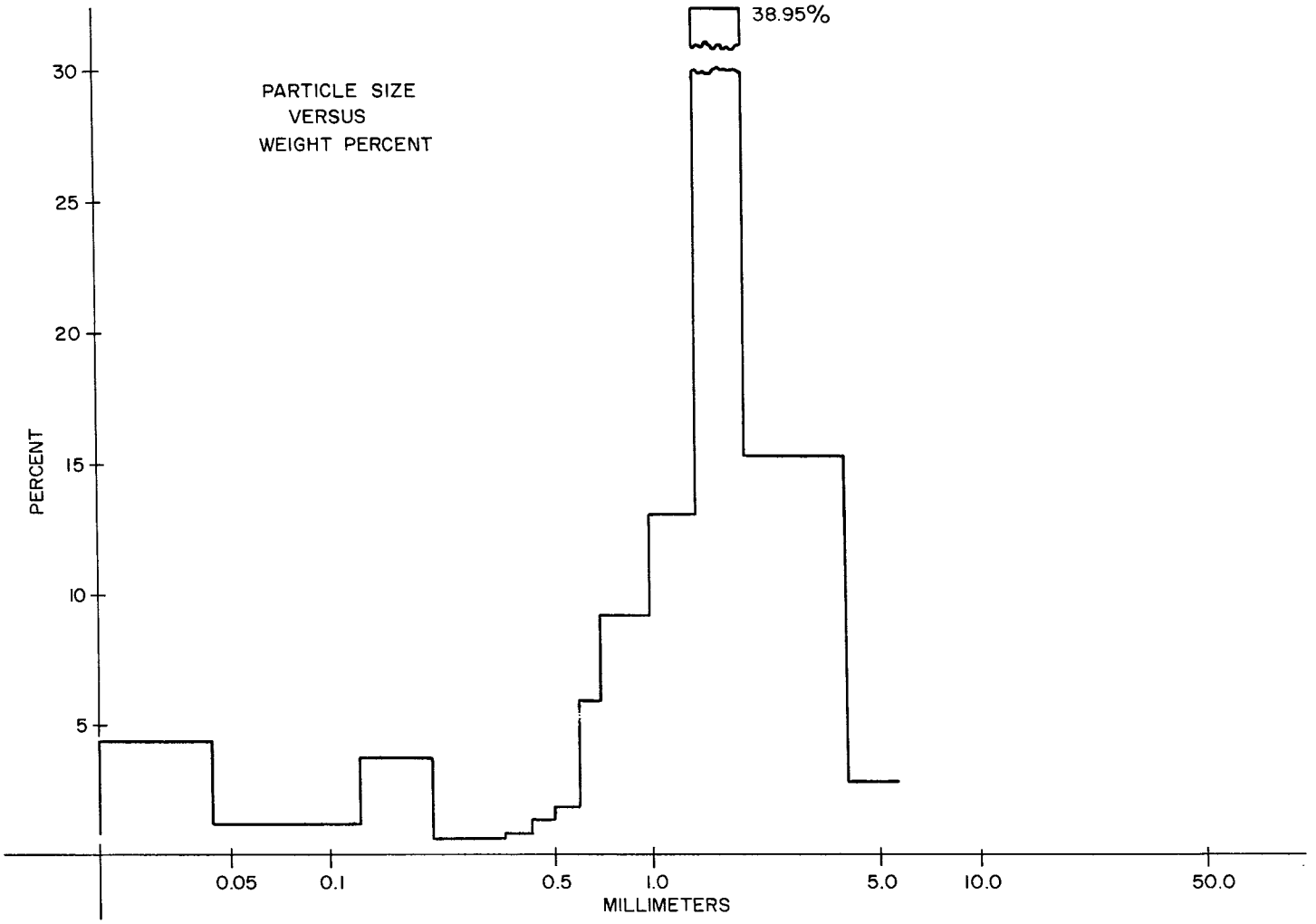

Figure C-5. Test 6

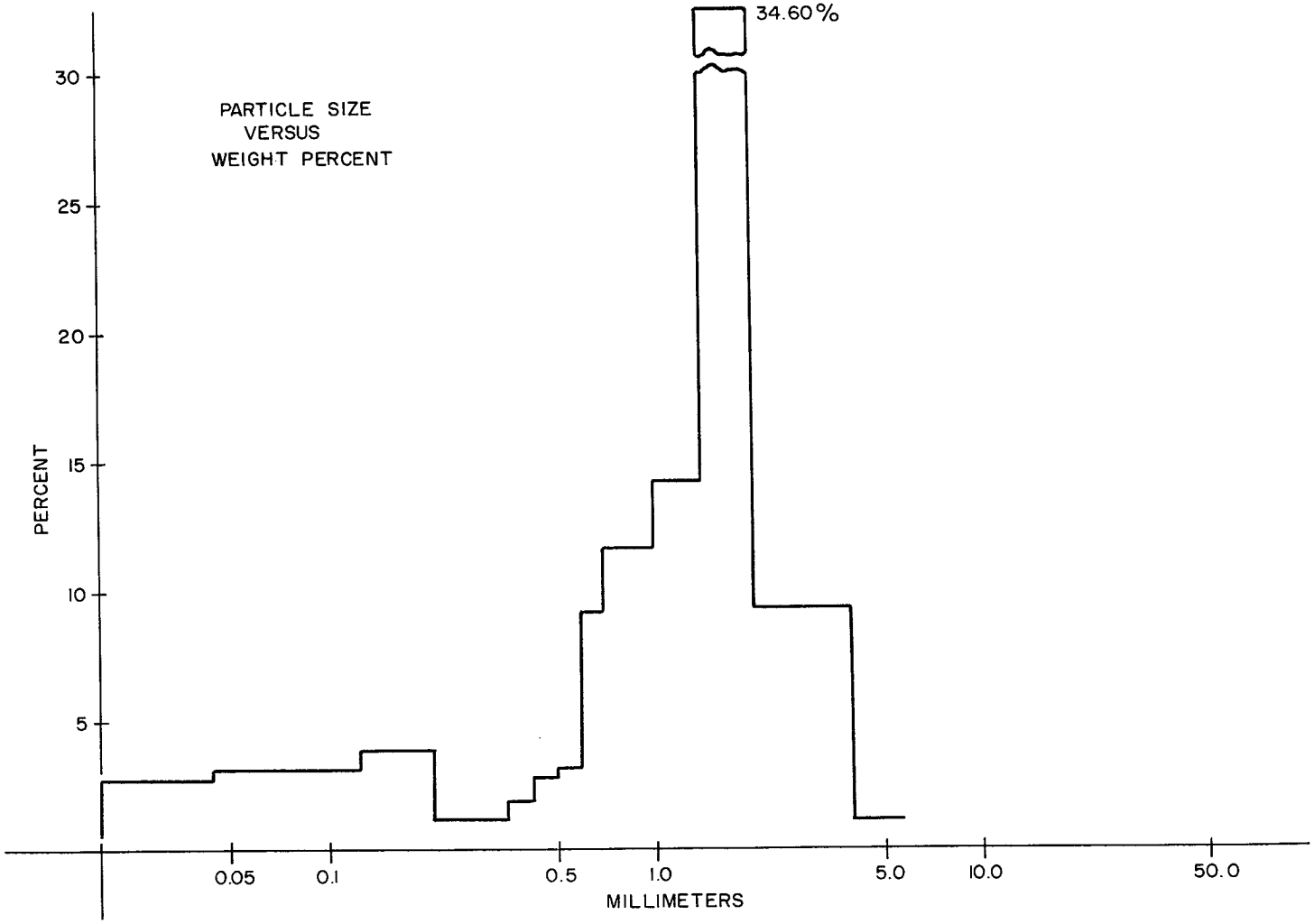

Figure C-6. Test 7

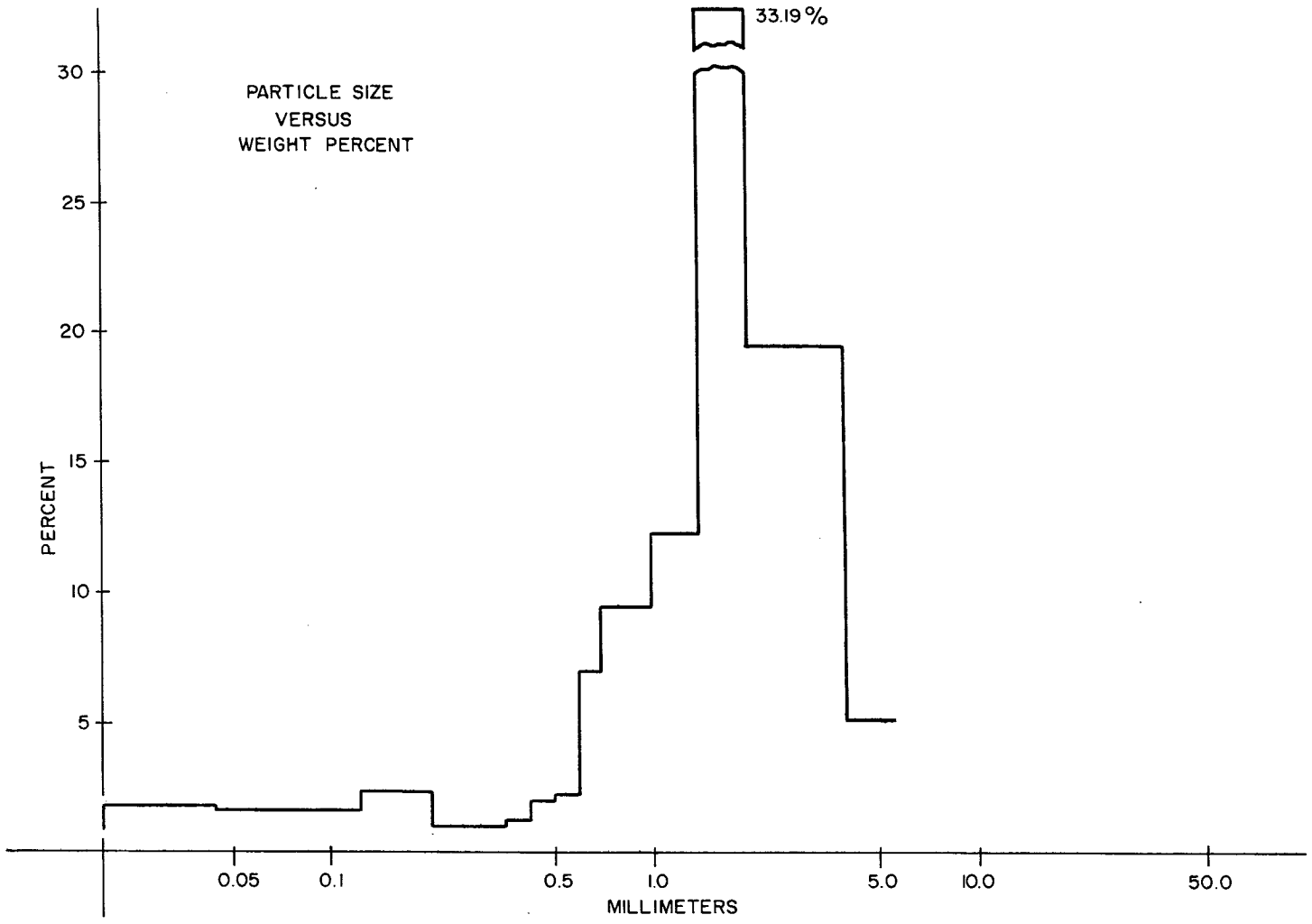

Figure C-7. Test 8

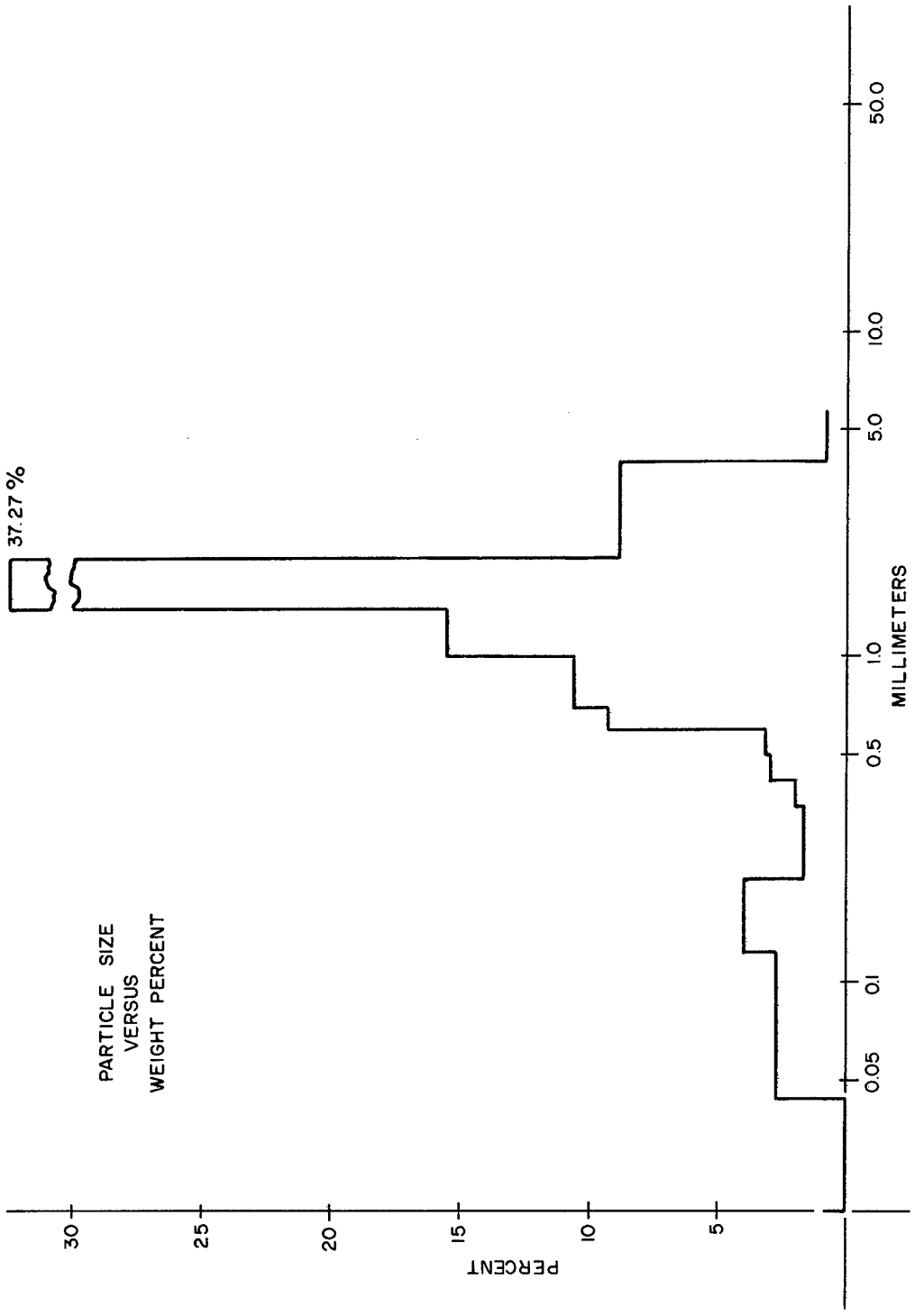

Figure C-8. Test 9

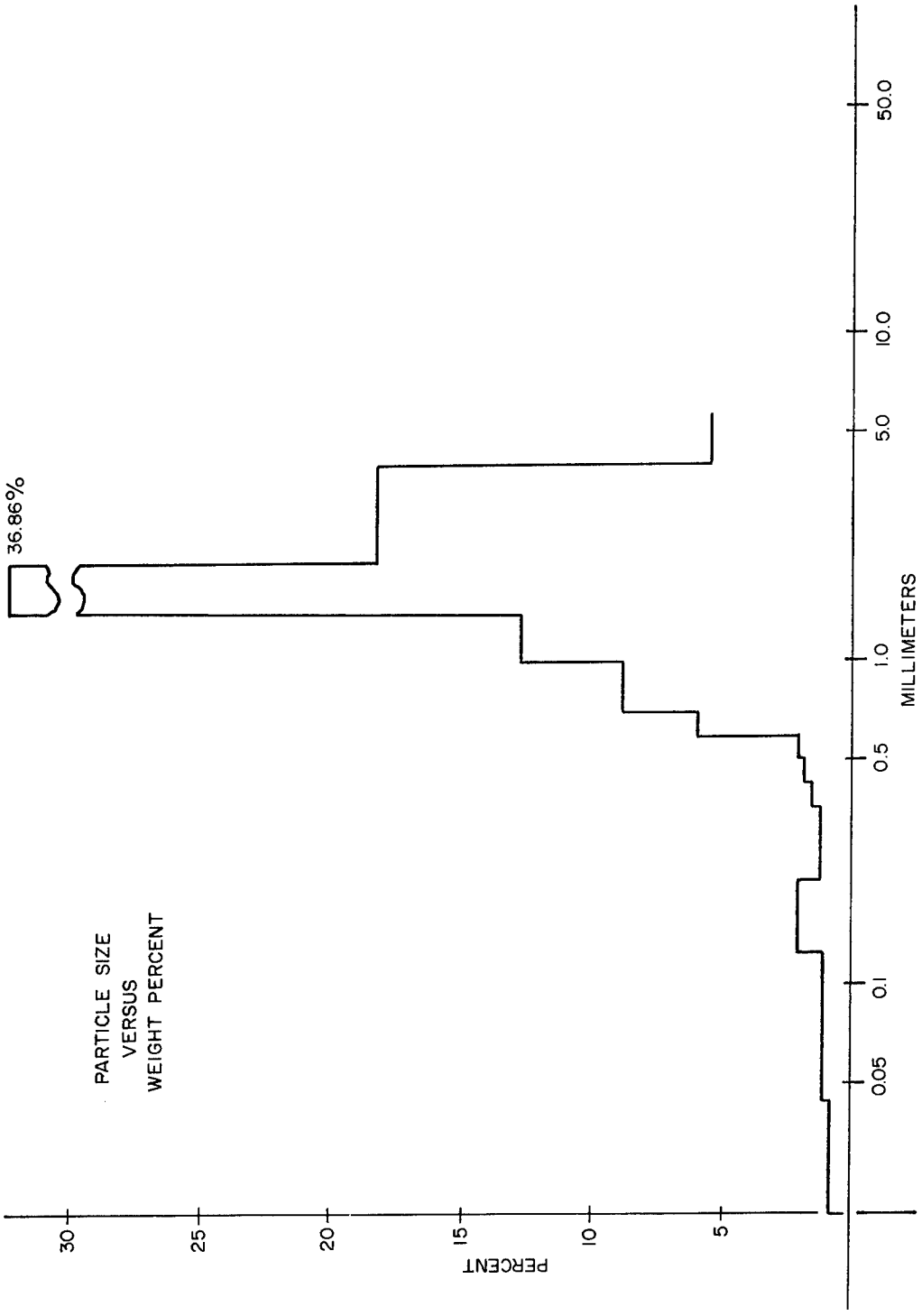

Figure C-9. Test 10

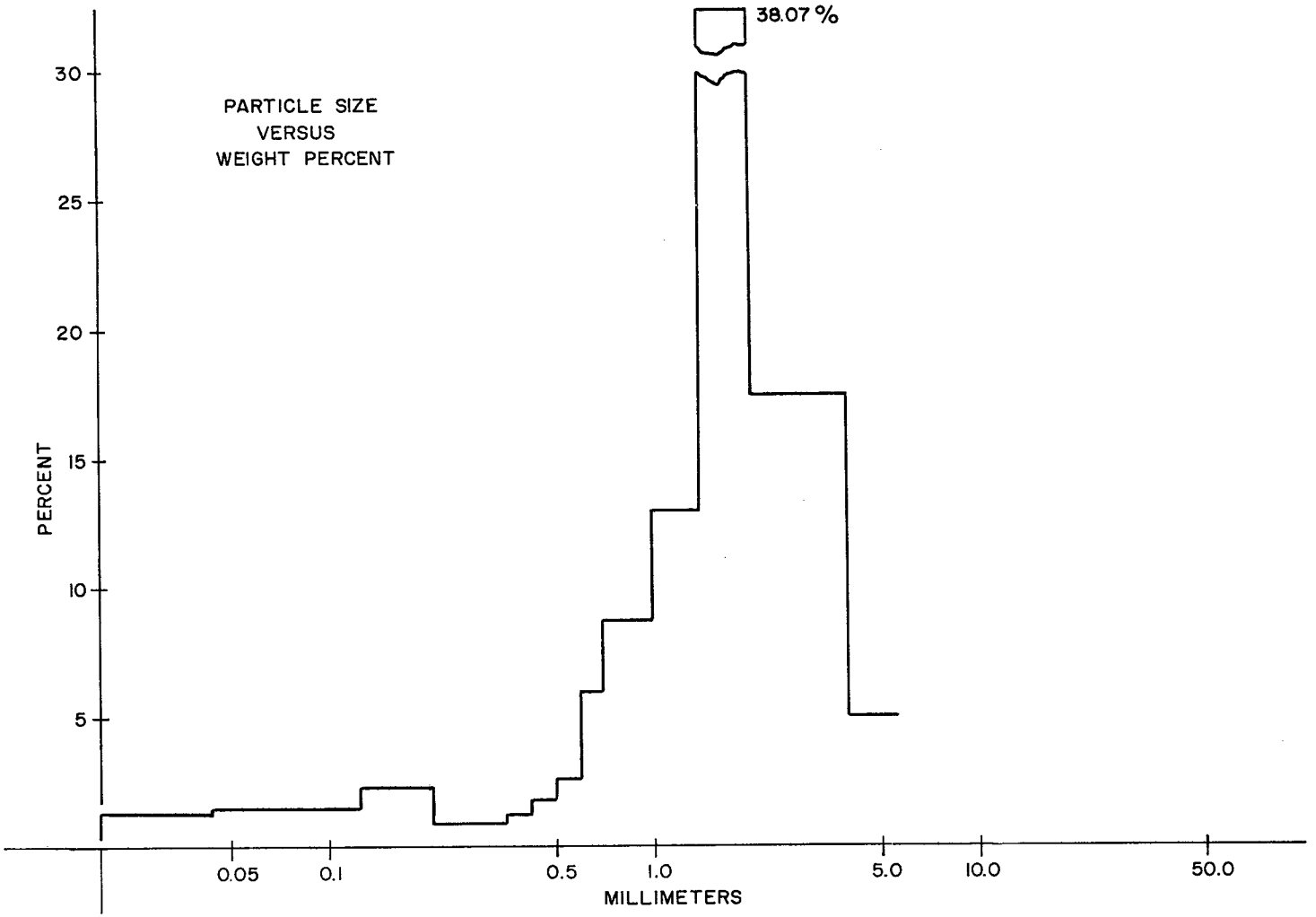

Figure C-10. Test 11

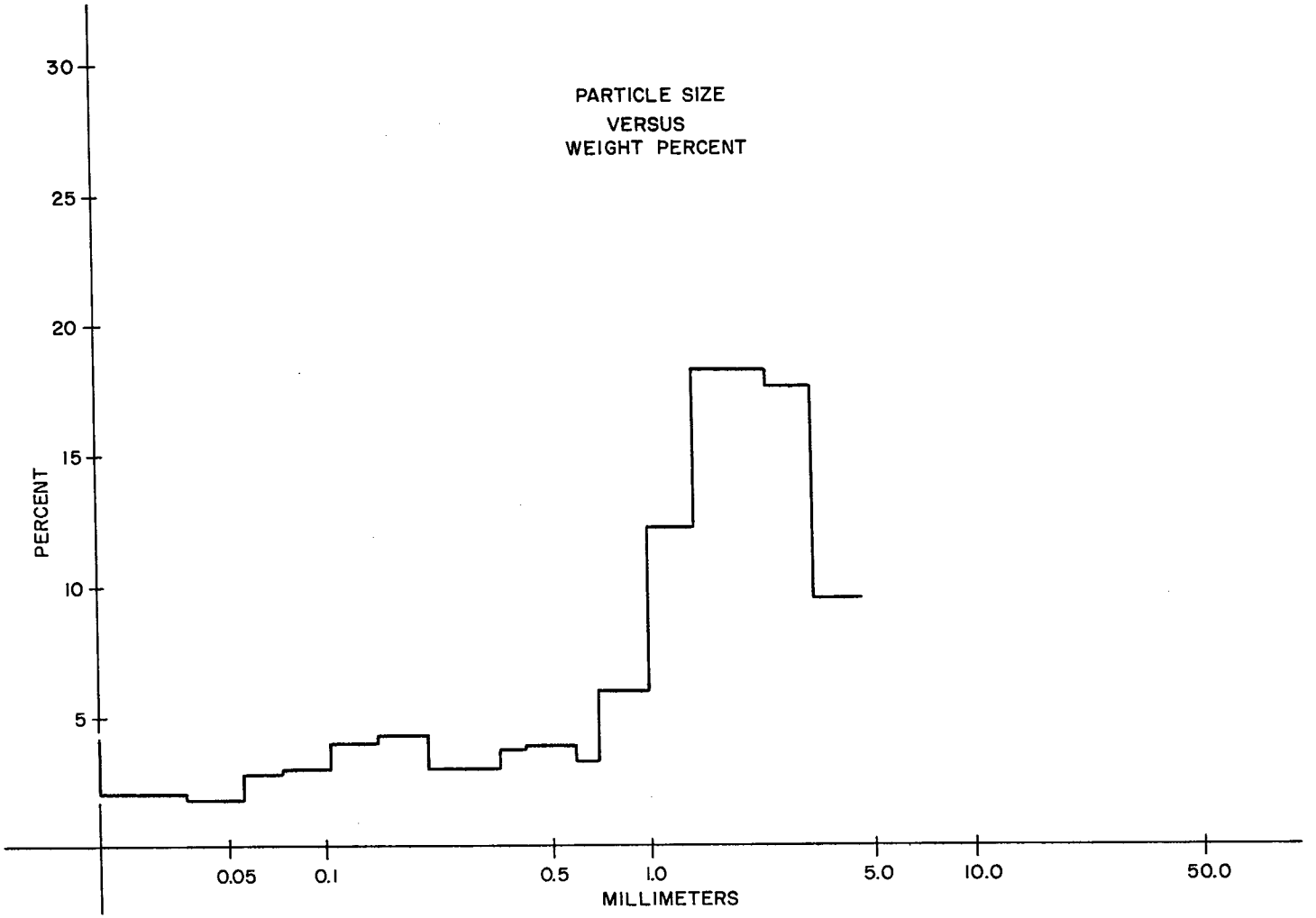

Figure C-11. Test 14

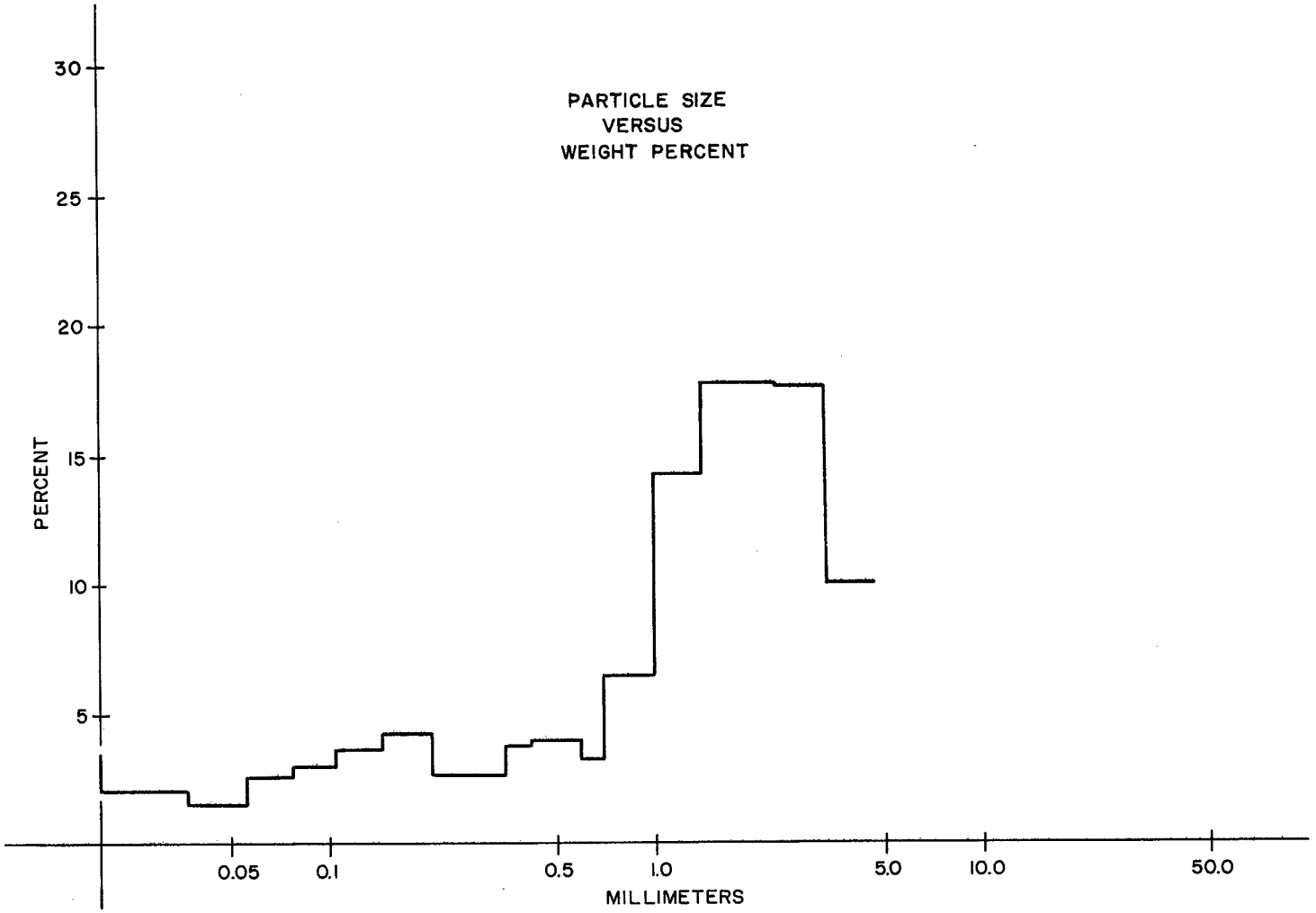

Figure C-12. Test 15

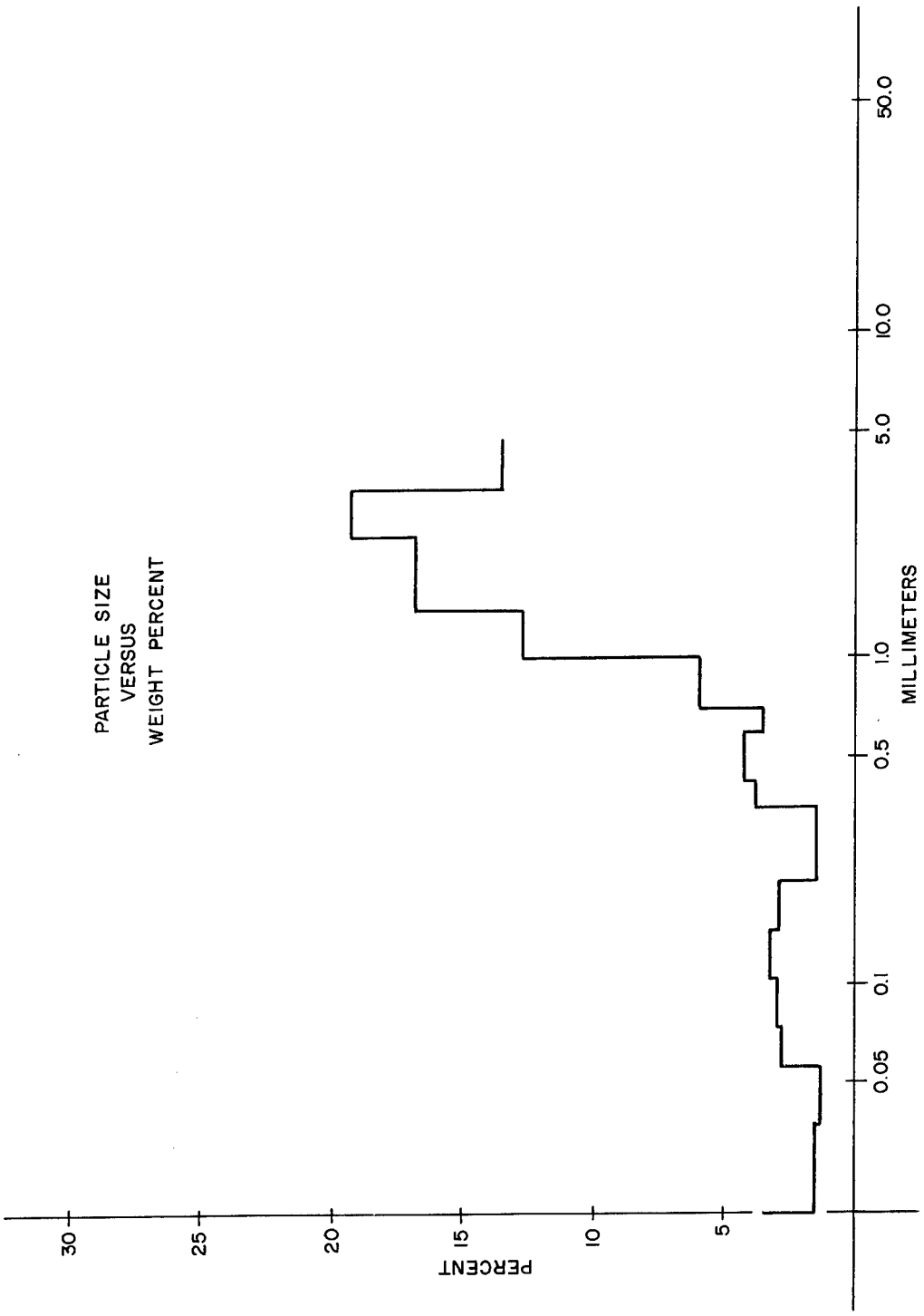

Figure C-13. Test 16

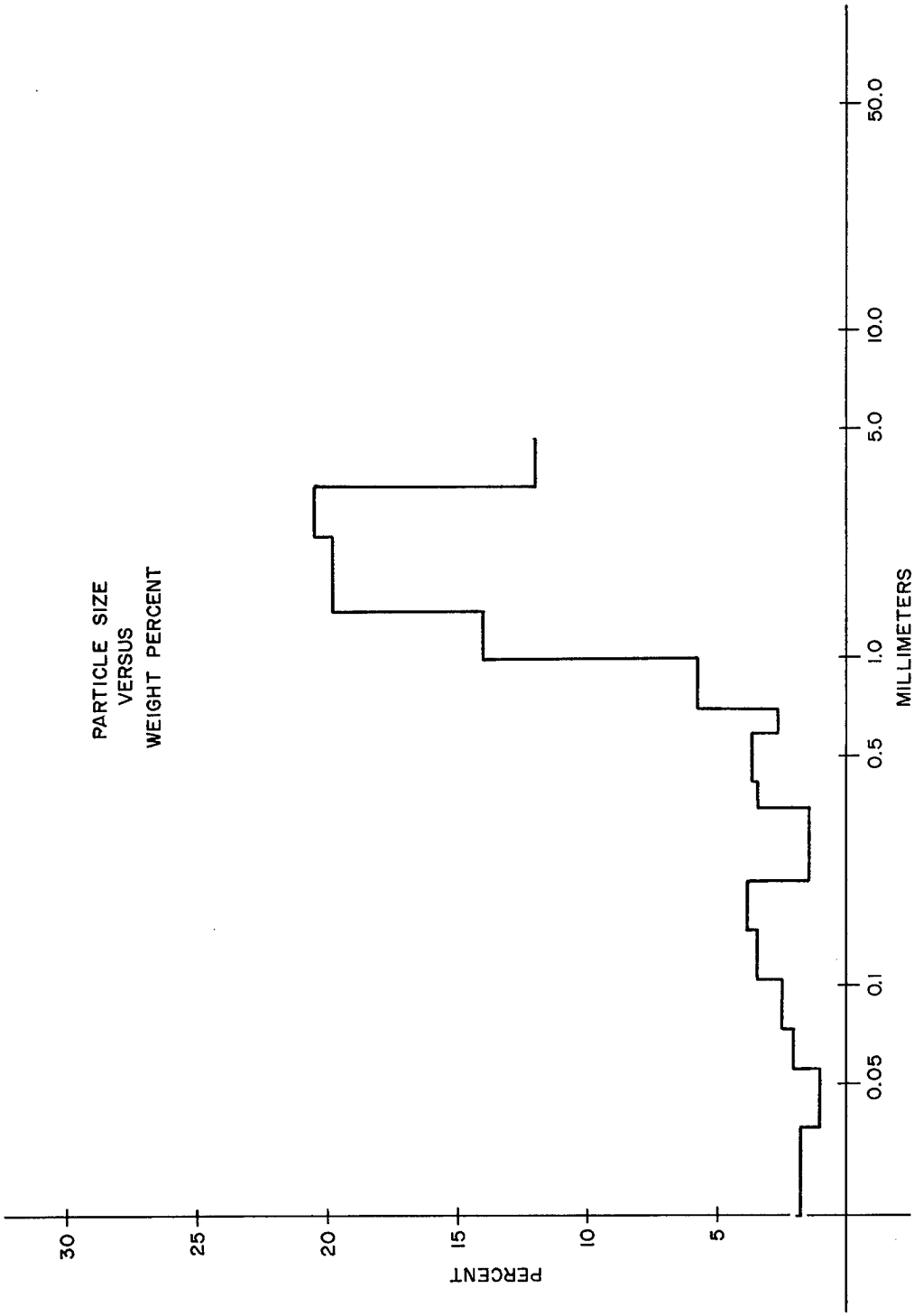

Figure C-14. Test 18

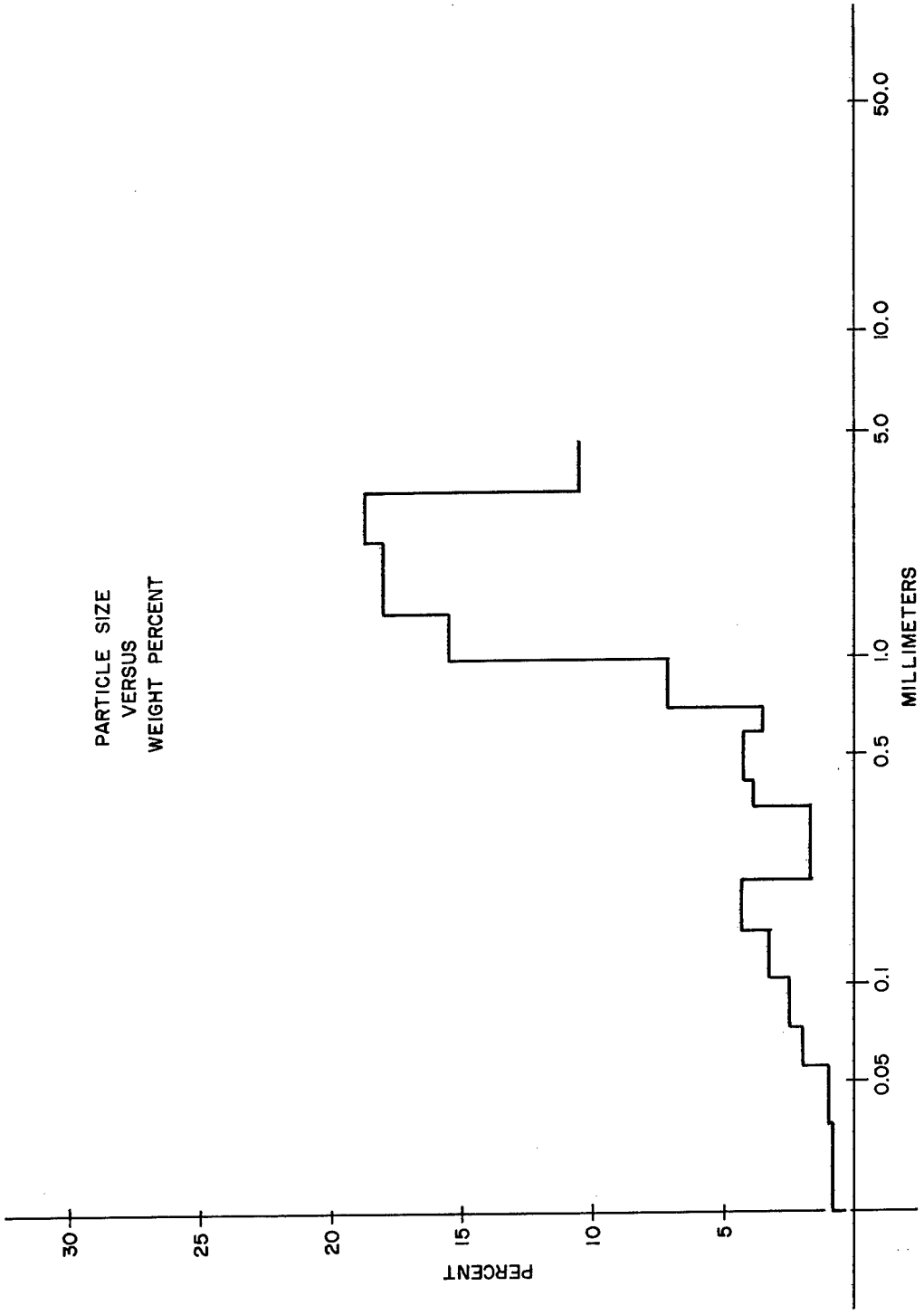

Figure C-15. Test 19

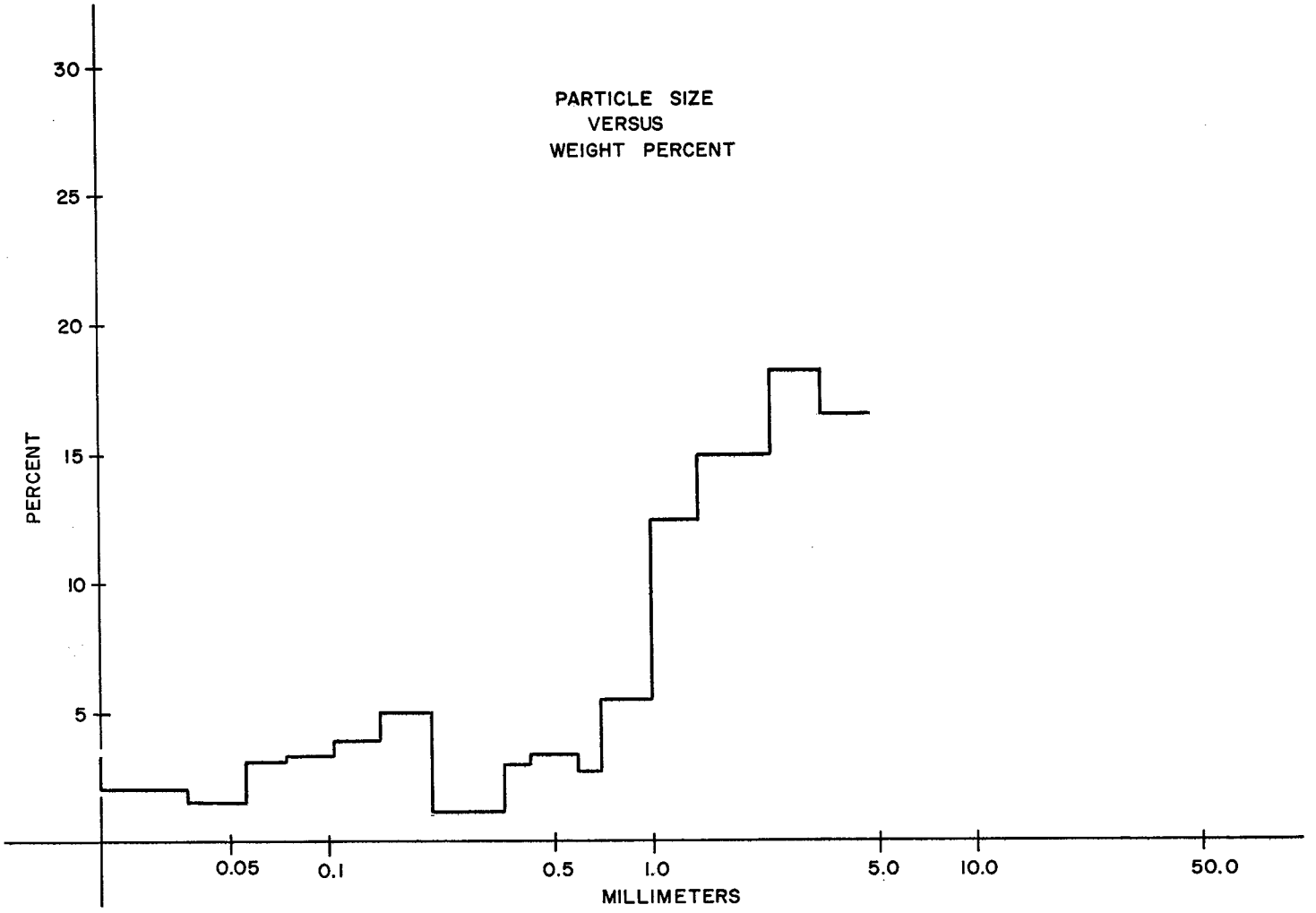

Figure C-16. Test 20

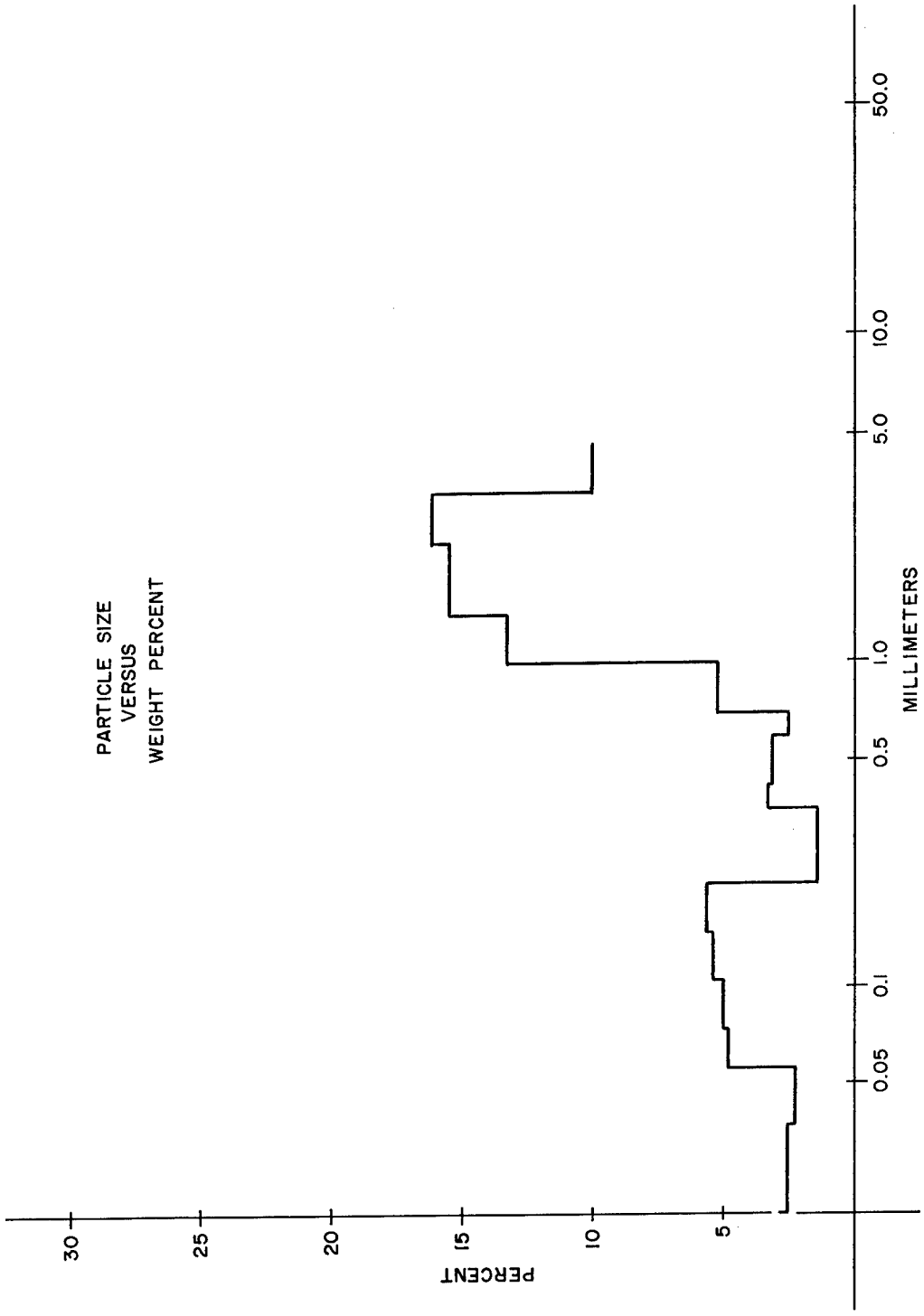

Figure C-17. Test 22

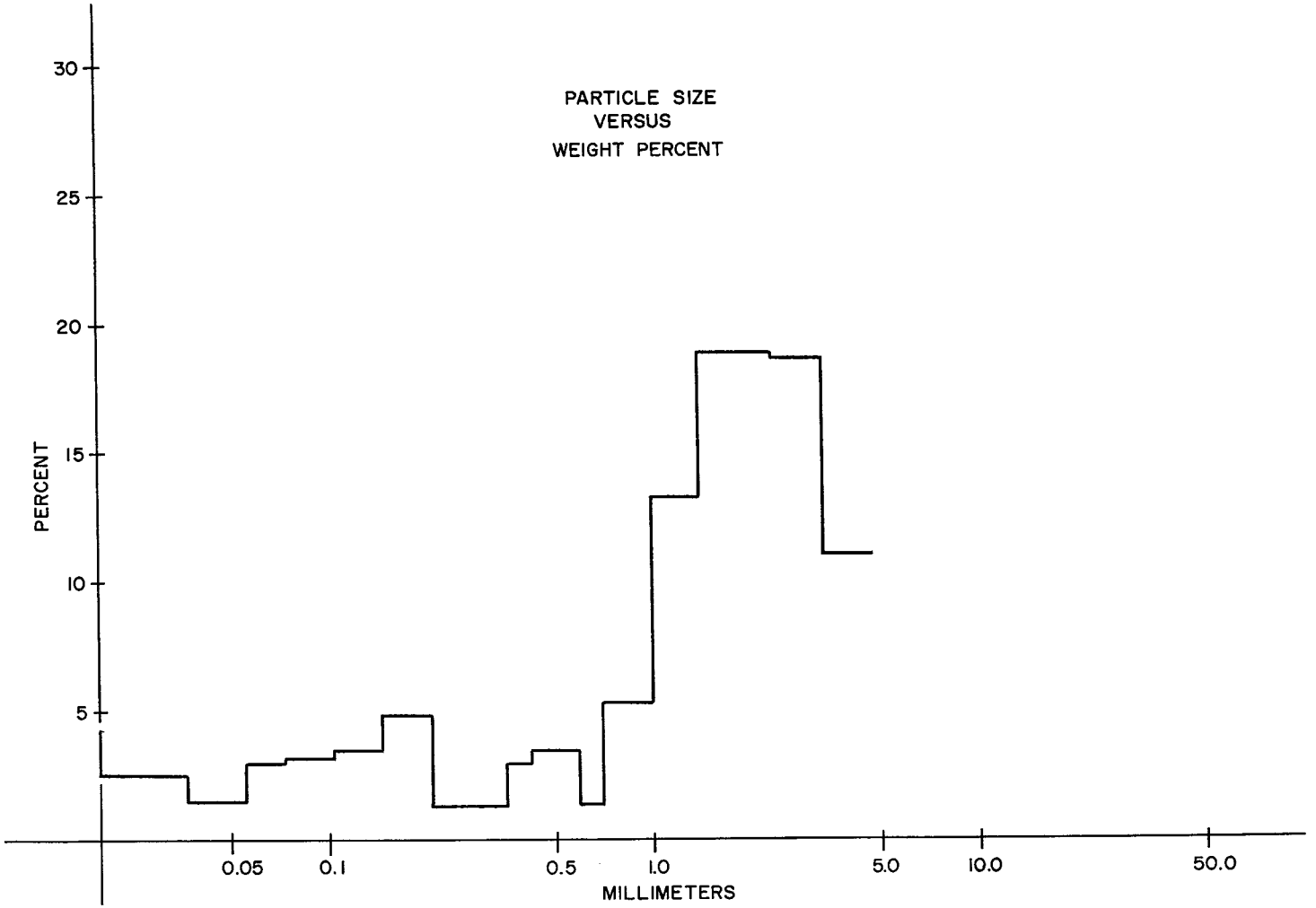

Figure C-18. Test 23

APPENDIX D

ROVER/NERVA DEVELOPMENT DESTRUCT
(Particle Size versus Accumulated Weight Percent)

The curves in this appendix show the accumulated weight percent plotted against the screen size. These data are presented on semilog paper and then on log-probability paper. The data show the percentage of particles less than a specific size or the sizes of particles less than a specific percentage.

Also shown is the composite (maximum-minimum) curve for the groups of tests performed with the same test configuration. These data show the reproducibility of results from these tests.

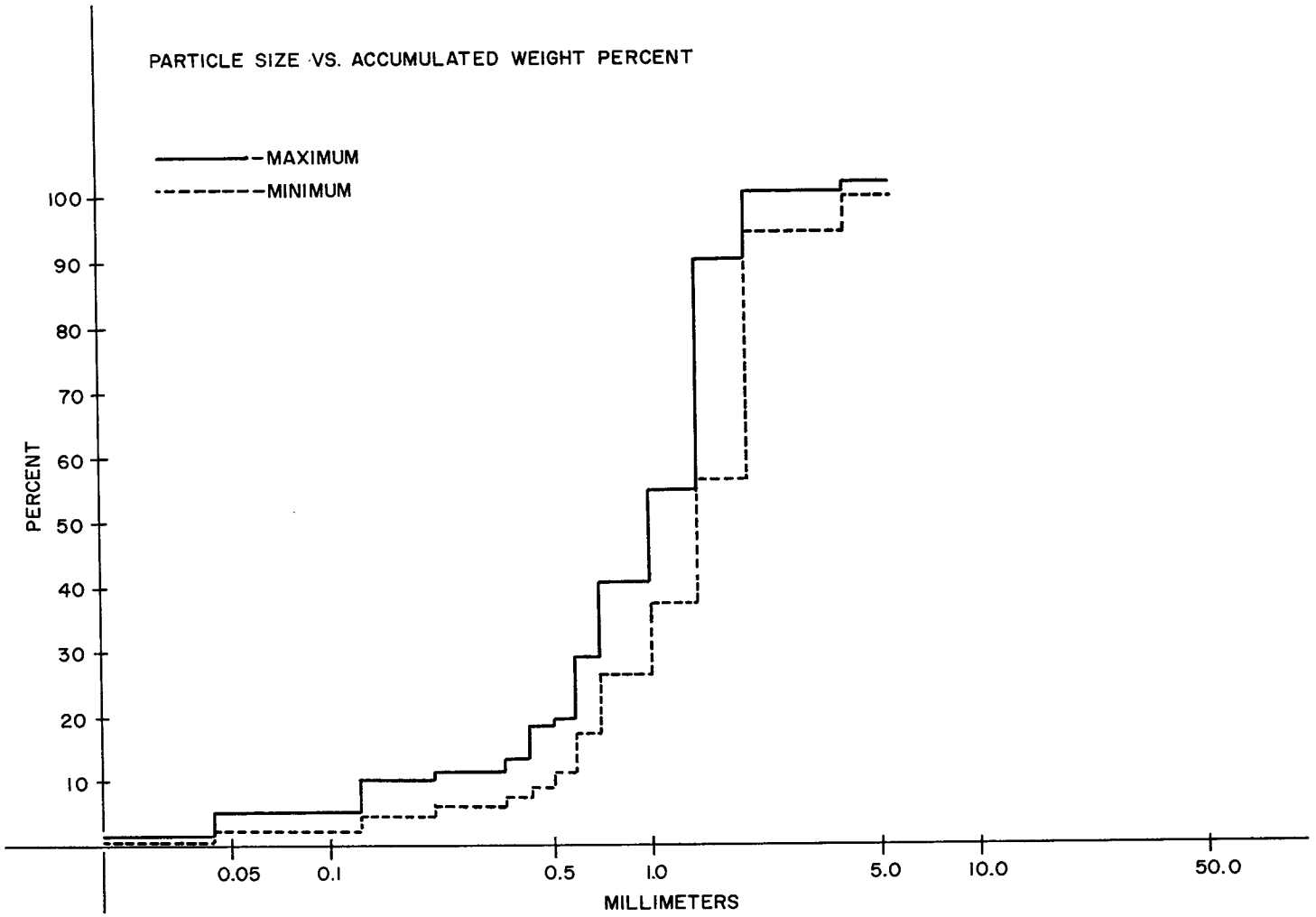

Figure D-1. Maximum-Minimum Curve for Tests 3, 6, 7, 8, 9, 10, and 11

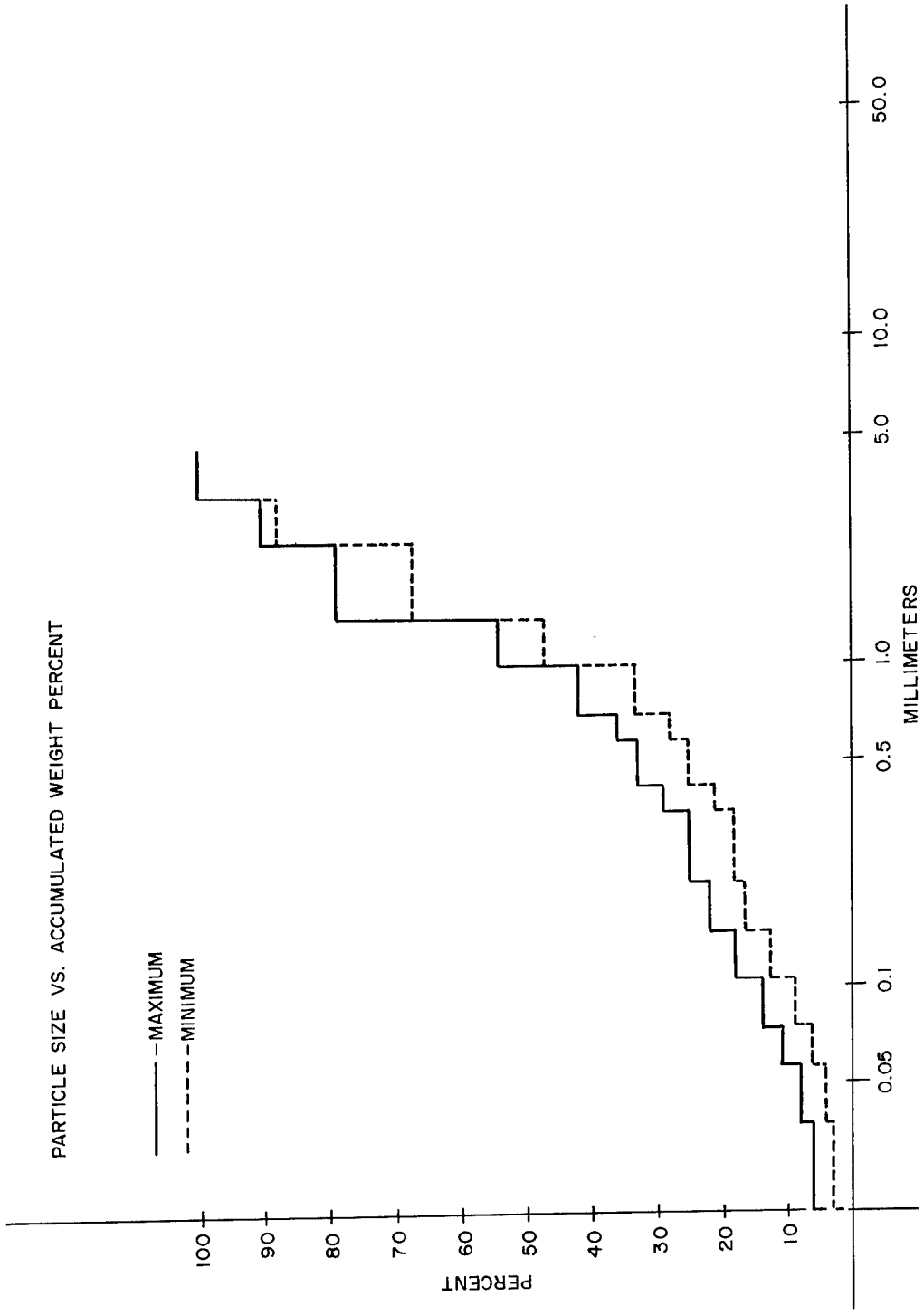

Figure D-2. Maximum-Minimum Curves for Tests 14, 15, 18, and 19

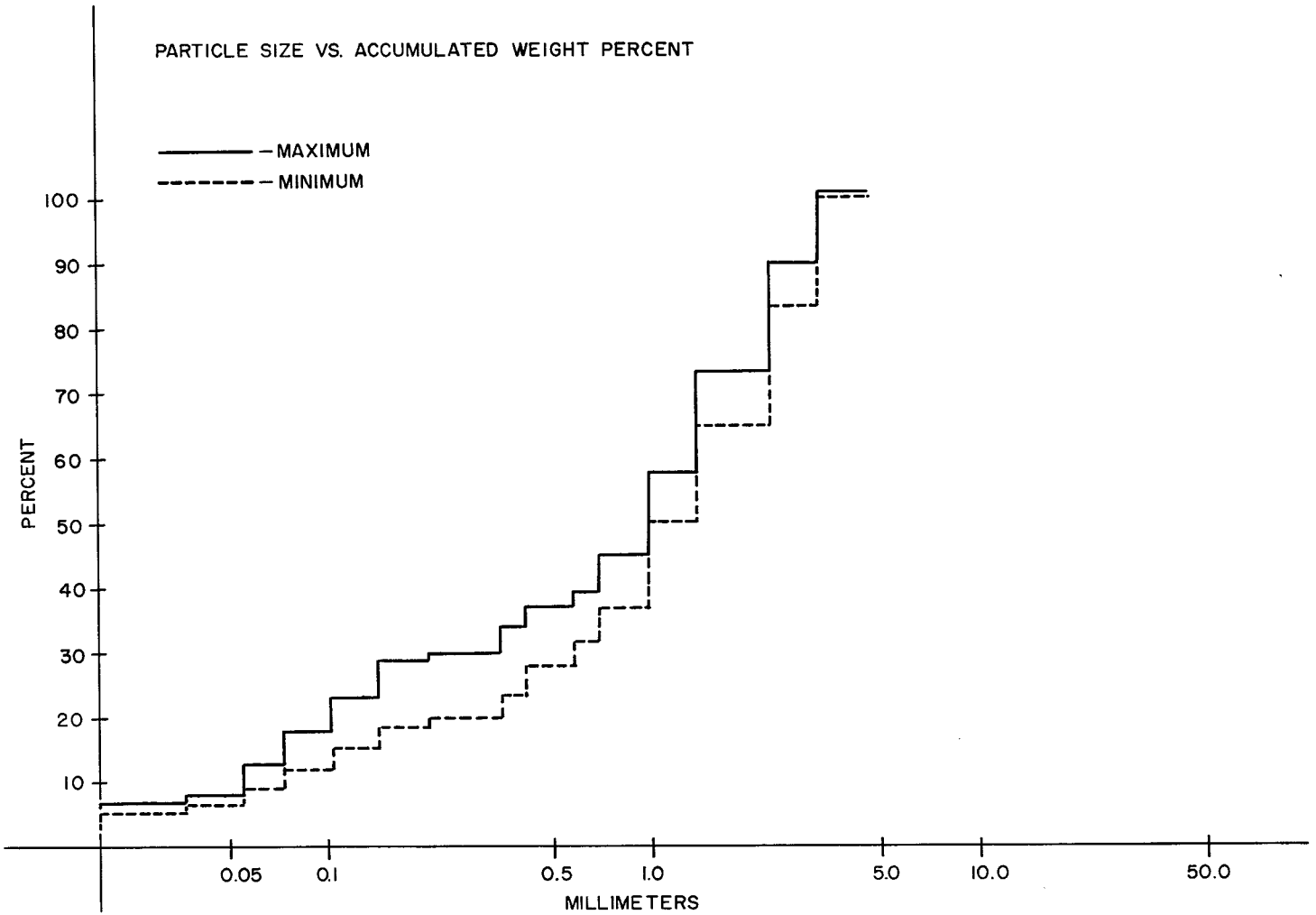

Figure D-3. Maximum-Minimum Curves for Tests 16, 20, 22, and 23

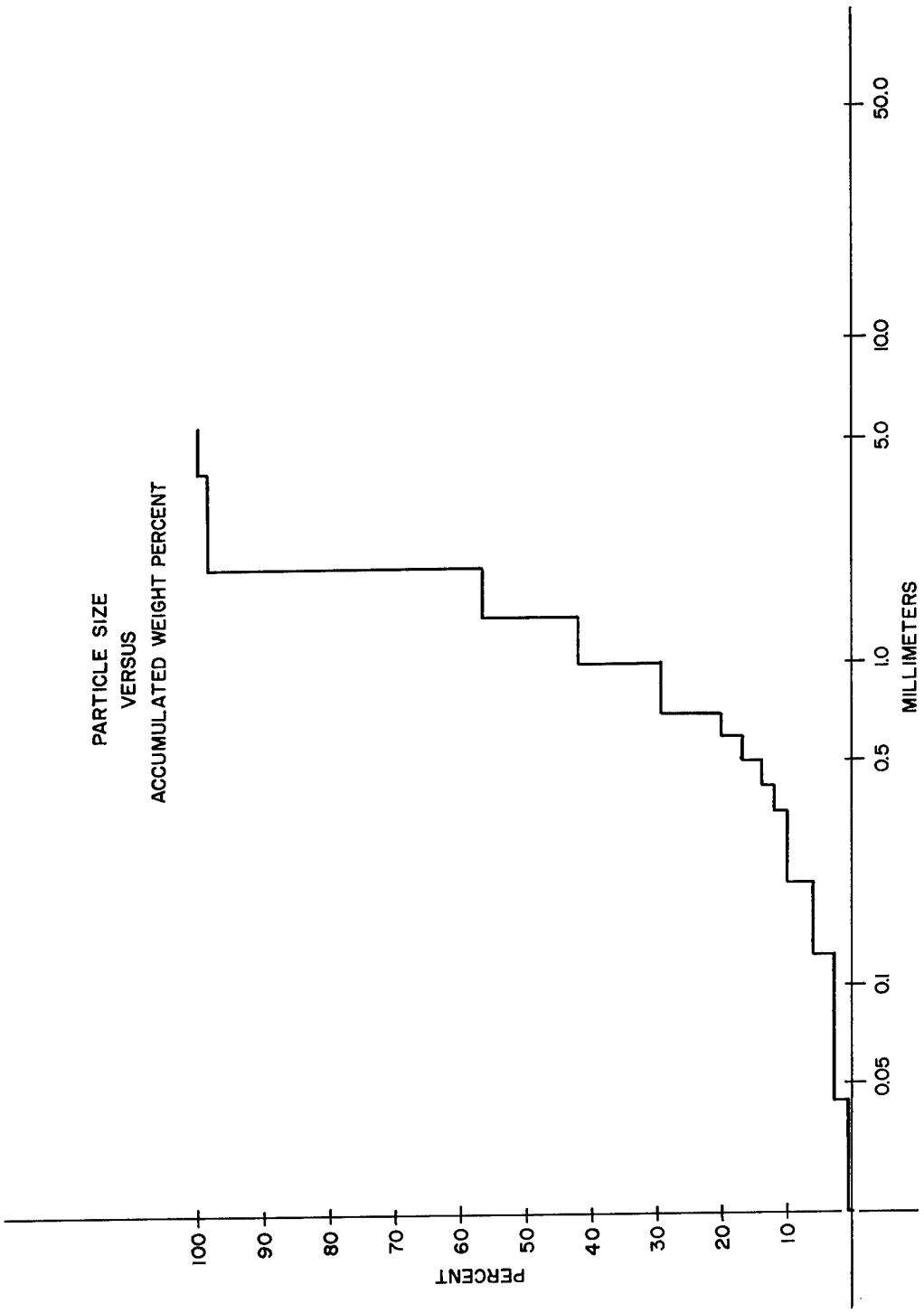

Figure D-4. Test 3

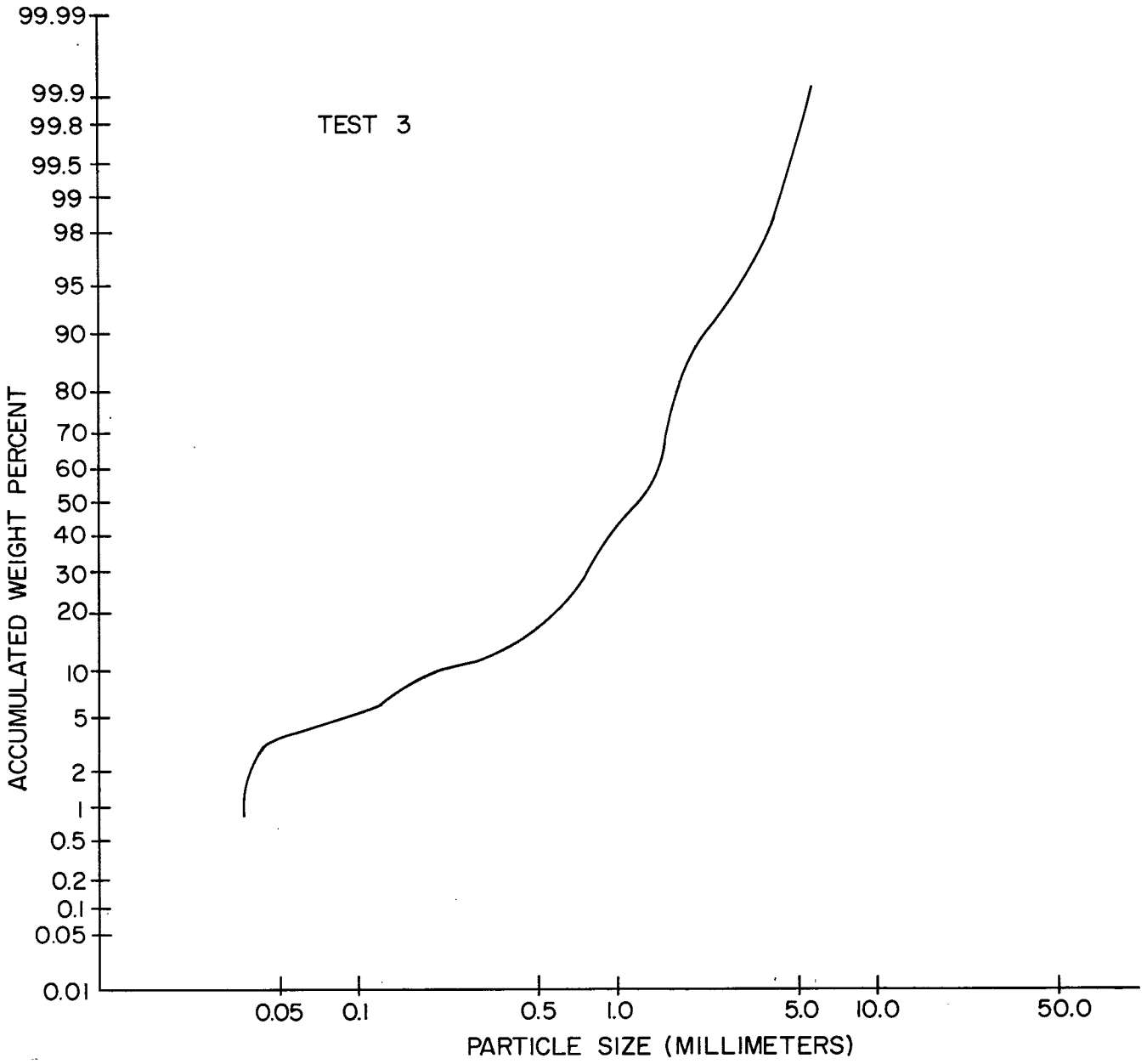

Figure D-4 (cont). Log Probability versus Particle Size

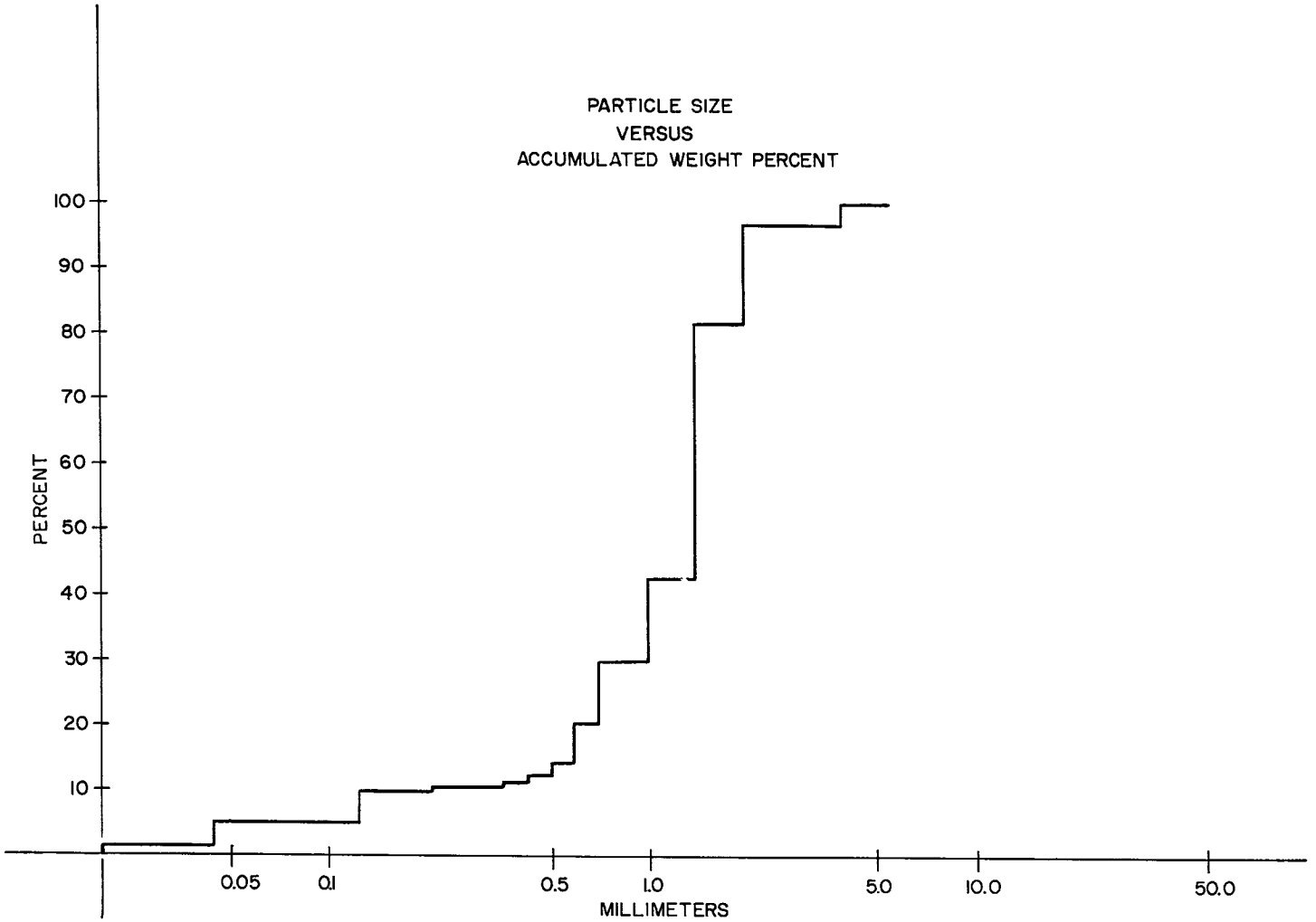

Figure D-5. Test 6

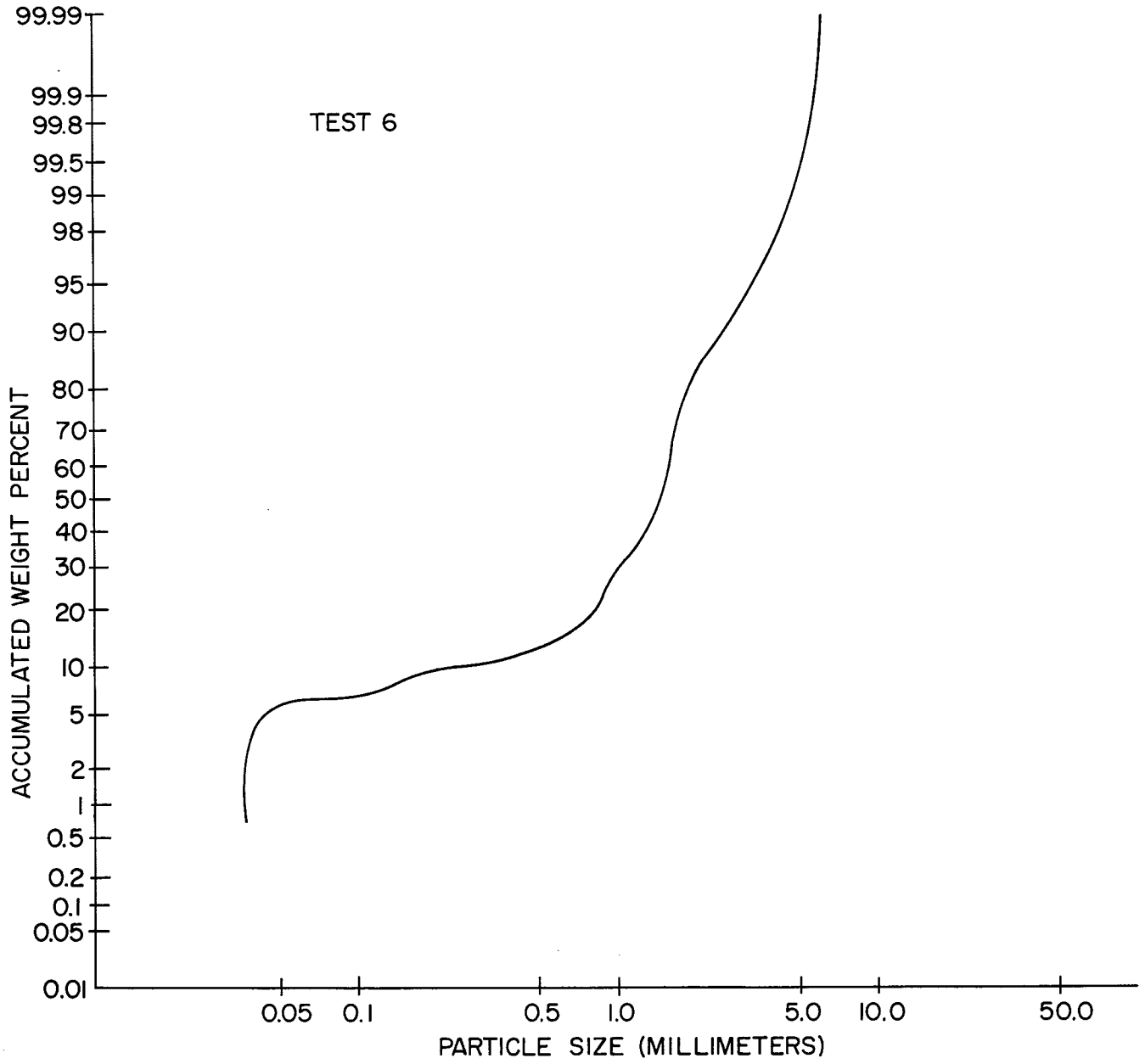

Figure D-5 (cont). Log Probability versus Particle Size

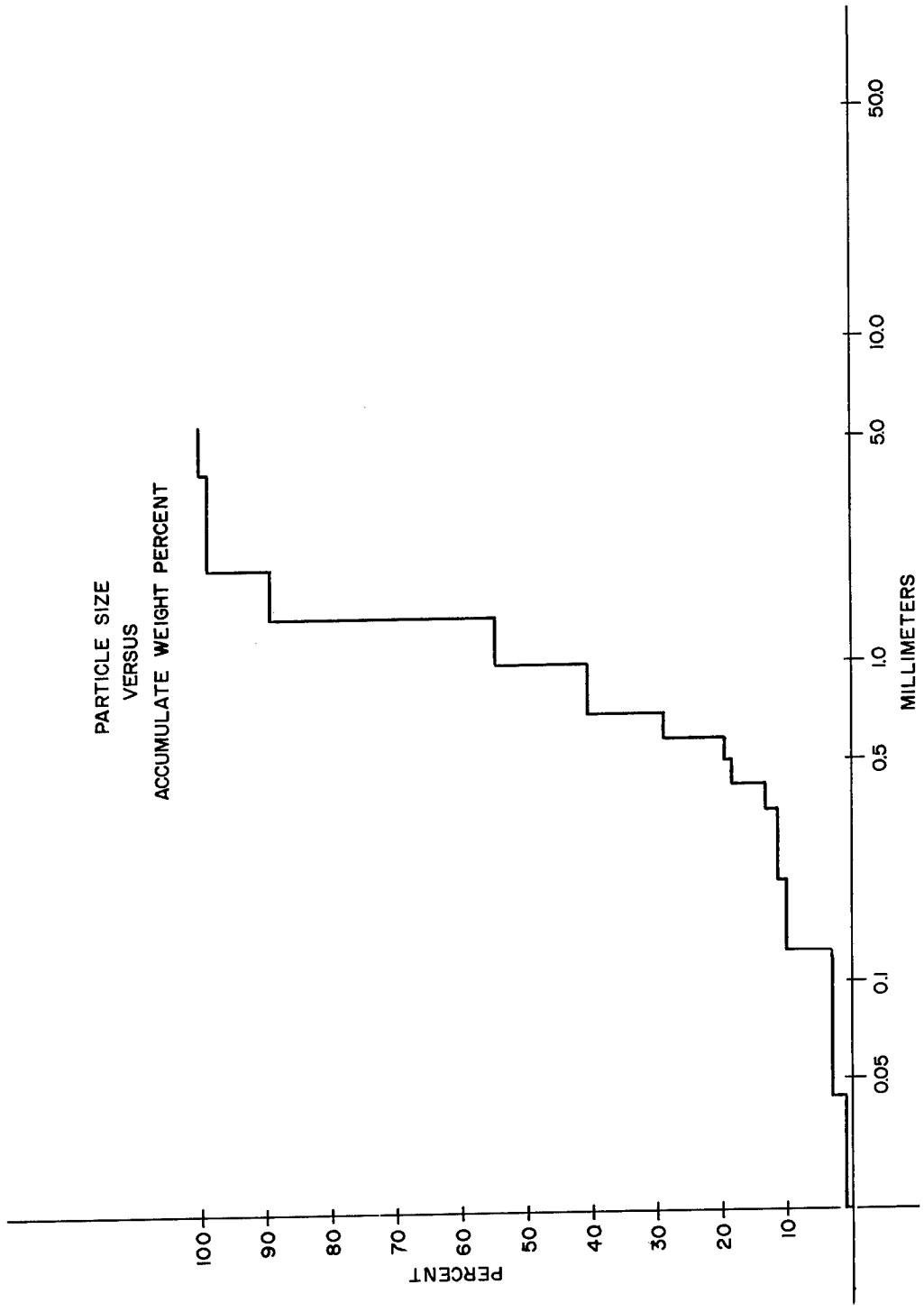

Figure D-6. Test 7

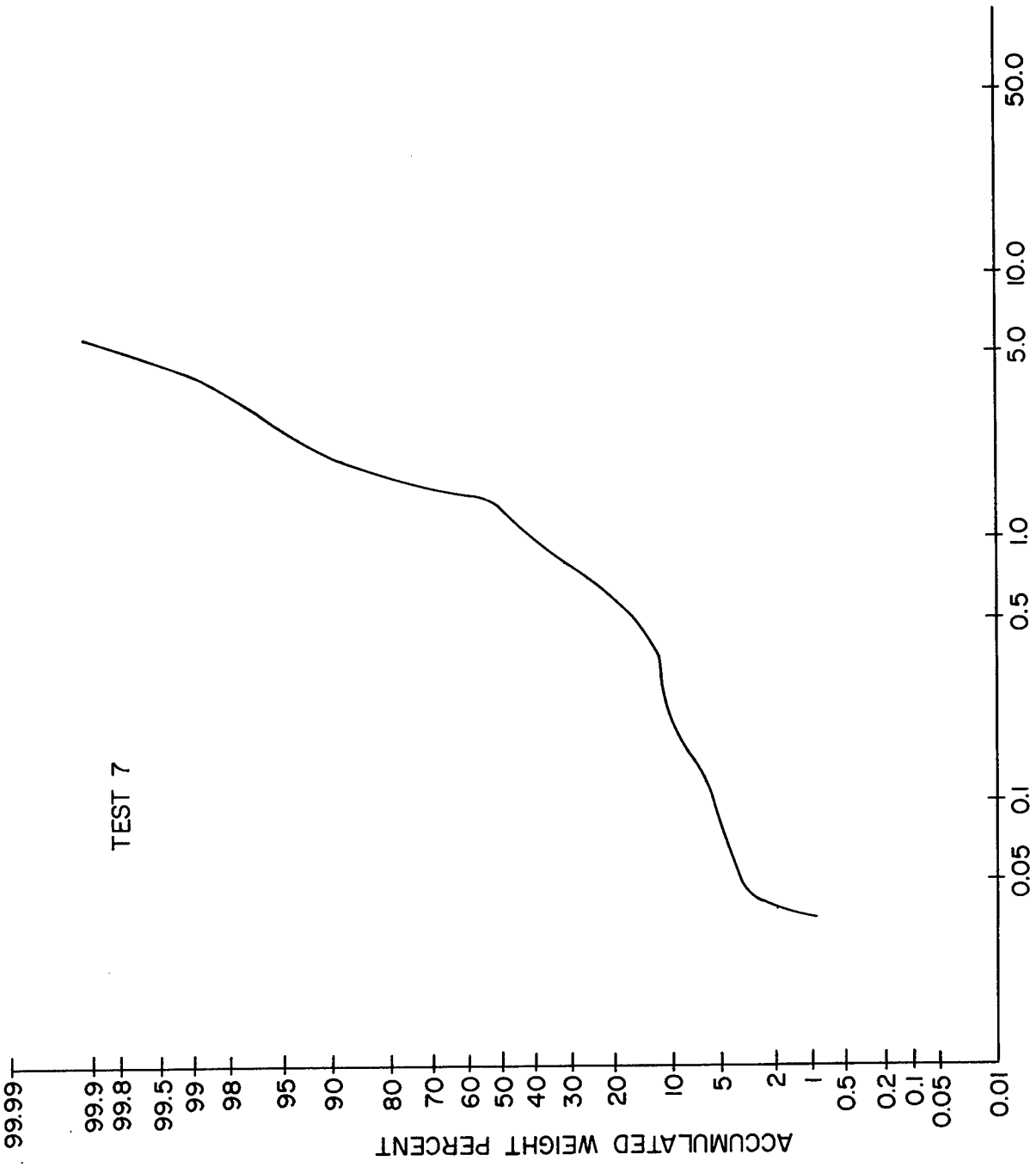

Figure D-6 (cont) Log Probability versus Particle Size

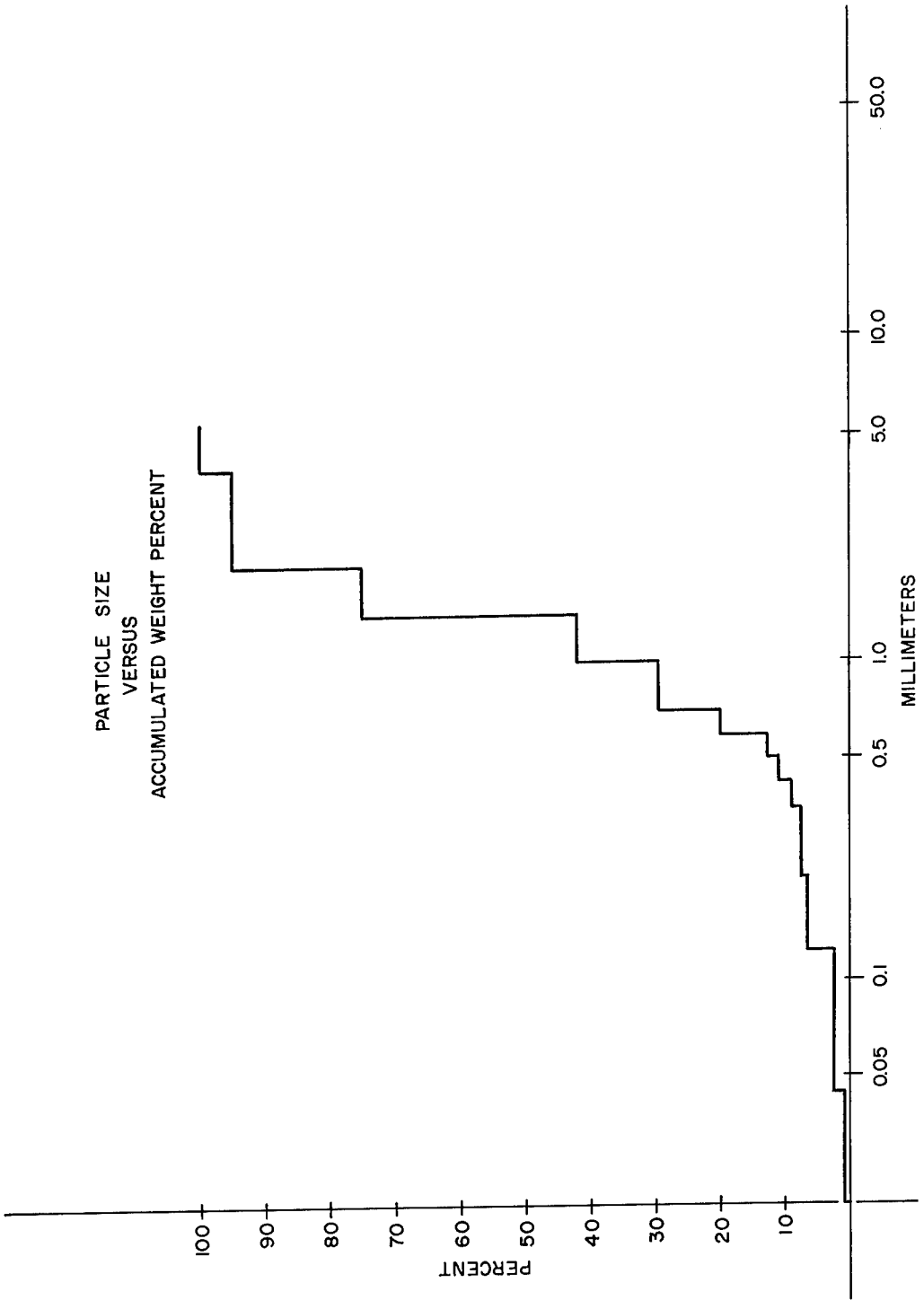

Figure D-7. Test 8

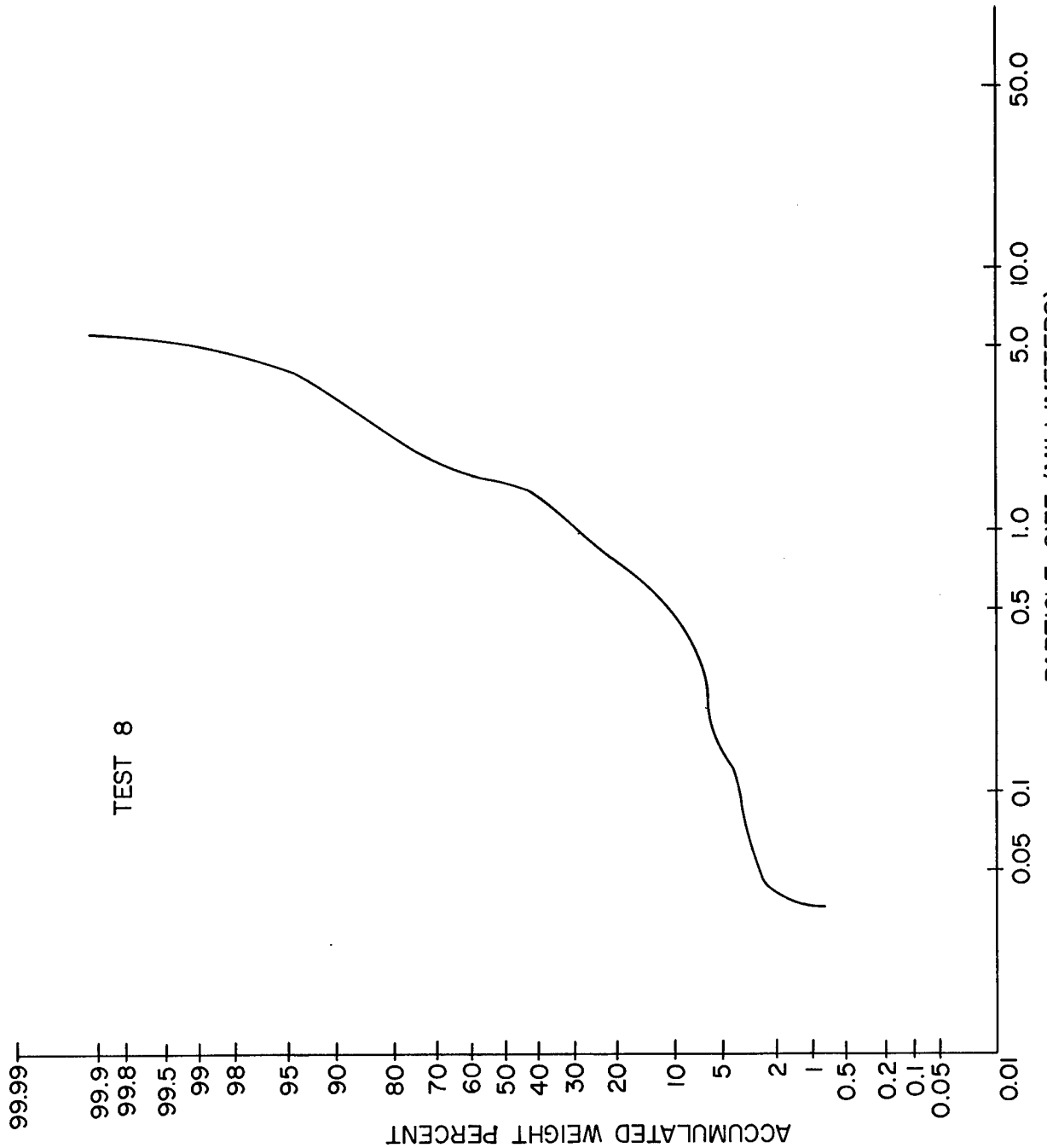

Figure D-7 (cont). Log Probability versus Particle Size

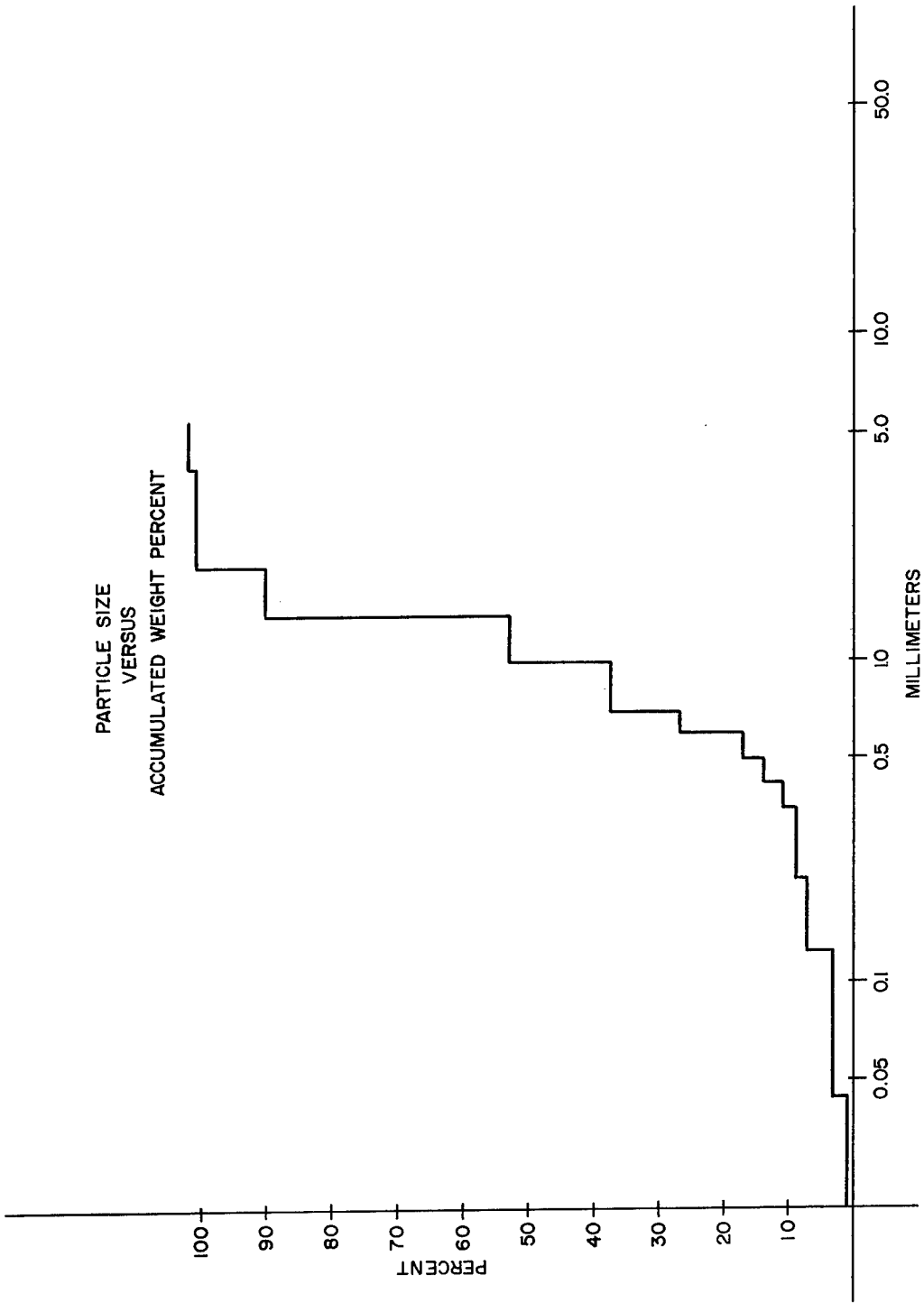

Figure D-8. Test 9

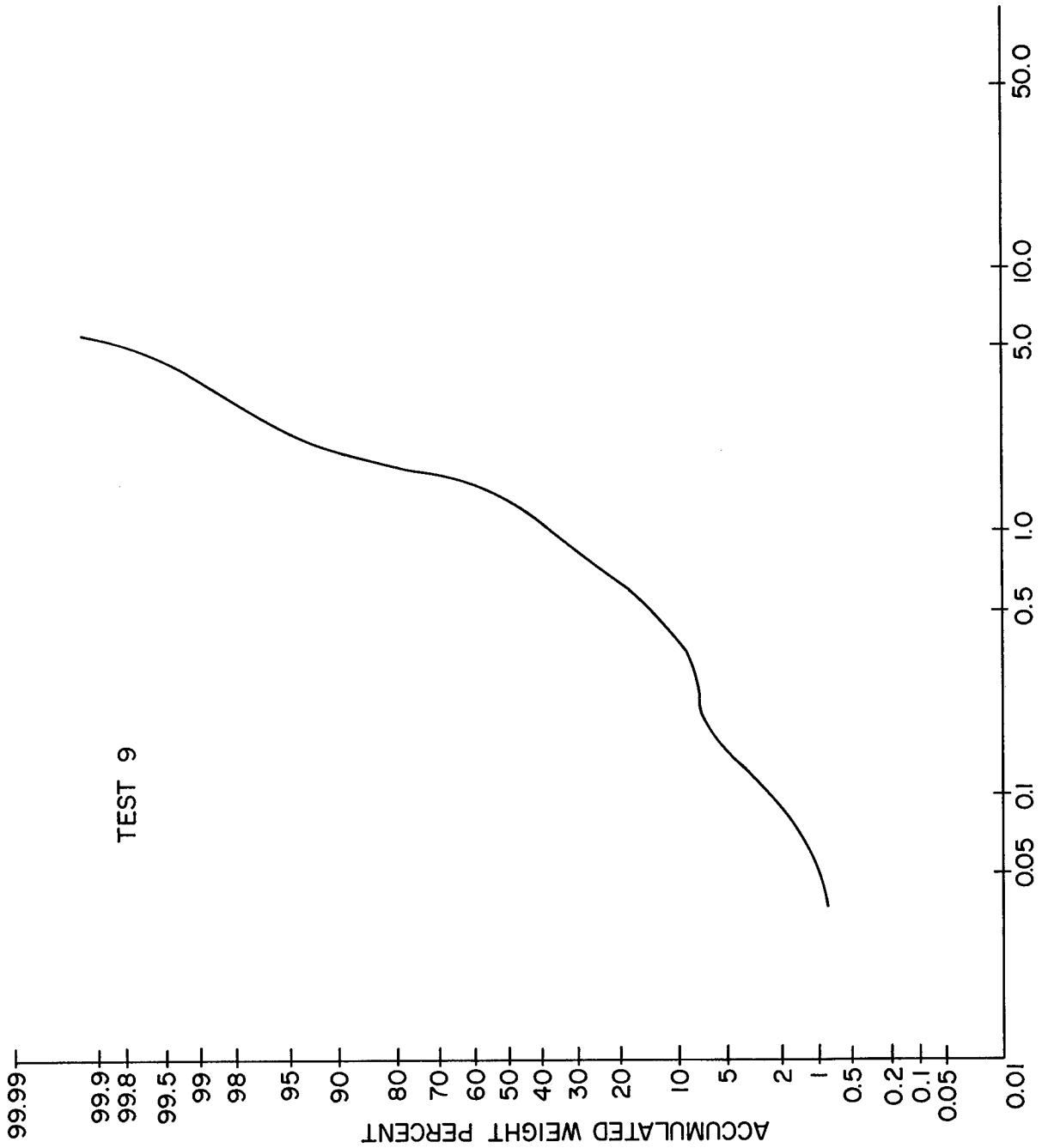

Figure D-8 (cont). Log Probability versus Particle Size

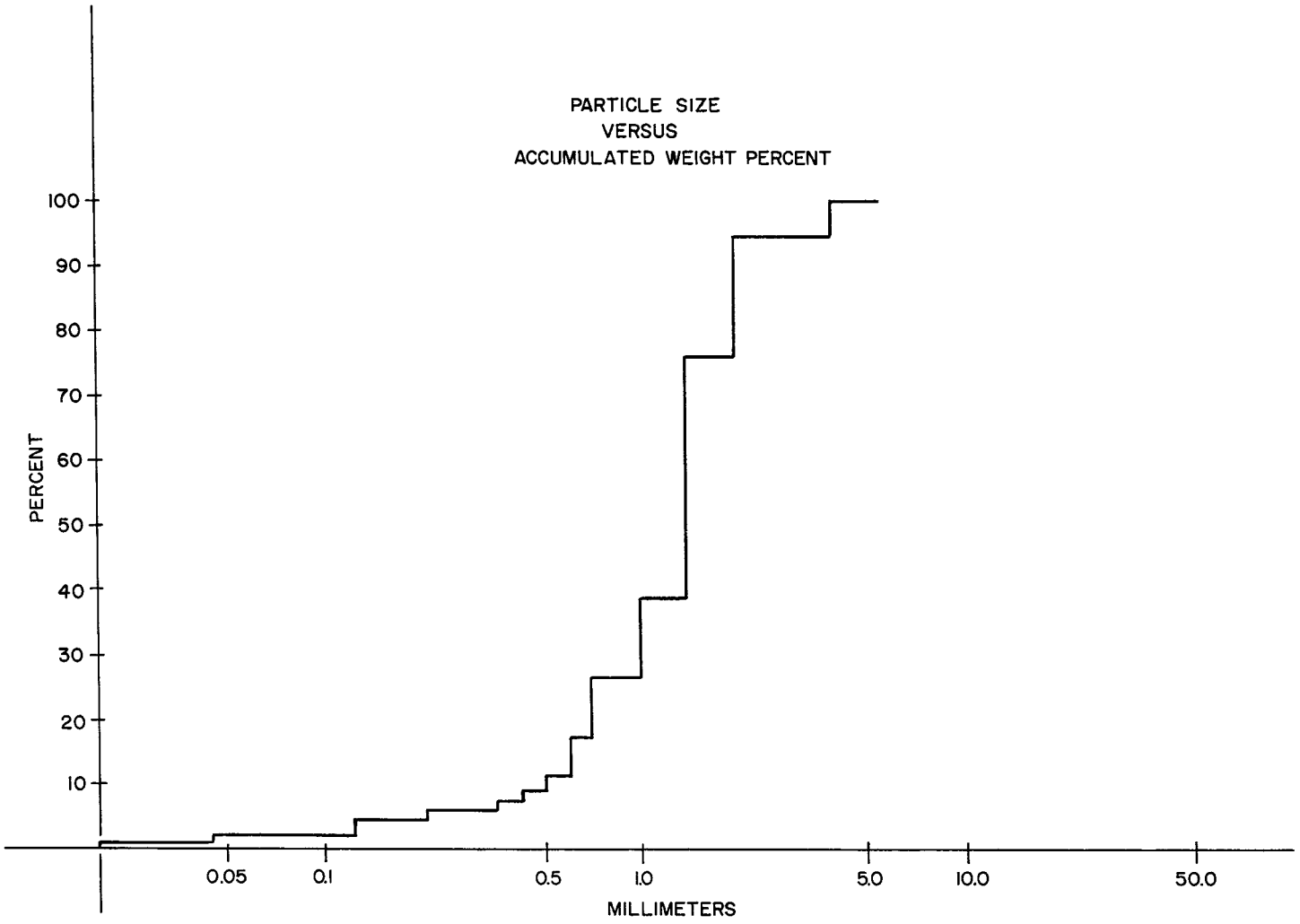

Figure D-9. Test 10

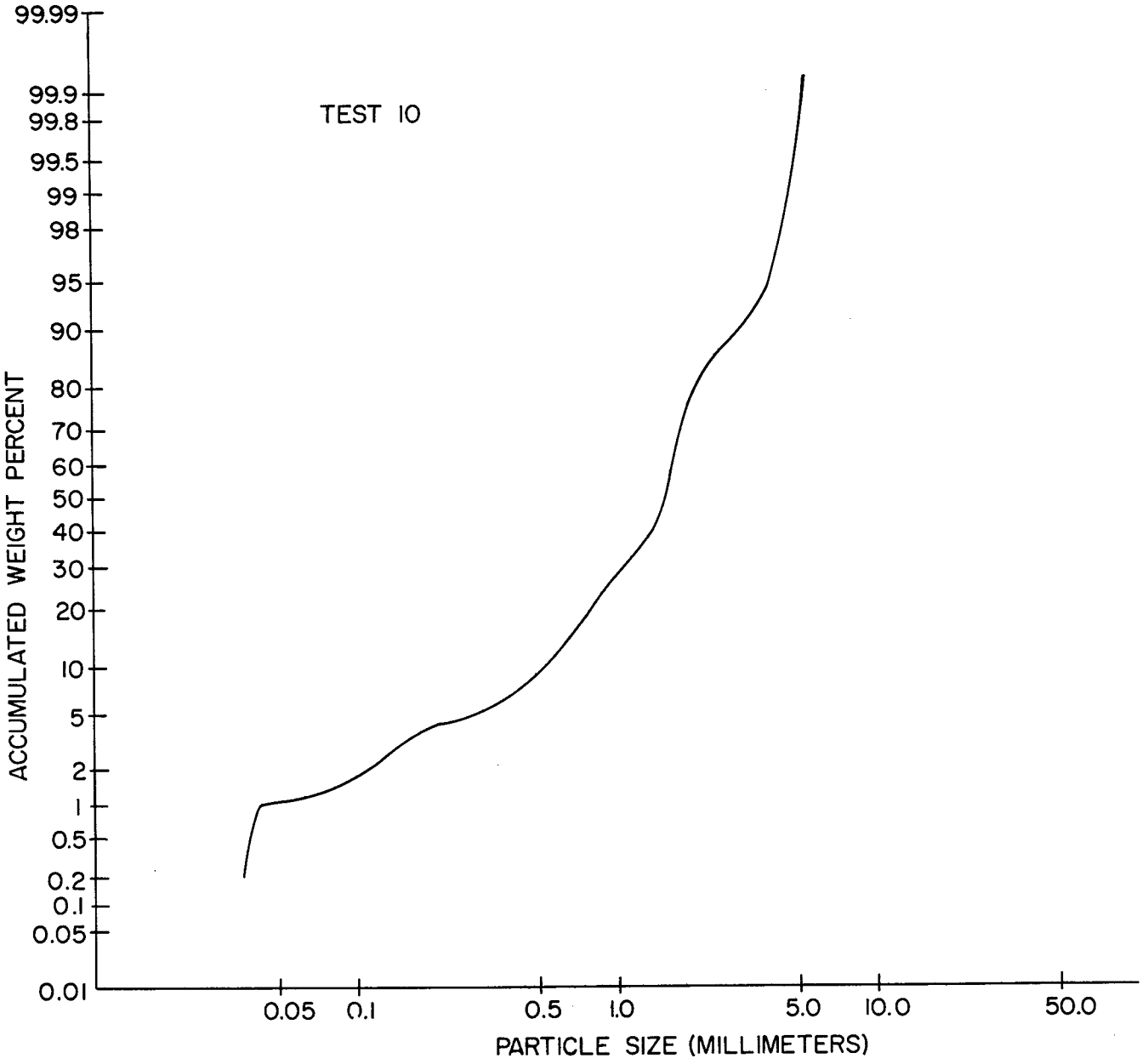

Figure D-9 (cont). Log Probability versus Particle Size

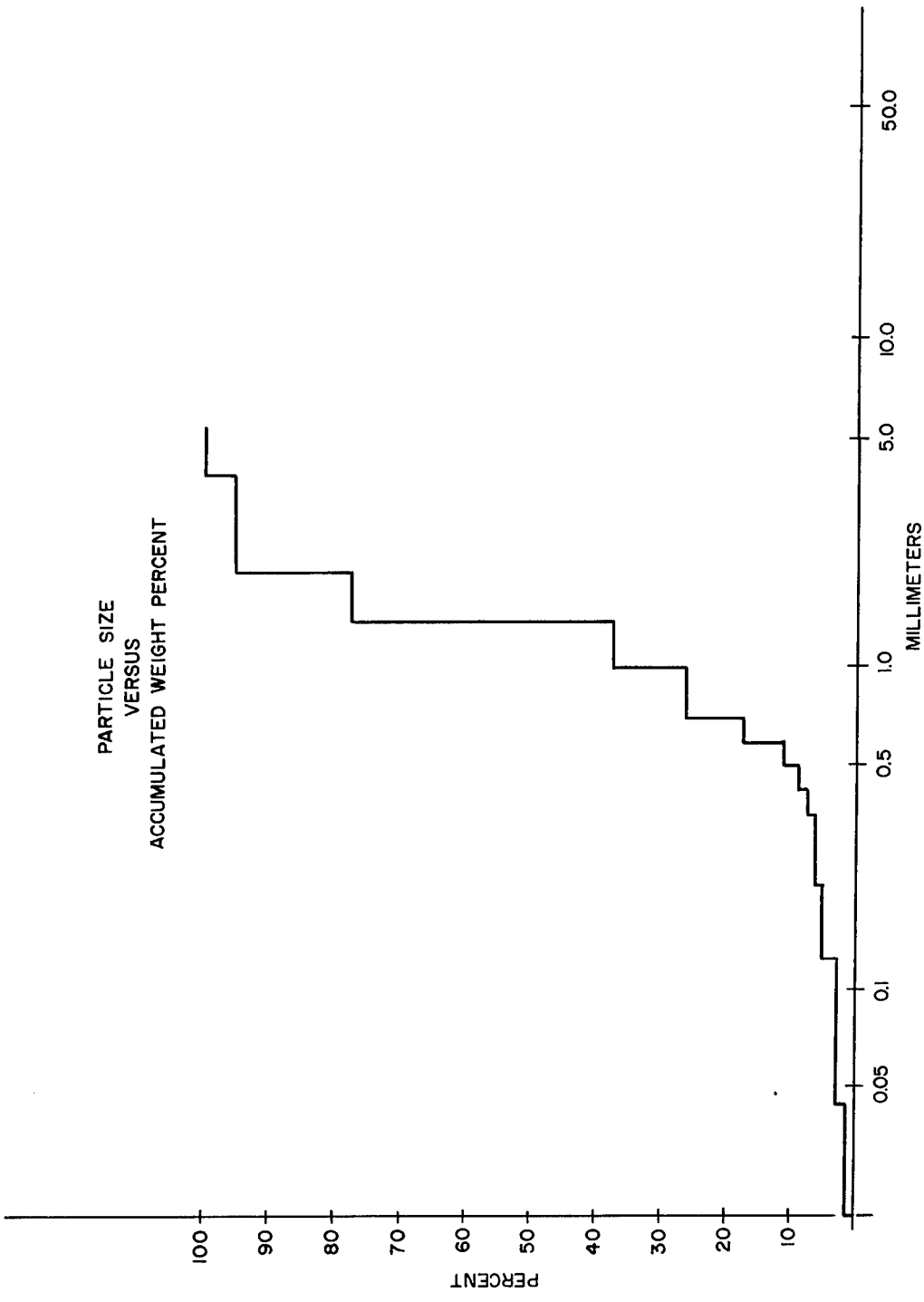

Figure D-10. Test 11

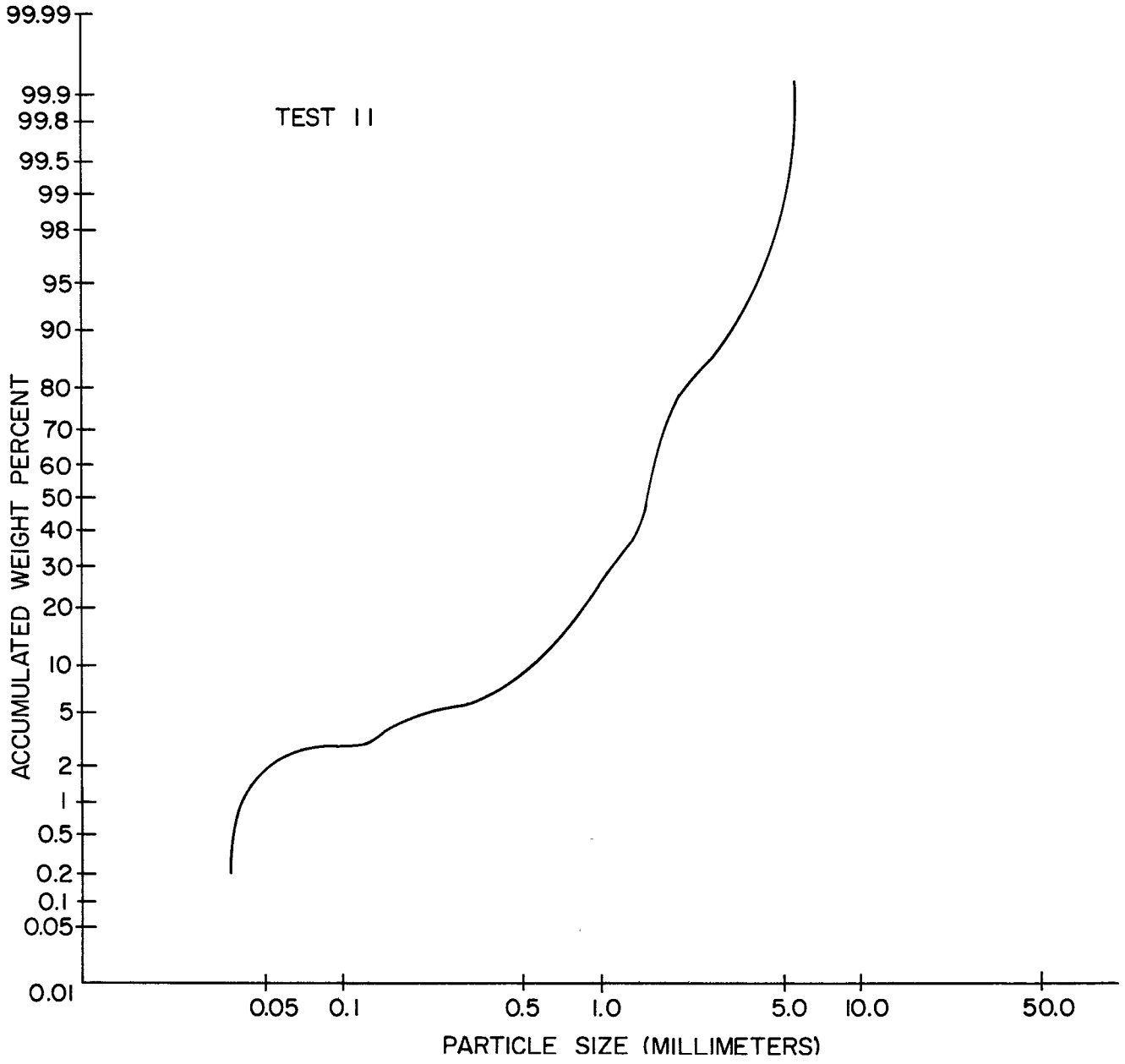

Figure D-10. (Cont). Log Probability Versus Particle Size

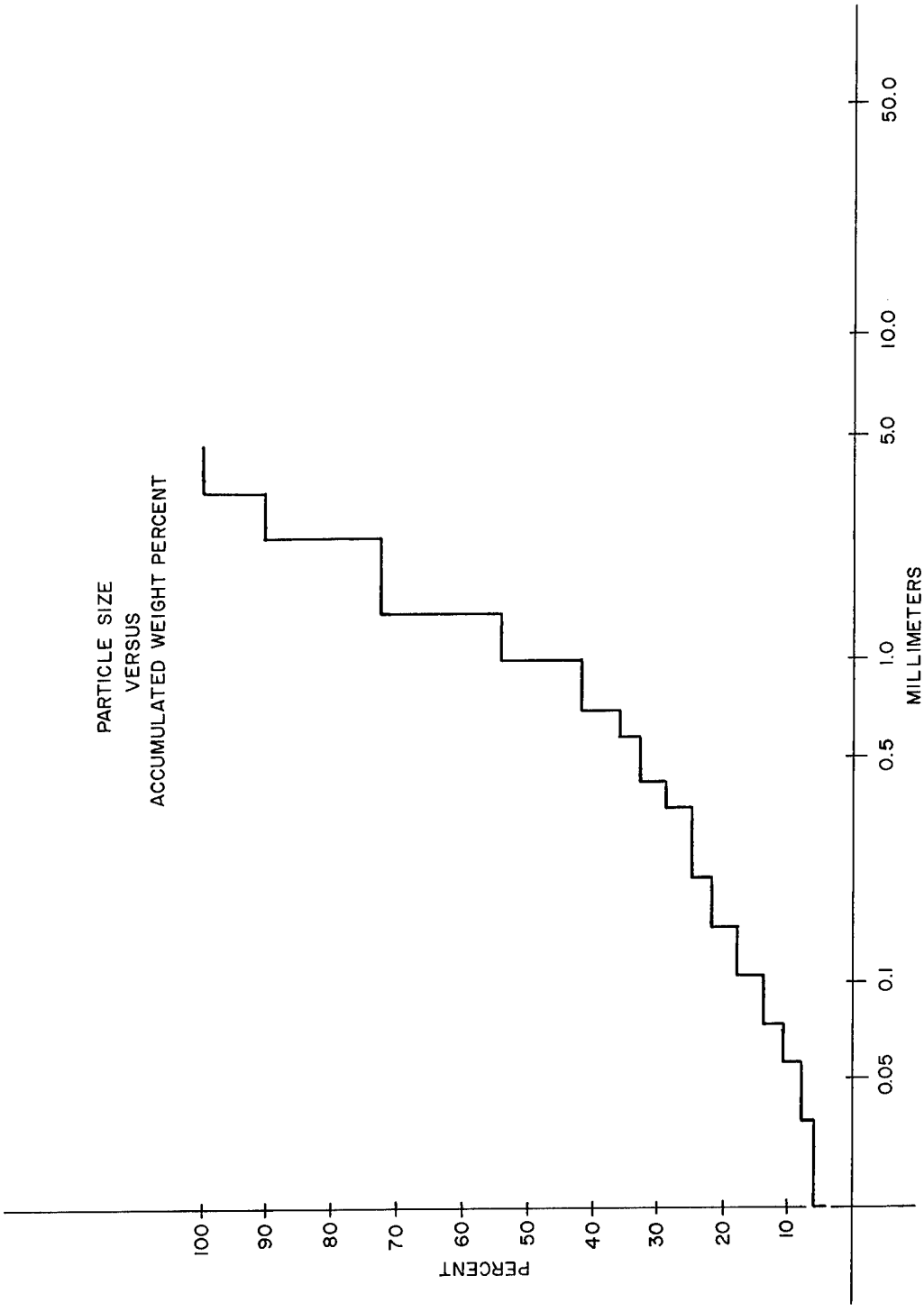

Figure D-11. Test 14

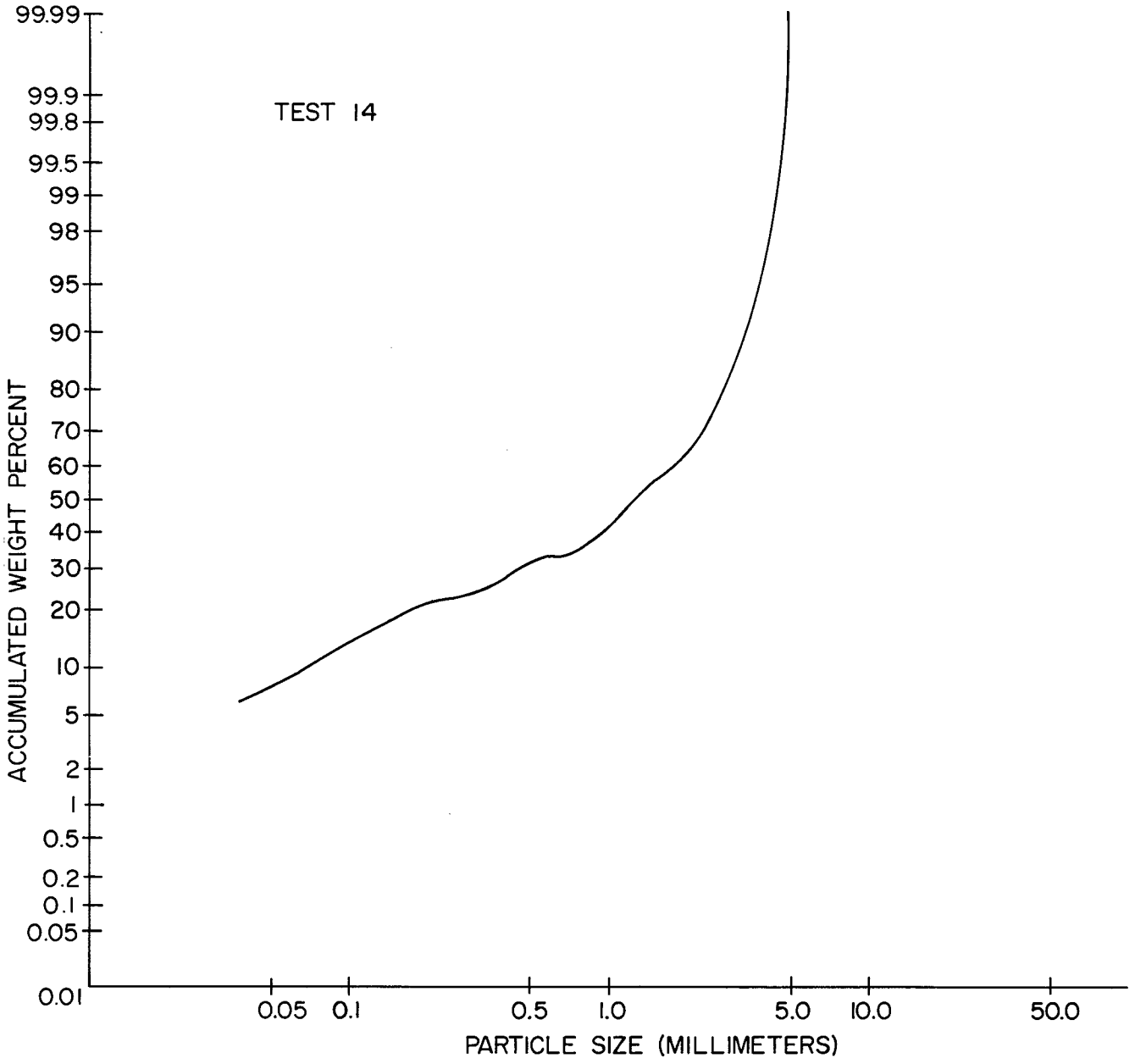

Figure D-11. (Cont). Log Probability versus Particle Size

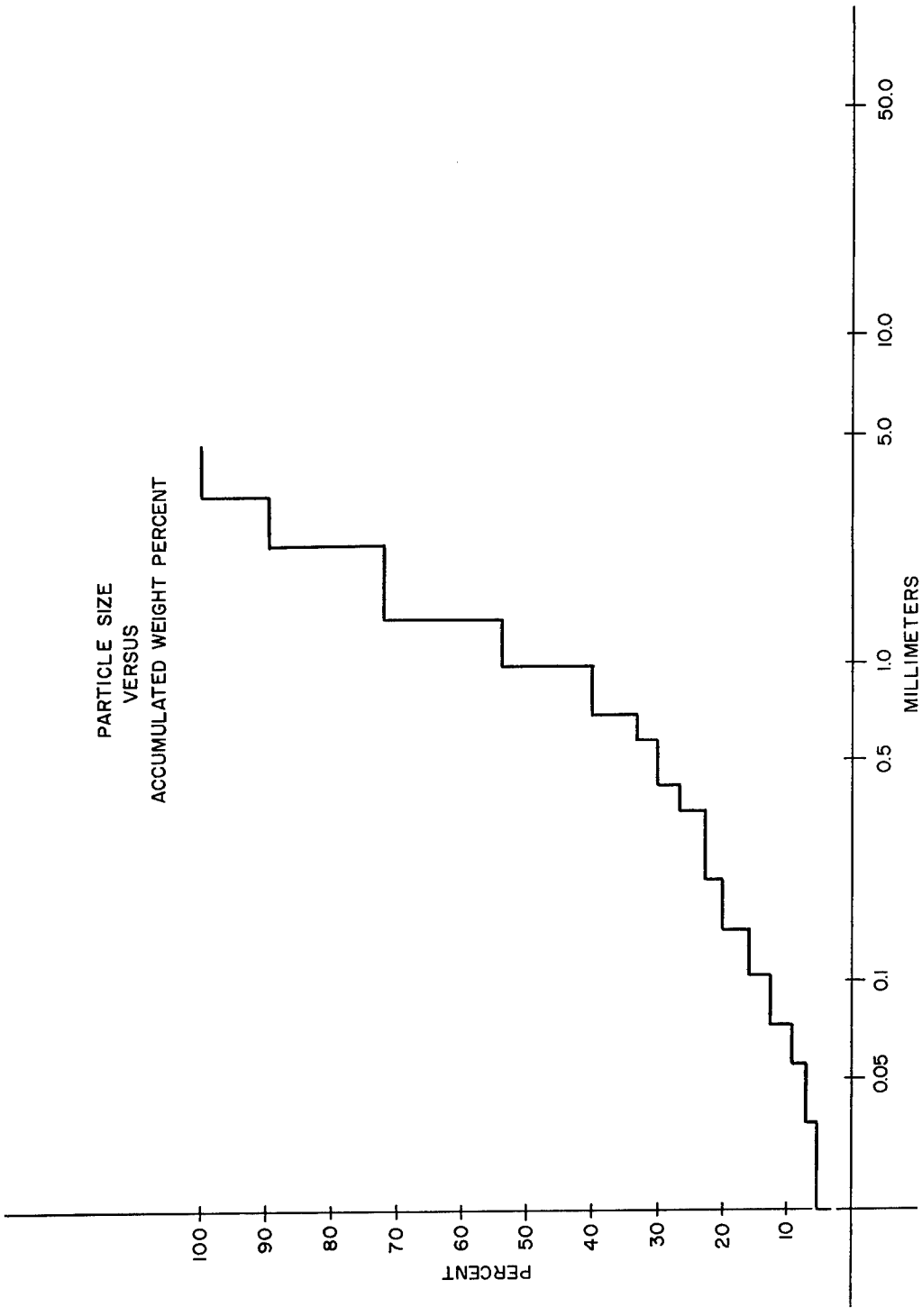

Figure D-12. Test 15

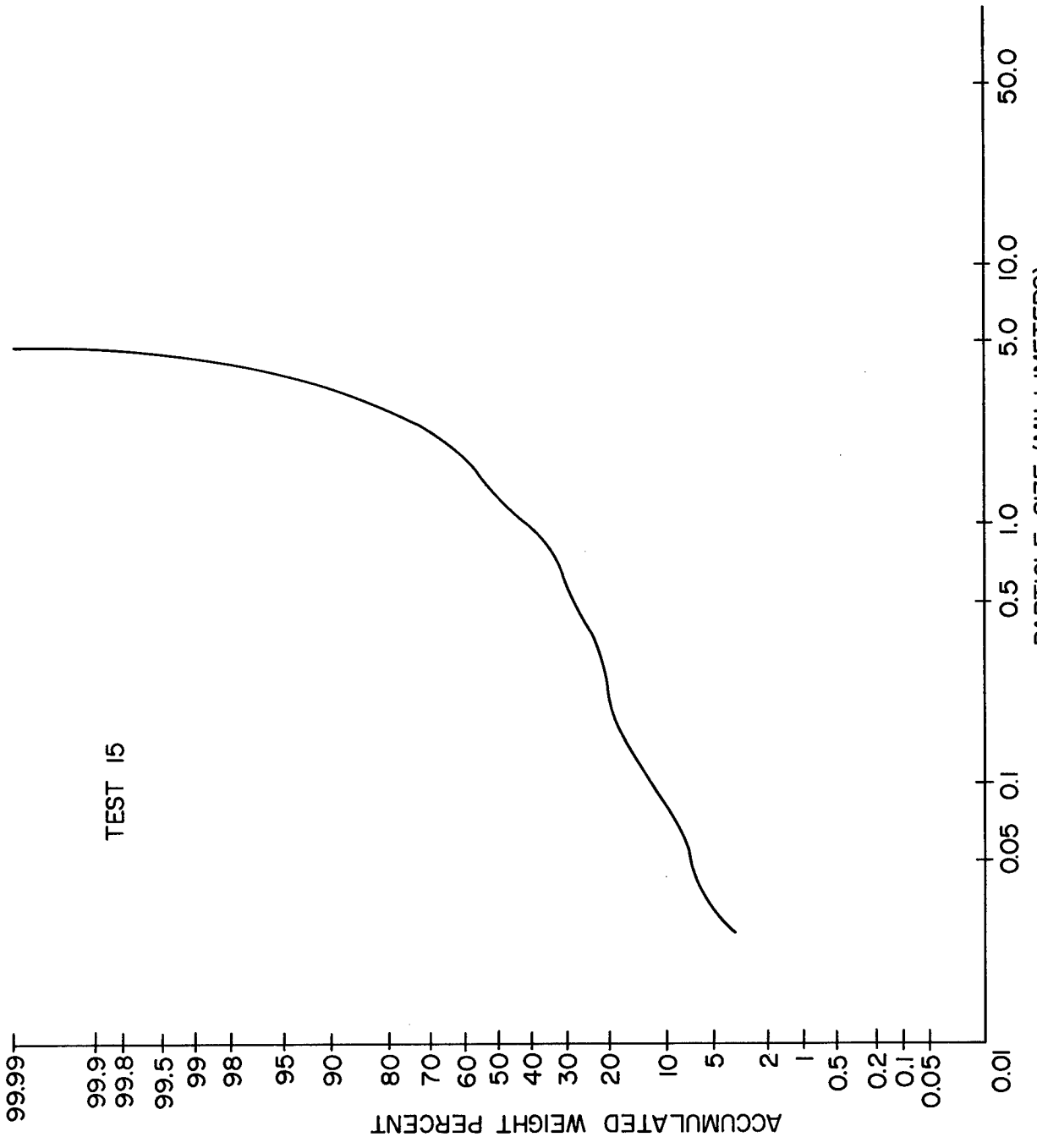

Figure D-12. (Cont). Log Probability versus Particle Size

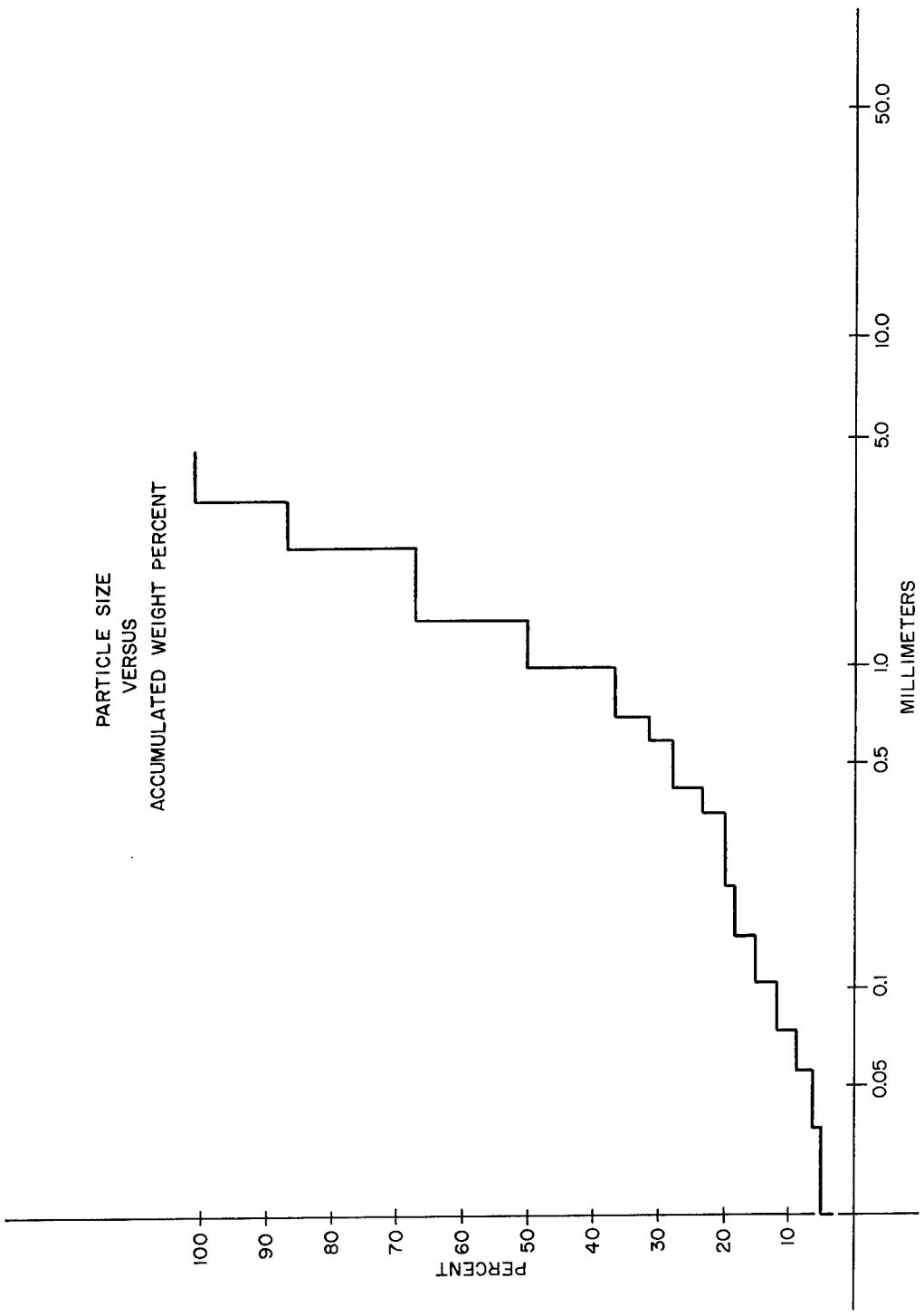

Figure D-13. Test 16

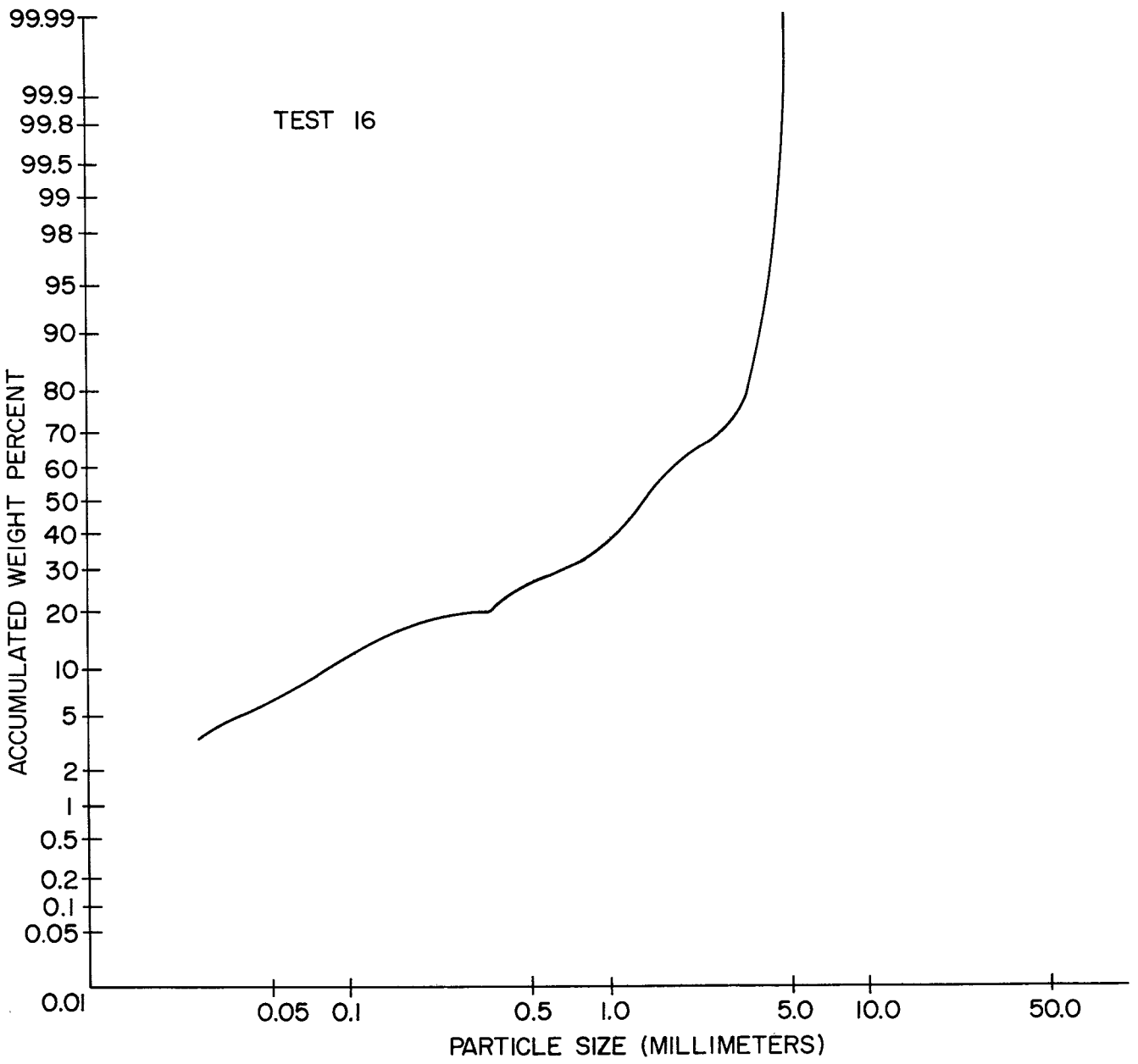

Figure D-13. (Cont). Log Probability versus Particle Size

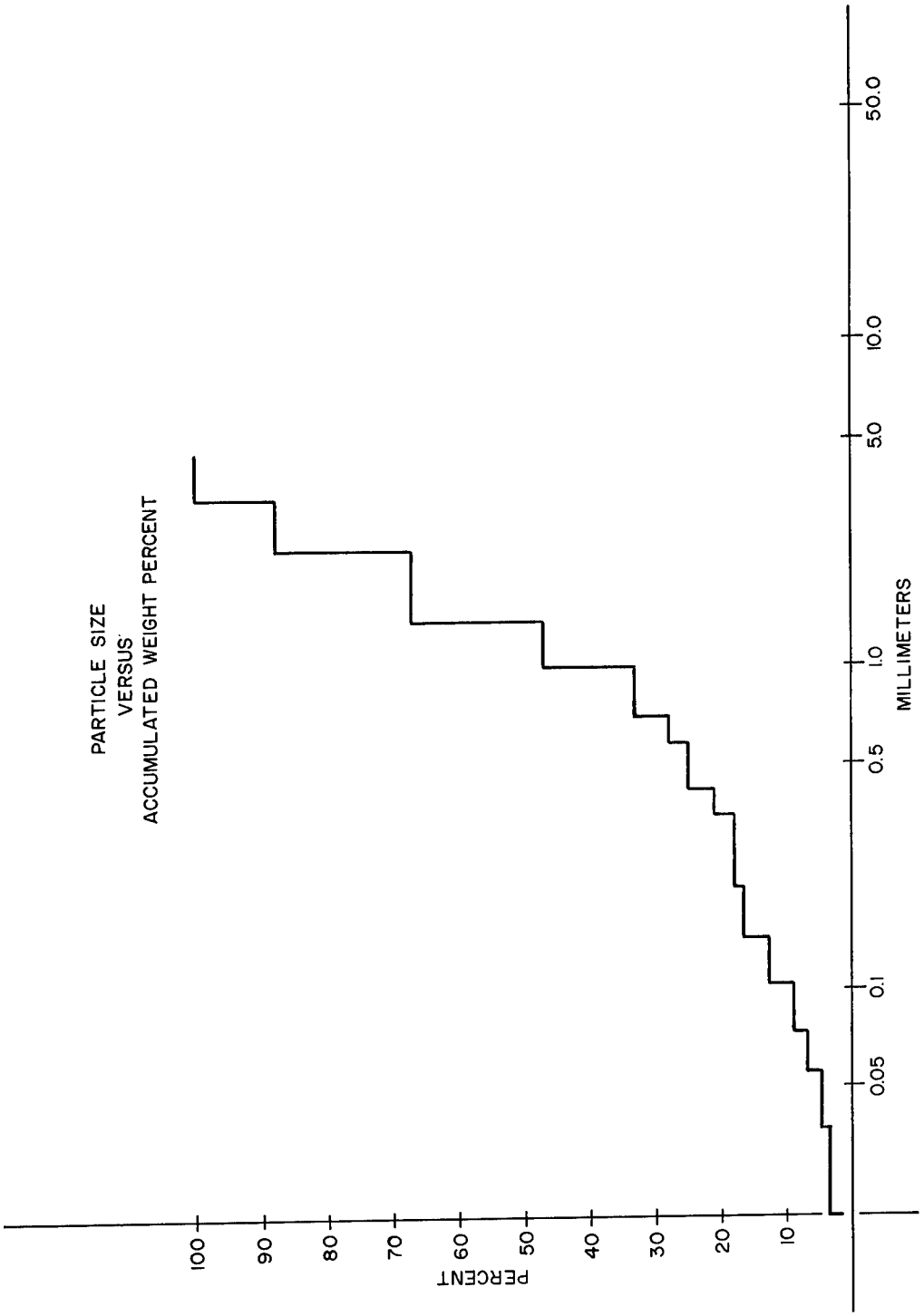

Figure D-14. Test 18

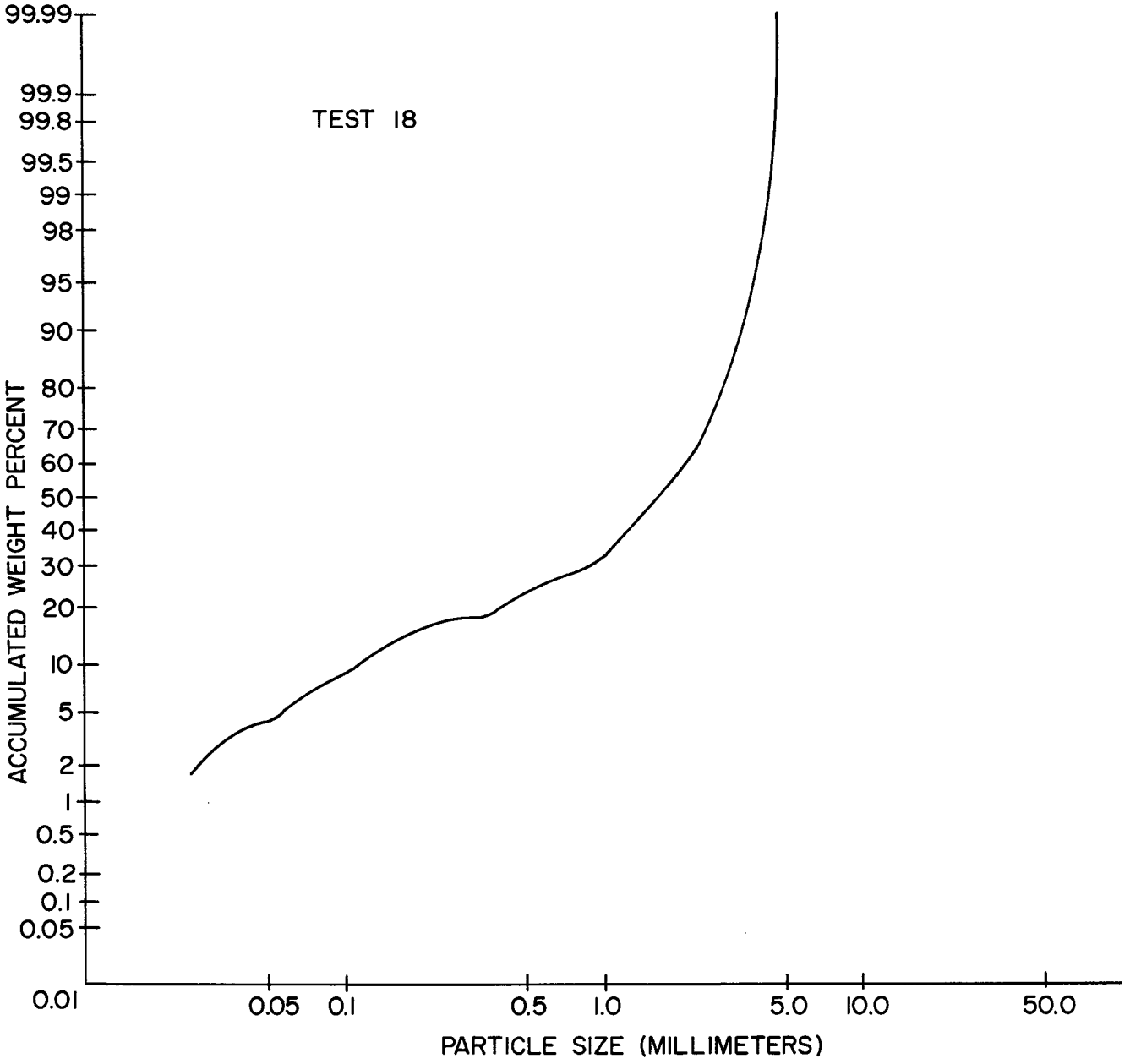

Figure D-14. (Cont). Log Probability versus Particle Size

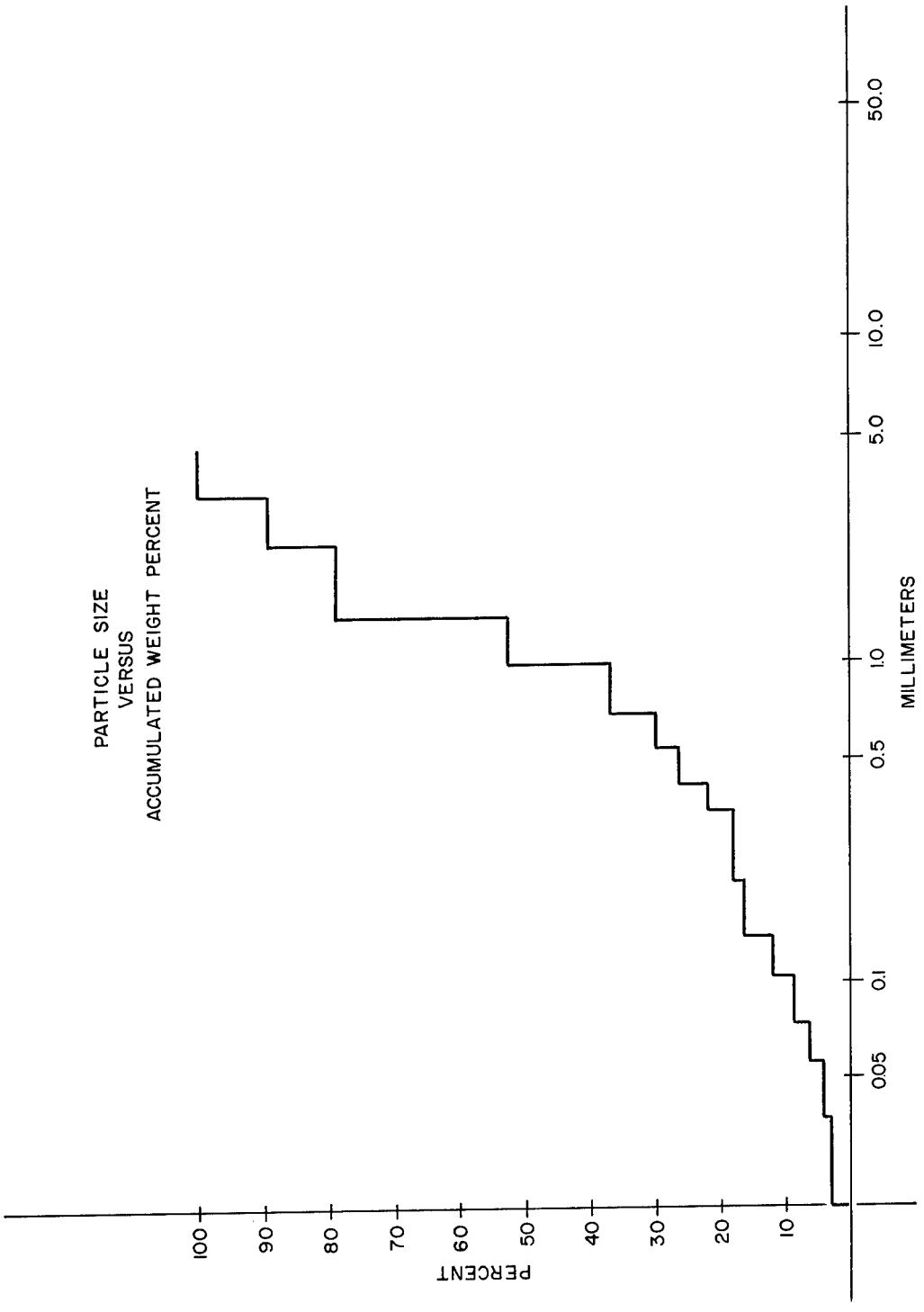

Figure D-15. Test 19

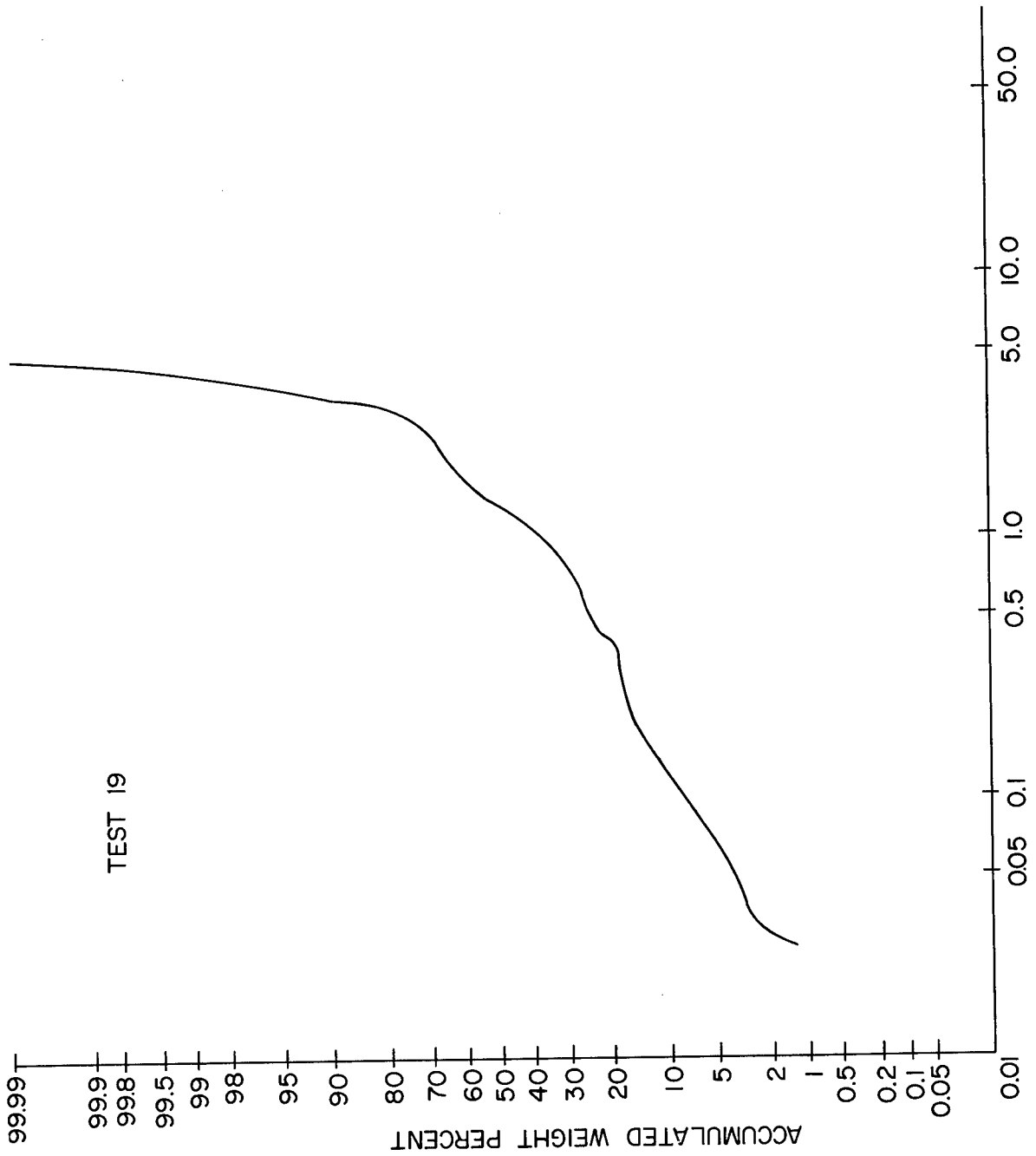

Figure D-15. (Cont). Log Probability versus Particle Size

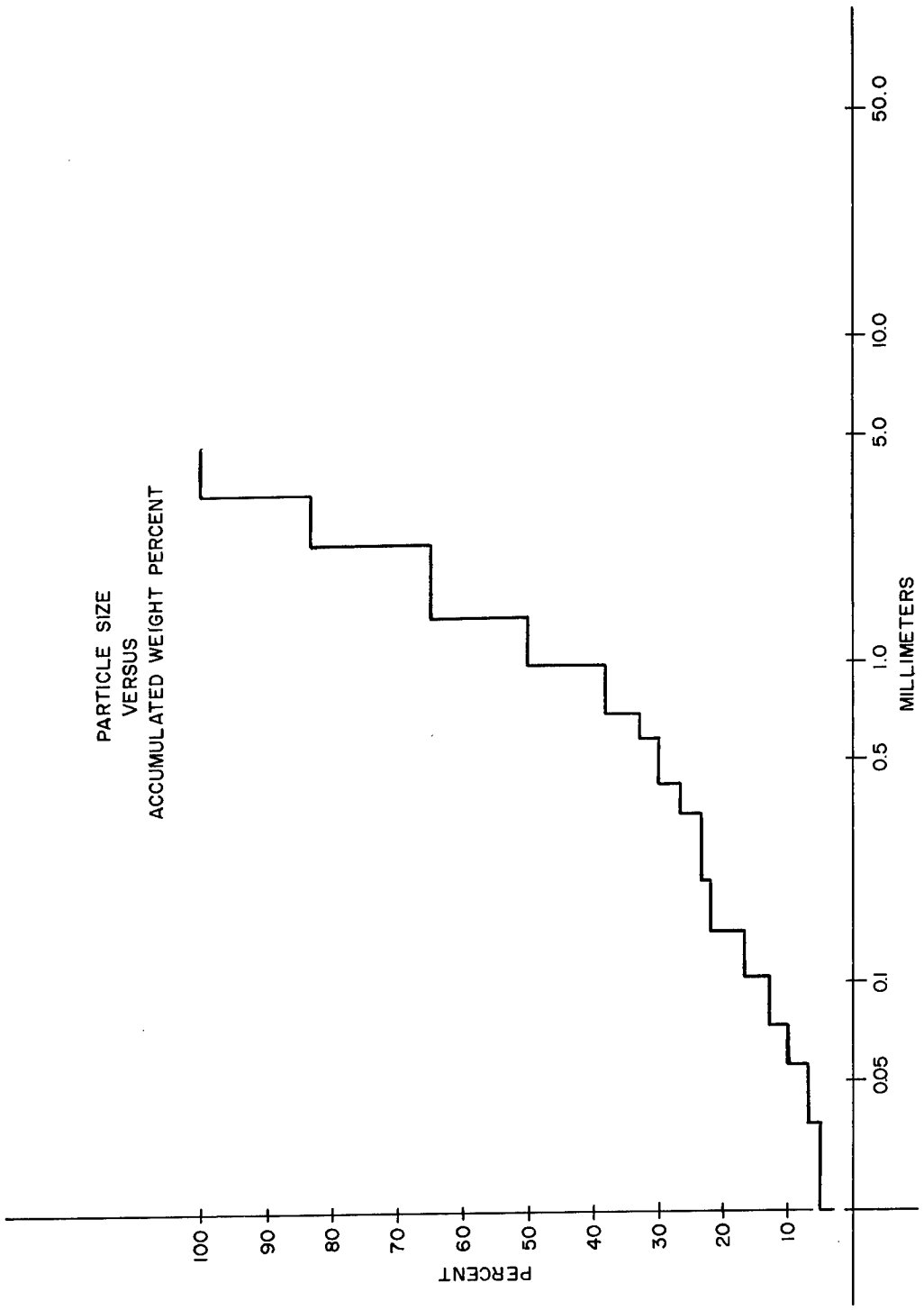

Figure D-16. Test 20

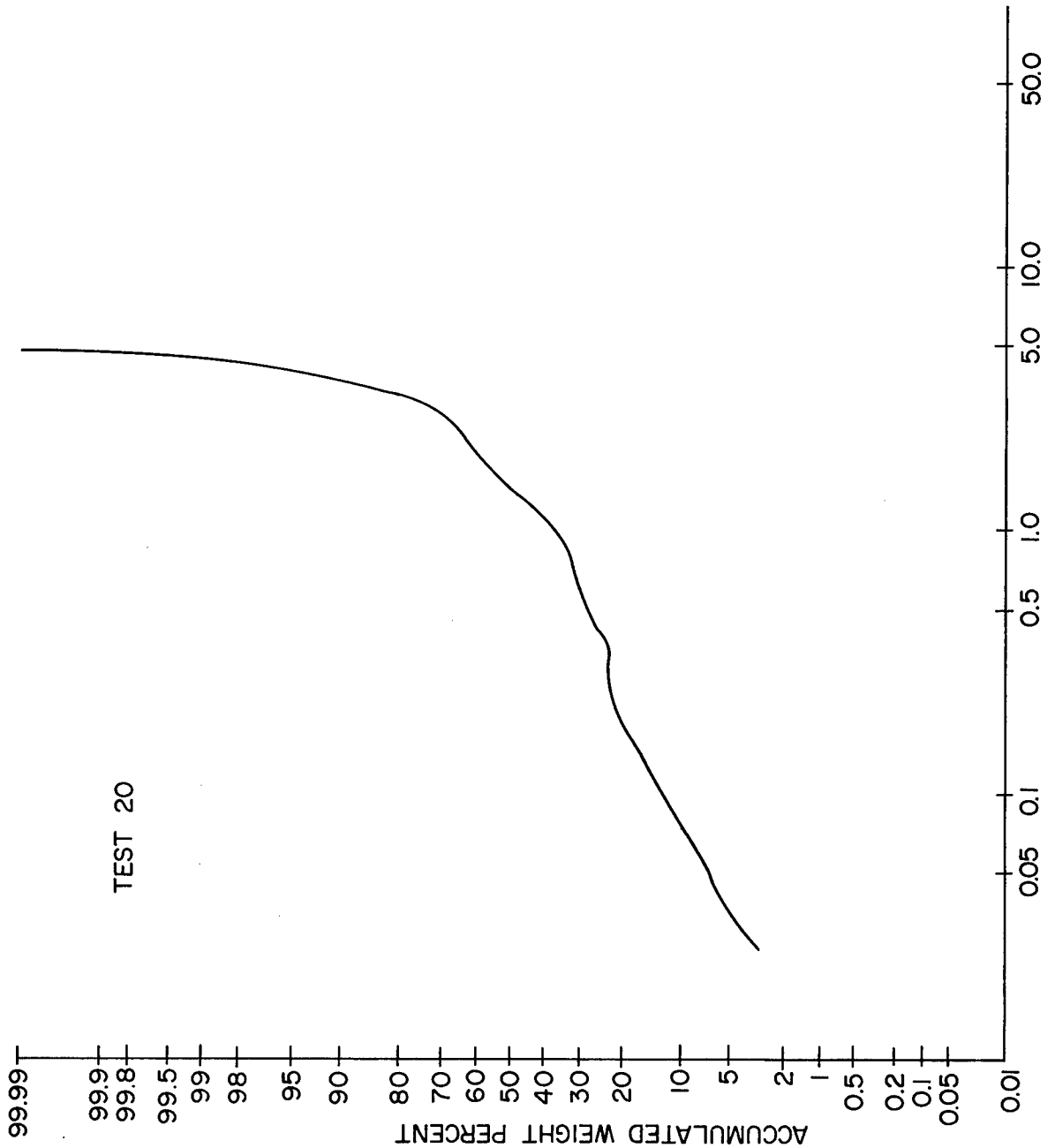

Figure D-16. (Cont). Log Probability versus Particle Size

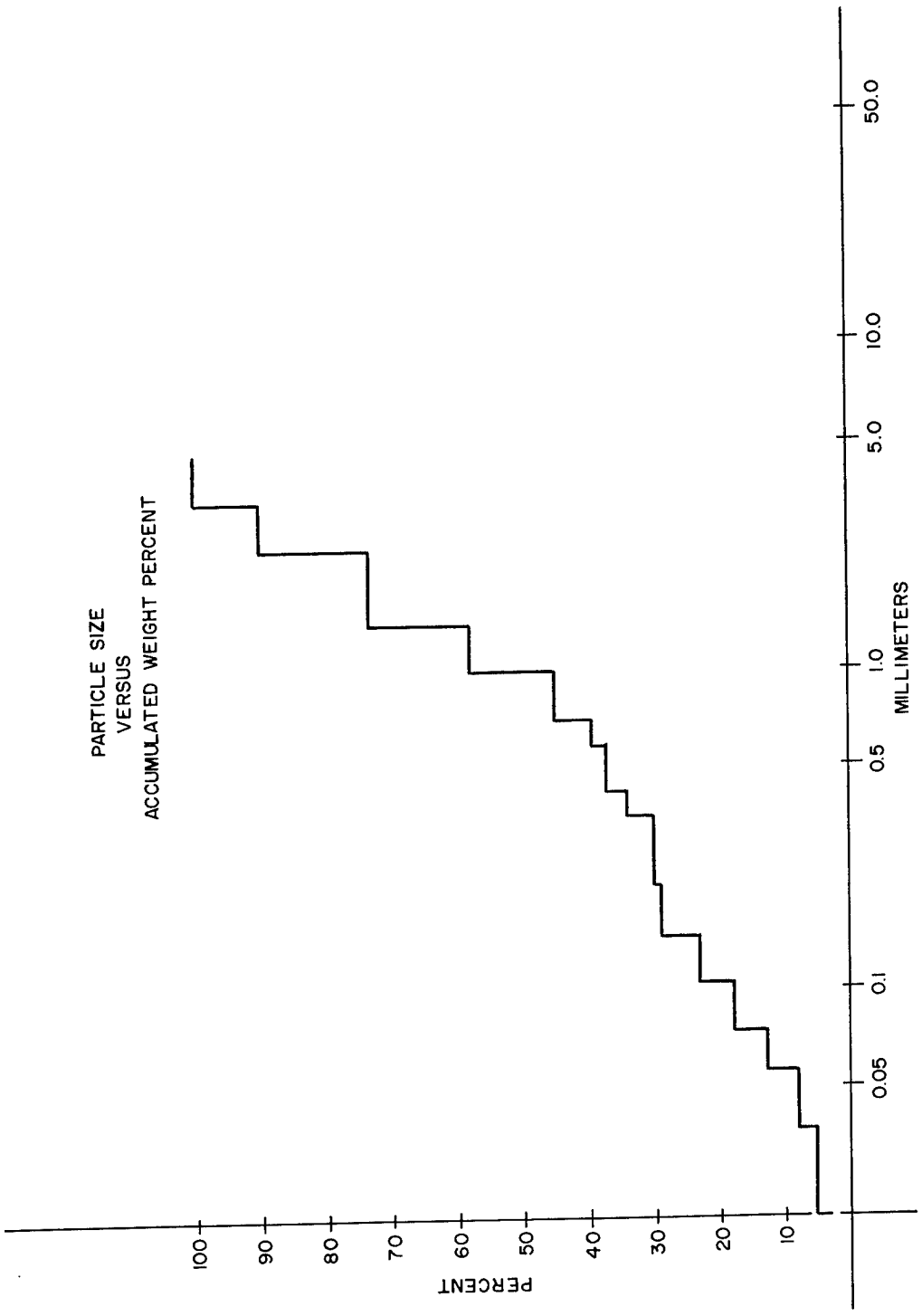

Figure D-17. Test 22

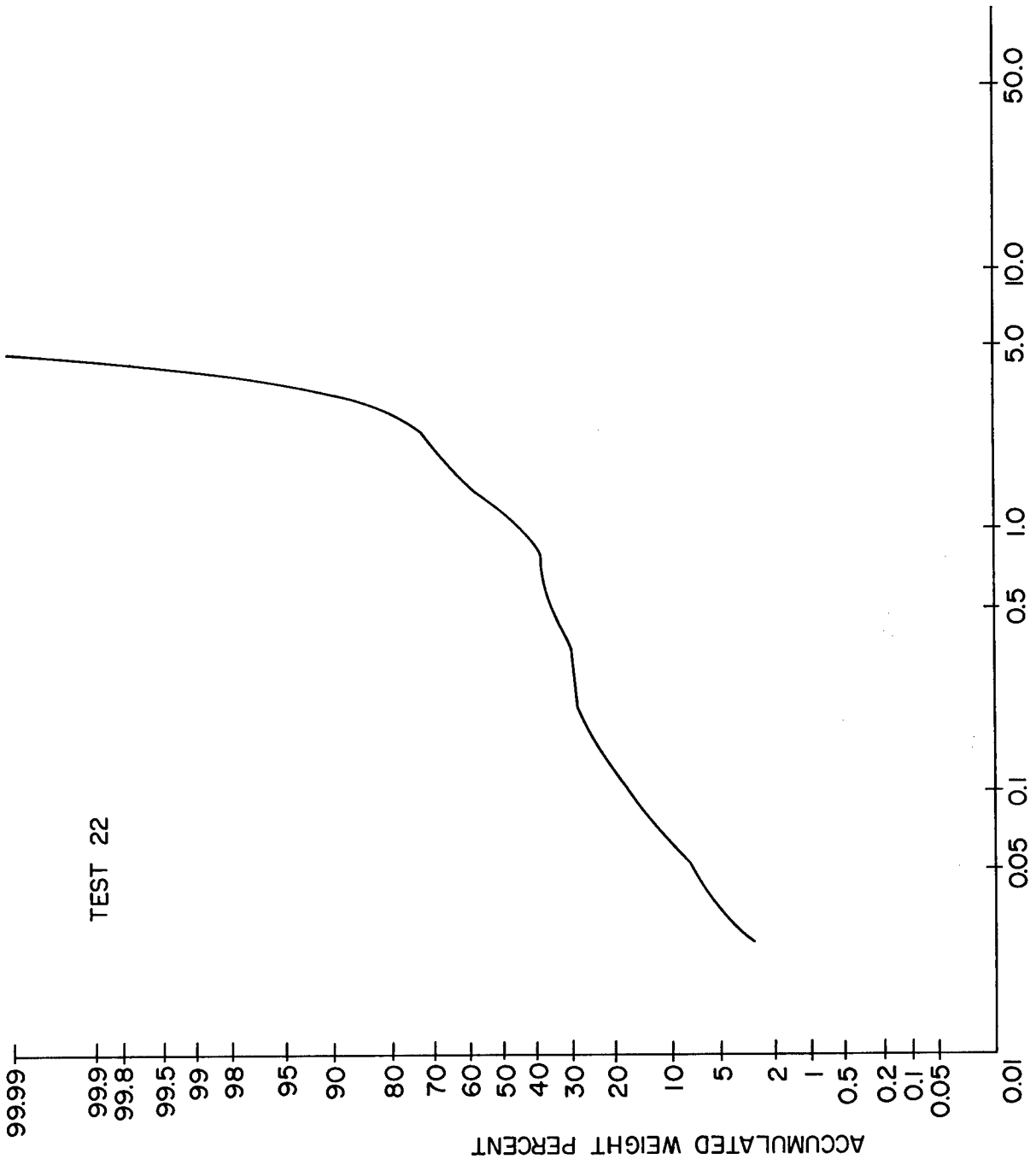

Figure D-17. (Cont). Log Probability versus Particle Size

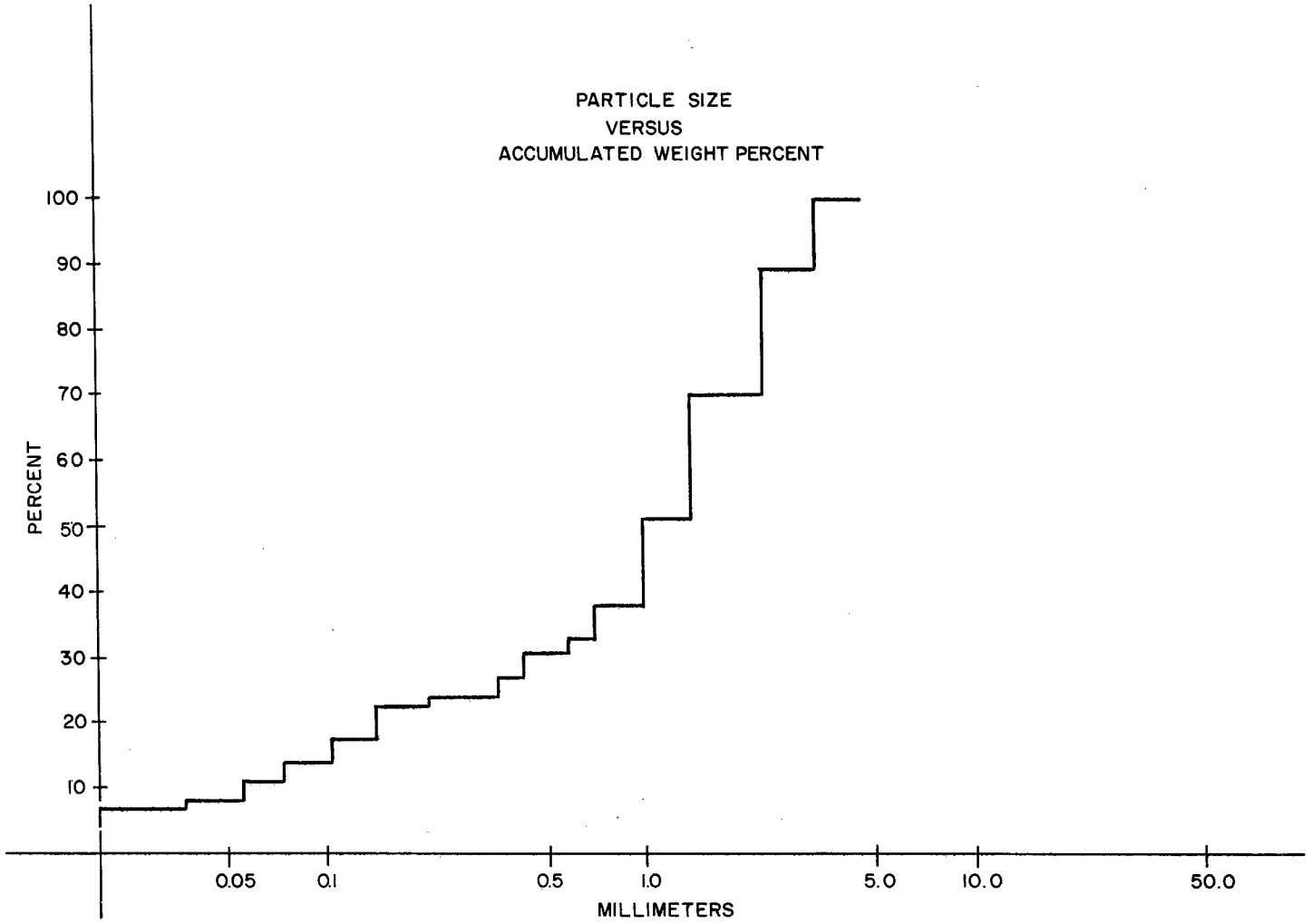

Figure D-18. Test 23

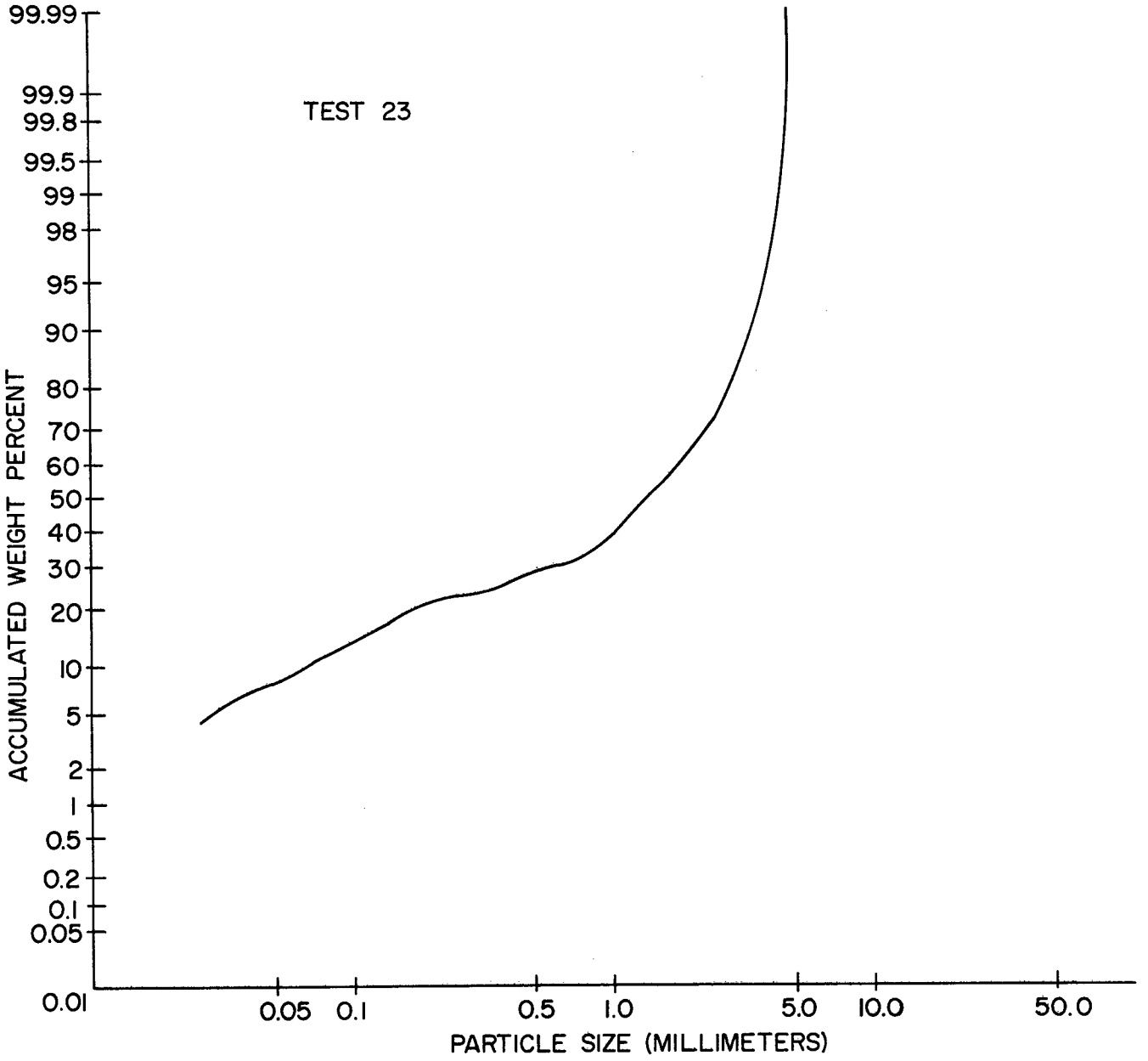

Figure D-18. (Cont). Log Probability versus Particle Size

APPENDIX E

VELOCITY DATA

VELOCITY DATA

Velocity data from photographic film were determined from selected development tests. The lead times required for analyzing the photographic film did not allow the data from all tests to be recorded. The data that were tabulated for several tests are representative of the velocities experienced during the solid graphite block tests (Groups 1 and 2) and the scale model tests (Group 3).

The increased containment and the formation of jets in scale model tests reduced the velocity substantially.

Group 1 and 2 test velocities

Test 5		Test 9		Test 11	
Displacement from Ground Zero (ft)	Average Velocity (fps)	Displacement from Ground Zero (ft)	Average Velocity (fps)	Displacement from Ground Zero (ft)	Average Velocity (fps)
1.27	882	1.85	1229	1.17	1421
1.62	938	2.68	1186	2.2	1335
1.92	882	3.54	1176	2.9	1185
2.22	882	4.31	1146	Average	1314
2.52	938	Average	1184		
2.84	941				
3.11	882				
3.45	1000				
3.75	941				
4.05	882				
4.35	1000				
4.64	882				
4.95	941				
Average	922				

Group 3 test velocities

Horizontal Displacement from Ground Zero (ft)	Average Velocity (fps)	Vertical Displacement from Ground Zero (ft)	Average Velocity (fps)	Angle (degrees)
		Test 20		
3.4	493			
4.5	551			
5.3	551			
6.0	544			
6.8	551			
7.5	544			
8.0	522			
8.1	489			
9.3	451	0.82	39.0	5.0
10.5	476	0.89	40.4	4.9
11.0	468	0.92	40.0	4.8
12.0	483	1.17	47.1	5.9
13.4	462	1.4	48.0	6.0
		Test 23		
3.5	362			
6.8	352	0.81	41.9	6.8
11.0	379	1.45	50.0	7.5
14.7	381	2.04	52.8	7.9
19.0	394	2.60	53.8	7.8

These velocity data plotted indicate the reduced velocity caused by containment and jet formation.

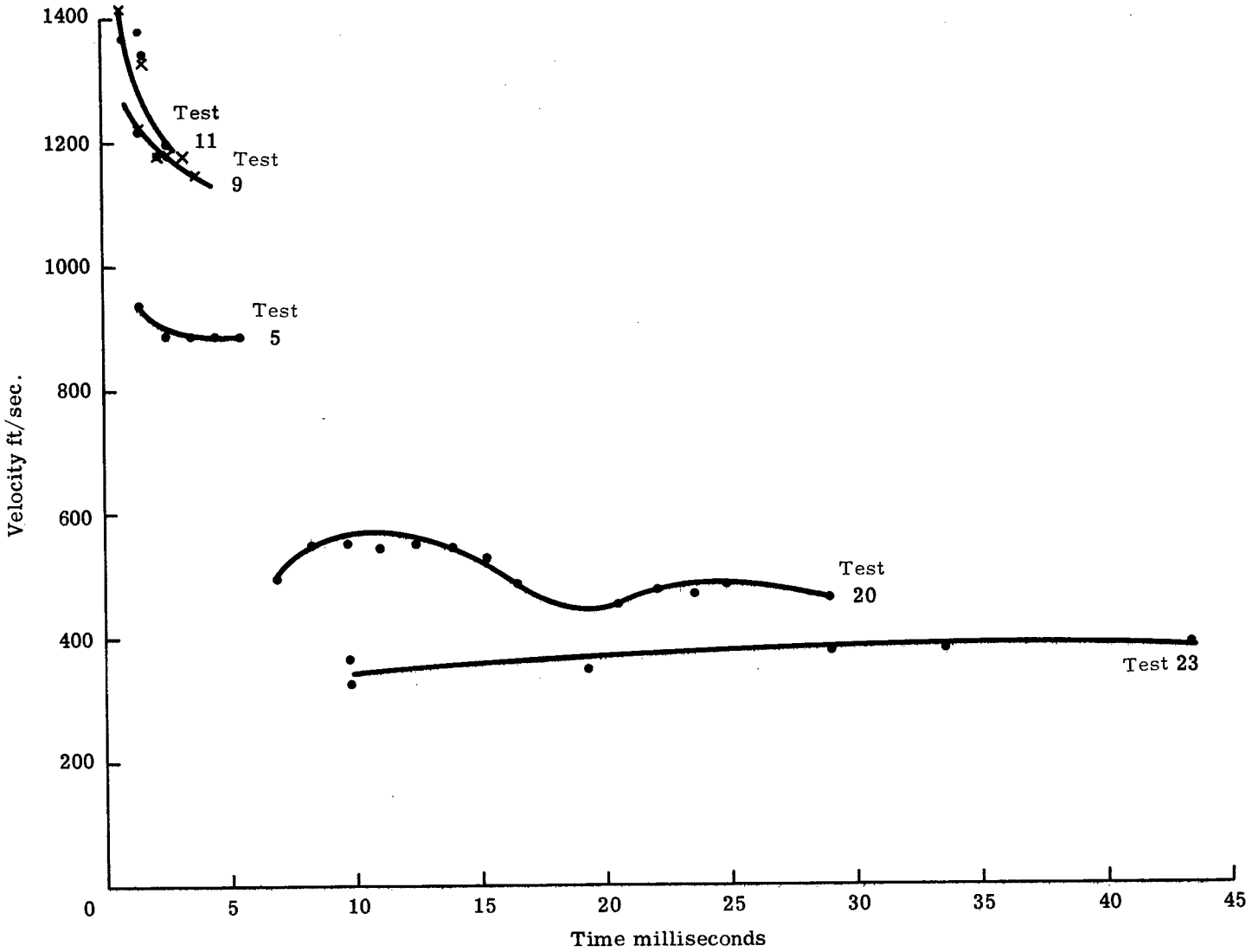

Particle Velocity Versus Time

APPENDIX F

ROVER/NERVA DEVELOPMENT DESTRUCT
(Photographs of representative particles from each screen size)

The photographs in this appendix show representative particles from each screen size used to grade the particles collected in the polystyrene foam during explosive destruct. Each photo shows the particle size represented and the magnification used to give a good picture of the shape of the particles in that screen size.

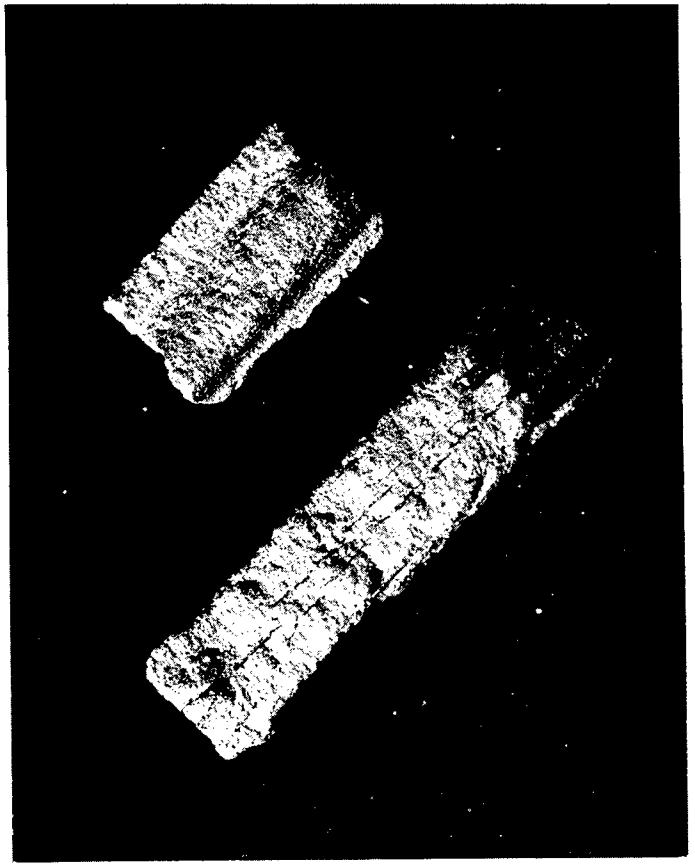

Particle size: 4.76 mm
Magnification: 4X

Particle size: 3.36 mm
Magnification: 4X

Particle size: 2.38 mm
Magnification: 4X

Particle size: 1.41 mm
Magnification: 4X

Particle size: 1.00 mm
Magnification: 4X

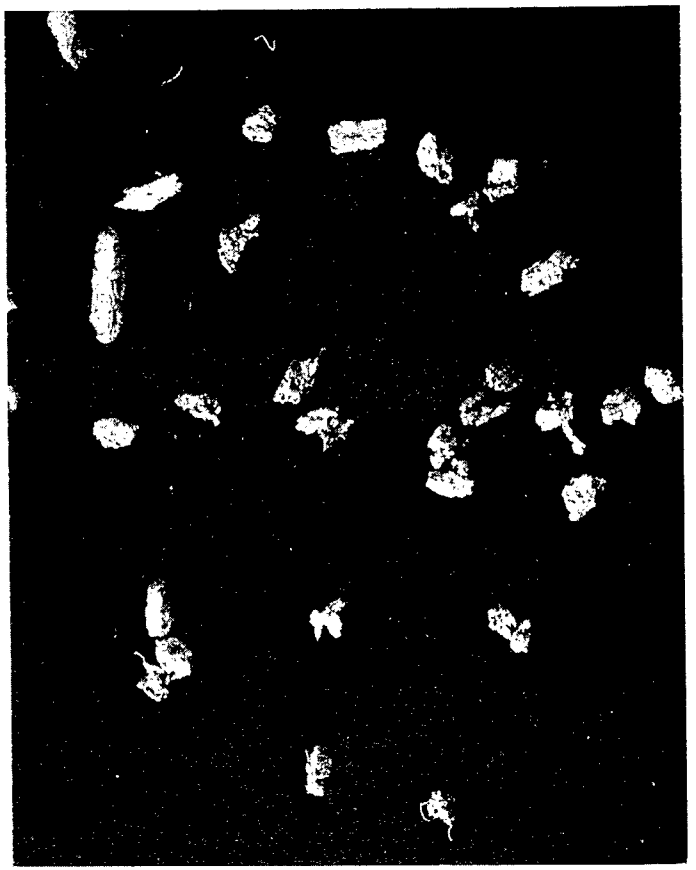

Particle size: 0.841 mm
Magnification: 4X

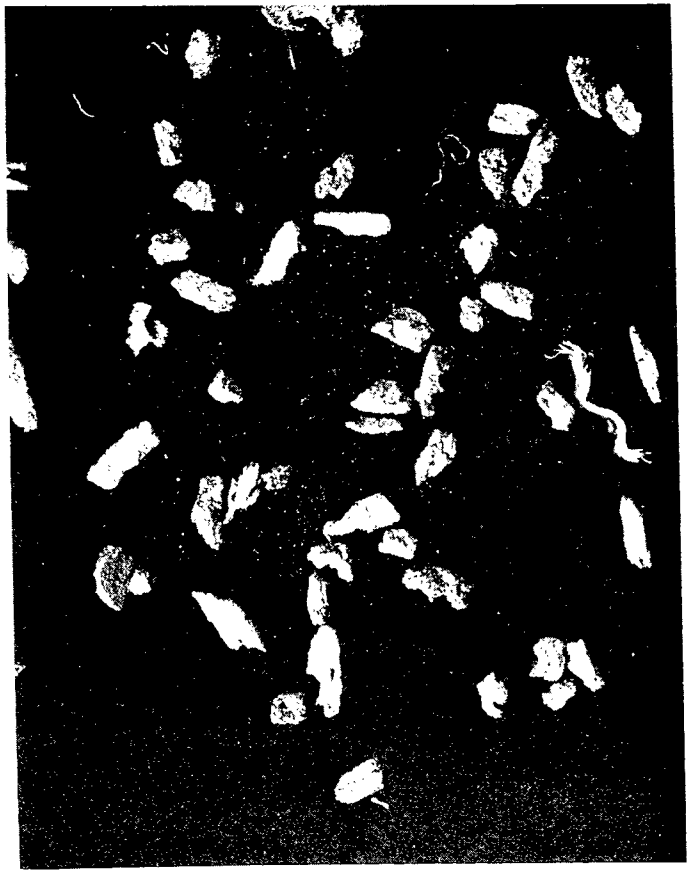

Particle size: 0.707 mm
Magnification: 4X

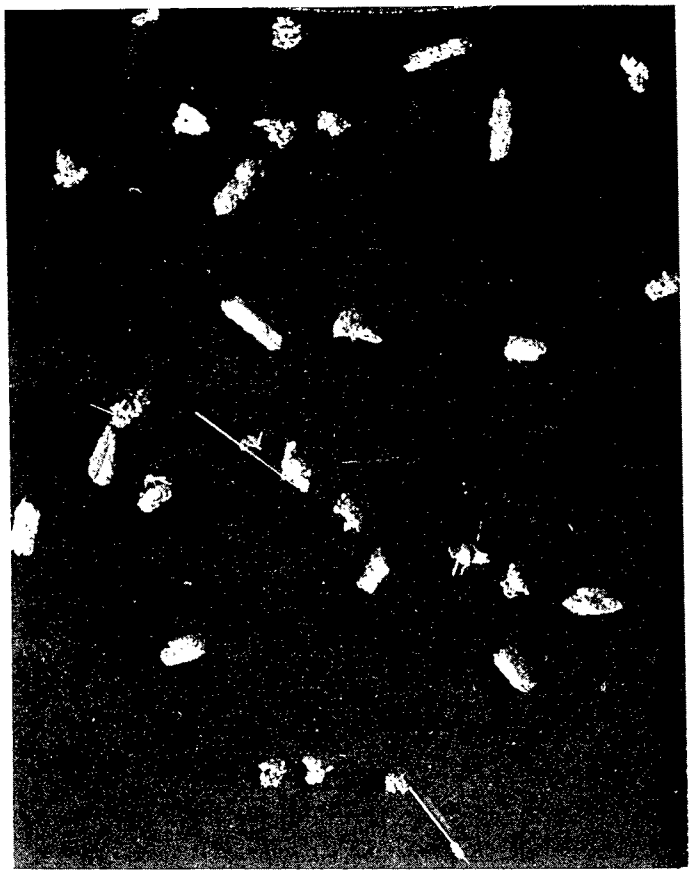

Particle size: 0.595 mm
Magnification: 4X

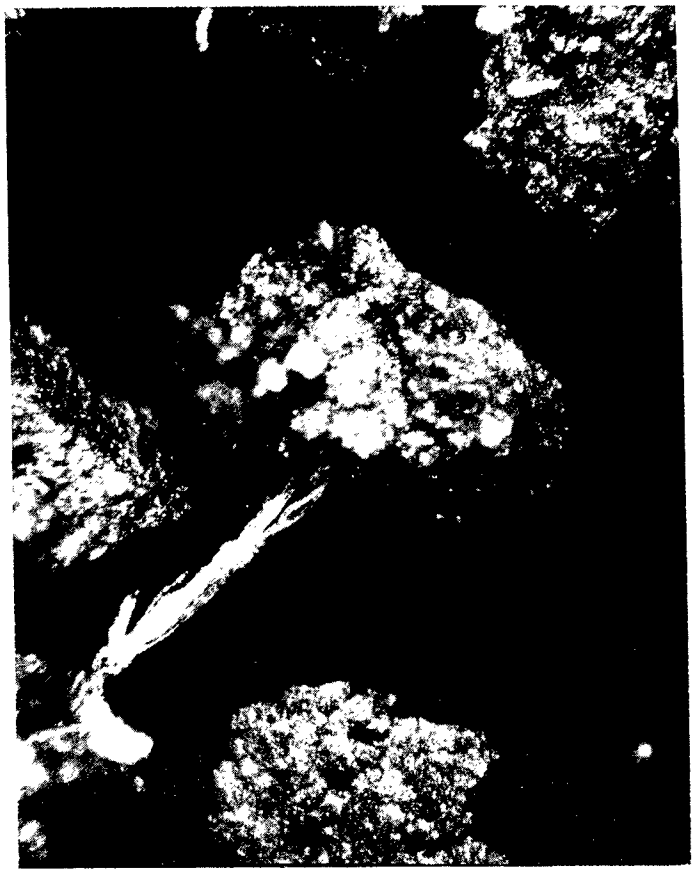

Particle size: 0.420 mm
Magnification: 63X

Particle size: 0.354 mm
Magnification: 63X

Particle size: 0.210 mm
Magnification: 63X

Particle size: 0.149 mm
Magnification: 63X

Particle size: 0.105 mm
Magnification: 63X

Particle size: 0.074 mm
Magnification: 63X

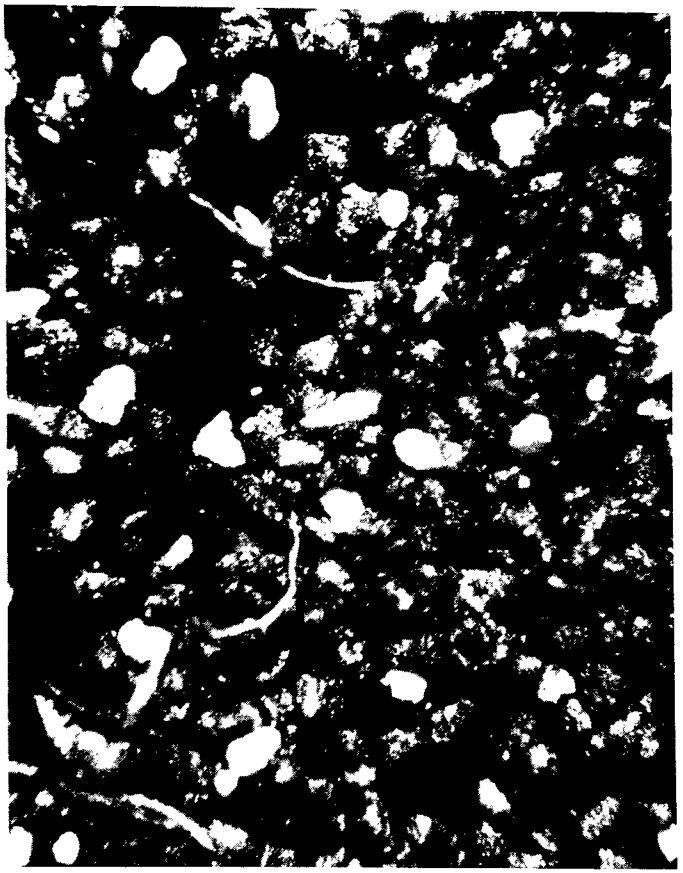

Particle size: 0.063 mm
Magnification: 63X

Particle size: 0.053 mm
Magnification: 63X

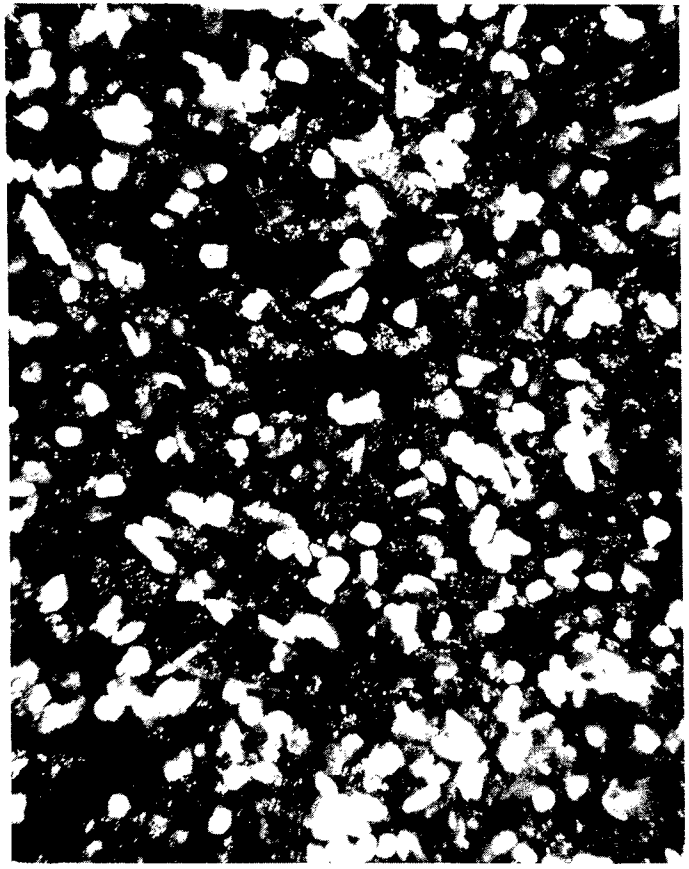

Particle size: 0.044 mm
Magnification: 63X

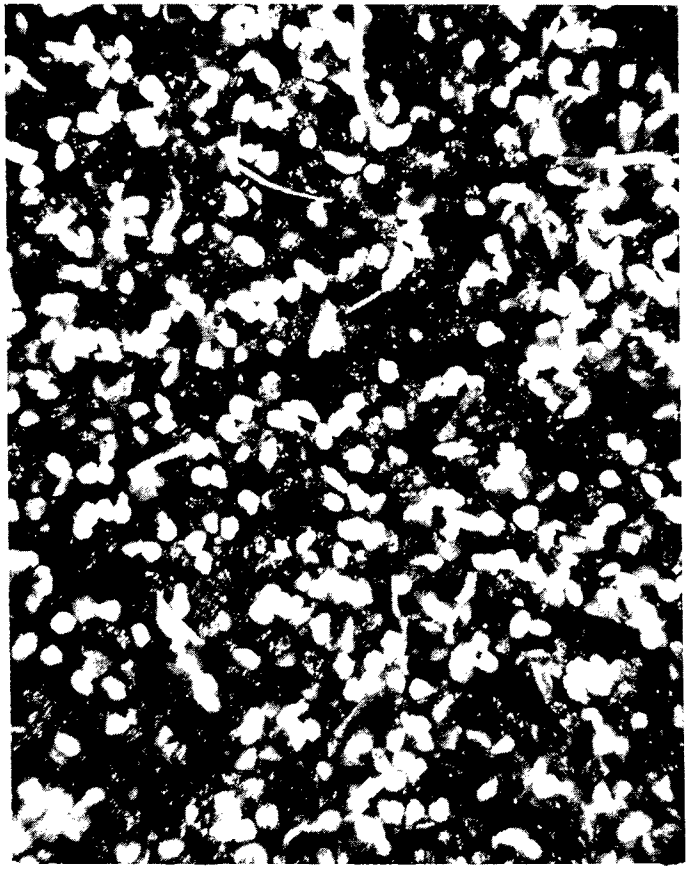

Particle size: 0.037 mm
Magnification: 63X

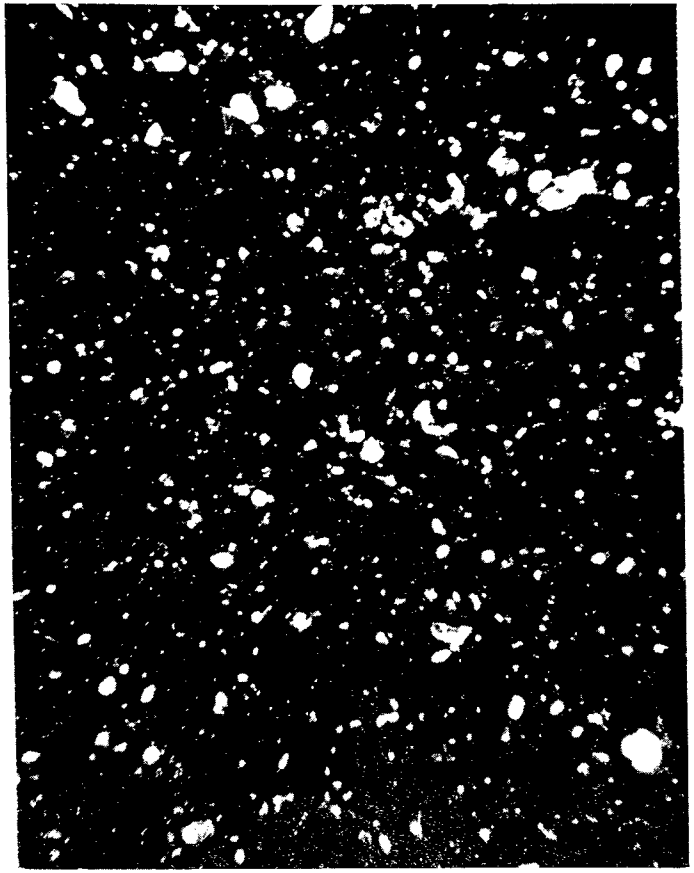

Particle size: Less than 0.037 mm
Magnification: 63X

DISTRIBUTION:

USAEC
Asst. General Manager for Reactors
Washington, D. C. 20545
Attn: J. A. Swartout

USAEC, DSNS
Washington, D. C. 20545
Attn: H. B. Finger, Director (1)
G. P. Dix, Chief, Safety Branch, SEPO (1)
W. A. Yingling, SNPO (1)
C. P. McCallum, Safety Branch, SEPO (1)
R. T. Carpenter, Chief, Isotopic Power System Branch, SEPO (1)
C. E. Johnson, Chief, Reactor Power Systems Branch, SEPO (1)

USAEC
Division of Reactor Development & Technology
Washington, D. C. 20545
Attn: J. A. Lieberman

USAEC
Office of the Assistant General
Council for Patents
Washington, D. C. 20545
Attn: Roland A. Anderson

USAEC
Division of Isotope Development
Washington, D. C. 20545
Attn: A. Berman (1)
W. K. Kern (1)

USAEC
Division of Military Application
Washington, D. C. 20545
Attn: Brig. General D. L. Crowson, USAF

USAEC
Division of Biology and Medicine
Washington, D. C. 20545
Attn: H. D. Bruner, Asst. Director Medical and Health Research (1)
Dr. Roger McClellan (1)
J. Z. Holland, Chief, Fallout Studies Br. (1)

USAEC
Reactor Division of Safety Standards
Washington, D. C. 20545
Attn: J. J. Dinunno, Asst. Director

USAEC
Director of Regulation
Washington, D. C. 20545
Attn: H. L. Price

USAEC
DSNS, Space Nuclear Prop. Office
Washington, D. C. 20545
Attn: R. S. Decker, Jr., Chief, Safety Branch (3)

USAEC
Division of Technical Information
Headquarters Library, G-017
Washington, D. C. 20545 (3)

Space Nuclear Propulsion Office
Lewis Research Center
21000 Brookpark Road
Cleveland, Ohio 44135
Attn: L. Nichols

USAEC New York Operations Office
376 Hudson Street
New York, New York 10014
Attn: A. L. Rizzo, Health & Safety Lab. (1)
J. Harley, Health & Safety Laboratory (1)
G. Silverman (1)
W. Sullivan (1)

USAEC Albuquerque Operations Office
P. O. Box 5400
Albuquerque, New Mexico 87115
Attn: S. A. Upson, Director, Research and Classification Div. (1)

USAEC Canoga Park Area Office
P. O. Box 591
Canoga Park, California
Attn: J. V. Levy, Area Manager (1)
C. A. Malmstrom (1)

USAEC
San Francisco Operations Office
2111 Bancroft Way
Berkeley, California 94704
Attn: Technical Services Division

USAEC
Chicago Operations Office
9800 South Cass Avenue
Argonne, Illinois 60439
Attn: Chief, Office Services Branch

U. S. Atomic Energy Commission
Oak Ridge Operations Office
Mail and Document Accountability Sect.
P. O. Box E
Oak Ridge, Tennessee 37831
Attn: Director, Research and Development Div.

Headquarters
Air Force Systems Command (SCIZN)
Washington, D. C. 20331
Attn: Nuclear Safety Branch

Director Nuclear Safety (AFINS)
Chief, Reactor & Advanced Systems Div.
Kirtland Air Force Base, New Mexico
Attn: Col. D. C. Jameson (AFINS-R)

DISTRIBUTION (cont):

Deputy, the Inspector General, USAF
Director Nuclear Safety
Kirtland Air Force Base, New Mexico
Attn: Col. George Ogburn (AFINSR)

Director
Air Force Weapons Laboratory
Kirtland Air Force Base
Albuquerque, New Mexico
Attn: WLIL
For: Lt. Col. M. N. Nold (WLRB) (1)
Lt. Col. H. L. Harris (WLAS) (1)

Space Systems Division
Air Force Unit Post Office
Los Angeles, California 90045
Attn: Technical Library

Air University Library
Maxwell Air Force Base, Alabama
Attn: Elizabeth C. Perkins, AUL3T-7143

Armed Forces Radiobiology Research Ins.
Defense Atomic Support Agency
Washington, D. C. 20014
Attn: Library

Atomics International
P. O. Box 309
Canoga Park, California 91304
Attn: R. L. Detterman

Atomics International
Div. North American Aviation, Inc.
1629 K Street, NW
Washington, D. C.
Attn: Miles Huntsinger, Washington Representative

Battelle Memorial Institute
505 King Avenue
Columbus, Ohio 43201
Attn: Dr. H. W. Russell

Battelle Memorial Institute
Pacific Northwest Laboratory
P. O. Box 999
Richland, Washington 99352
Attn: Dr. Roy Thompson

Brookhaven National Laboratory
Technical Information Division
Upton, Long Island, New York 11973
Attn: Research Library

The Boeing Company
P. O. Box 3707
Seattle, Washington 98124
Attn: Maynard D. Pearson, Aero-Space Division

Chief, Defense Atomic Support Agency
P. O. Box 2610
Washington, D. C. 20301
Attn: Document Library Branch

Douglas Aircraft Company, Inc.
Missile and Space Systems Division
3000 Ocean Park Boulevard
Santa Monica, California
Attn: Sid Gromich, Advanced Space Technology

Edgerton, Germeshausen and Grier, Inc.
P. O. Box 98
Goleta, California

E. I. du Pont de Nemours and Company
Savannah River Laboratory
Aiken, South Carolina 29802
Attn: W. B. Scott, Document Div.

General Atomic Division
General Dynamics Corporation
P. O. Box 608
San Diego, California 92112
Attn: Library

General Electric Company
570 Lexington Avenue
New York, New York 10022
Attn: Richard W. Porter, Consultant
Aerospace Science and Technology

General Electric Company
Valley Forge Space Technology Center
Philadelphia, Pennsylvania
Attn: Carl Gamertsfelder, Advanced Requirements
Planning Department

General Electric Company
Valley Forge Space Technology Center
Philadelphia, Pennsylvania
Attn: S. M. Scala

Hittman Associates
P. O. Box 2685
4715 East Wabash Avenue
Baltimore, Maryland

Lockheed Missiles and Space Co.
P. O. Box 504
Sunnyvale, California
Attn: H. H. Greenfield, Manager
Nuclear Power Development (1)
Dr. R. C. Lee (1)
Harold F. Plank (1)

Los Alamos Scientific Laboratory
P. O. Box 1663
Los Alamos, New Mexico 87544
Attn: Report Librarian (2)
Dr. L. D. P. King (1)
Dr. Wright Langham (1)

DISTRIBUTION (cont):

Lovelace Foundation for Medical Education
and Research
5200 Gibson Blvd., SE
Albuquerque, New Mexico
Attn: Dr. Clayton S. White, Director of Research

Martin Company Nuclear Division
Middle River, Maryland 21203
Attn: D. G. Harvey (1)
W. A. Hagis (1)

Minnesota Mining and Manufacturing Co.
P. O. Box 6505
St. Paul, Minnesota
Attn: H. C. Zeman, Security Department

Minnesota Mining and Manufacturing Co.
425-13th Street, NW
Washington, D. C.
Attn: Reynolds Marchant, Government Liaison
SNAP and Nuclear

Monsanto Research Corporation
Mound Laboratory
P. O. Box 32
Miamisburg, Ohio 45352
Attn: G. R. Grove

NASA
Langley Research Center
Langley Station
Hampton, Virginia 23365
Attn: Librarian

NASA
Goddard Space Flight Center
Glenn Dale Road
Greenbelt, Maryland 20771
Attn: Charles Baxter, Nimbus Project (1)
A. W. Fihelly, Nimbus Project (1)

NASA
Lewis Research Center
21000 Brookpark Road
Cleveland, Ohio 44135
Attn: George Mandel

NASA
George C. Marshall Space Flight Center
Huntsville, Alabama 35812
Attn: W. Y. Jordan

NASA
Ames Research Center
Moffet Field, California
Attn: Glenn Goodwin

NASA
Headquarters
1512 H Street, NW
Washington, D. C. 20545
Attn: Thomas B. Kerr

NASA
Manned Spacecraft Center
Houston, Texas 77058
Attn: Chief, Technical Information Division

NASA
Scientific and Tech. Info. Facility
P. O. Box 5700
Bethesda, Maryland 20014
Attn: NASA Representative, S-AK/DL (2)

Nuclear Utility Services, Inc.
1730 M Street, NW
Washington, D. C. 20036
Attn: Morton S. Goldman, Manager Environmental
Safeguards

Phillips Petroleum Company
NRTS Technical Library
P. O. Box 2067
Idaho Falls, Idaho 83401

Radio Corporation of America
Astroelectronics Division
Princeton, New Jersey

Director, USAF Project RAND
Via Air Force Liaison Office
The Rand Corporation
1700 Main Street
Santa Monica, California 90406
Attn: Library

TRW Systems
P. O. Box 287
Redondo Beach, California
Attn: Dr. Donald Jortner

U. S. Naval Radiological Defense Lab.
Commanding Officer and Director
San Francisco, California 94135
Attn: Dr. P. E. Zigman

Union Carbide Research Institute
P. O. Box 278
Tarrytown, New York
Attn: Joseph Agresta, Space Sciences Group

Union Carbide Corporation
Nuclear Division
P. O. Box X
Oak Ridge, Tennessee 37831
Attn: E. Lamb, Isotope Dev. Ctr.

University of California
Lawrence Radiation Laboratory
P. O. Box 808
Livermore, California 94551
Attn: Technical Information Division

DISTRIBUTION (cont):

Westinghouse Electric Company
Astronuclear Laboratory
P. O. Box 10864
Pittsburgh 30, Pennsylvania
Attn: Joanne M. Bridges
Supervisor, Flight Safety Analysis Group

Aeronautical Systems Division
Wright-Patterson Air Force Base, Ohio 45433
Attn: Augustus Daniels, SEPRR

Division of Technical Information Ext.
USAEC
P. O. Box 62
Oak Ridge, Tennessee 37831 (50)

Clearinghouse for Federal Scientific and
Technical Information
5285 Port Royal Road
Springfield, Virginia 22151 (75)

Aerojet-General Corp.
P. O. Box 296
Azusa, California 91703
Attn: M. T. Grenier, Corporate Librarian

Westinghouse Electric Co.
Astronuclear Laboratory
P. O. Box 10864
Pittsburgh 30, Pennsylvania
Attn: H. P. Smith

Space Nuclear Propulsion Office
Lewis Research Center
21000 Brookpark Road
Cleveland, Ohio 44135
Attn: P. M. Ordin

U. S. Naval Radiological Laboratory
San Francisco, California 94135
Attn: J. D. Connor, Code 935

Aberdeen Proving Ground
Aberdeen, Maryland
Attn: H. Bechtol

Picatinny Arsenal
Dover, New Jersey
Attn: P. Sadlon

Watervliet Arsenal
Watervliet, New York
Attn: A. Muzicka

Los Alamos Scientific Lab.
P. O. Box 1663
Los Alamos, New Mexico 87544
Attn: E. E. Campbell

S. P. Schwartz, 1
R. W. Henderson, 1000
H. J. Bolles, 1111
C. C. Thacker, 1113
B. A. Ball, 1113
J. H. Findlay, 1400
S. A. Moore, 1540
E. H. Draper, 2000
A. Juskiewicz, 3311
D. R. Parker, 3311
R. J. Hansen, 4200
R. S. Claassen, 5100
J. R. Banister, 5120
T. B. Cook, 5200
J. D. Shreve, 5234
C. Winter, 5630
W. T. Moffat, 7220
H. E. Viney, 7250
L. E. Lamkin, 7300
G. H. Roth, 7320
H. J. Plagge, 7325
R. D. Jones, 7332
G. A. Fowler, 9000
D. B. Shuster, 9200
A. E. Bentz, 9232 (1), Attn: J. P. Martin, 9232 (1)
A. Y. Pope, 9300
V. E. Blake, 9310
H. E. Hansen, 9311 (3)
A. J. Clark, Jr., 9312 (1)
Attn: R. E. Berry, 9312 (3)
B. S. Hill, 9312 (1)
H. J. Gay, 9312 (1)
J. W. McKiernan, 9319 (2)
R. C. Maydew, 9320
H. R. Vaughn, 9321
W. H. Curry, 9322
E. C. Rightley, 9323
W. R. Barton, 9324
S. McAlees, 9325
K. J. Touryan, 9326
W. N. Caudle, 9327 (1)
Attn: J. Colp, 9327 (1)
J. L. Tischhauser, 9420
B. S. Biggs, 8000
B. R. Allen, 3421
M. G. Randle, 3428-1
W. F. Carstens, 3410
Attn: T. B. Heaphy, 3411 (1)
R. S. Gillespie, 3413 (2)
W. A. Jamieson, 8232
R. C. Smelich, 3415-3 (10)